

**COMPLEX FORMATION OF PYRIDINE OXIMES WITH DIVALENT TRANSITION
METAL IONS IN AQUEOUS SOLUTION**

MARKKU A. J. SALONEN

Department of Chemistry
Faculty of Science
University of Helsinki
Helsinki, Finland

Academic dissertation

*To be presented with permission of the Faculty of Science of the University of Helsinki
for public criticism in Auditorium A 129 of Department of Chemistry,
A. I. Virtasen aukio 1, on December 16th at 12 o'clock noon.*

Helsinki 2020

Supervisor

Professor Timo Repo
Department of Chemistry
University of Helsinki
Finland

Reviewers

Professor Konstantin Popov
Laboratory head of JSC “Fine Chemical R&D Centre”
Moscow, Russian Federation

Professor Mika Sillanpää
University of Johannesburg
South Africa

Opponent

Docent Ari Lehtonen
University of Turku
Finland

© Markku A. J. Salonen
ISBN 978-951-51-6897-9 (nid.)
ISBN 978-951-51-6898-6 (PDF)
<http://ethesis.helsinki.fi>

Unigrafia
Helsinki 2020

ABSTRACT

The complex formation equilibria of pyridine-2-aldoxime and its methyl or amido derivatives (HL) with cobalt(II), zinc(II), and cadmium(II) ions, and the protonation and complex formation equilibria of pyridine-2,6-carboxamidoxime (H_2L) with copper(II) and nickel(II) ions were studied in aqueous 0.1 M NaCl solution at 25 °C by potentiometric titrations with the use of glass electrode. The experimental data were analyzed with the least-squares computer program SUPERQUAD to determine the complexes formed and their stability constants. In addition, the structure of the crystallized pyridine-2,6-carboxamidoxime complex with the formula $[Ni(HL)_2] \cdot 4H_2O$ has been determined with X-ray measurements.

The complexes of types $Co(HL)^{2+}$ and $Co(HL)_2^{2+}$ are mainly octahedral with a high spin d^7 electron structure ($t_{2g}^5 e_g^2$) and their oxidation states are stable. The deprotonated bis complexes of type $Co(HL)L^+$ are often low spin ($t_{2g}^6 e_g$) and because of the easy loss of their only e_g electron they are easily oxidized to very inert low spin cobalt(III) complexes (t_{2g}^6). Only small amounts of cobalt(III) complexes cause the very slow attainment of equilibrium often already in the pH range 2–5. Pyridine-2-carboxamidoxime and pyridine-2-aldoxime and probably also 1-(2-pyridinyl)ethanone oxime forms also tris complexes $Co(HL)_3^{2+}$ and/or $Co(HL)_2L^+$.

The complex formation of pyridine-2-aldoxime in the pH range 5–10 could be studied by using very small cobalt(II) ion concentrations. There, all the cobalt(II) form the low spin CoL_2 , which quantitatively displaces also the tris complex $Co(HL)_2L^+$. 6-methylpyridine-2-aldoxime forms complexes $Co(HL)^{2+}$, CoL^+ , CoL_2 , $Co_2L_2OH^+$, $Co_2L_3^+$, and Co_2L_3OH , mainly in the pH range 6–10. The stabilities of the low spin CoL_2 , $Co_2L_3^+$, and Co_2L_3OH and their oxidation reactions are decreased by the steric requirements of the 6-methyl groups of the ligands.

Pyridine-2-acetamidoxime forms also a complex $Co(H_2L)^{3+}$ and pyridine-2-carboxamidoxime forms a complex $Co_2(HL)_2H_2L^{5+}$ with a positively charged ligand (H_2L^+).

Zinc(II) and cadmium(II) ions form with 6-methylpyridine-2-aldoxime only $Zn_2L_2^{2+}$, $Zn_2L_2OH^+$, and $Zn_2L_2(OH)_2$, and CdL^+ , CdL_2 , and $Cd_2L_2OH^+$. With pyridine-2-acetamidoxime, they form only $Zn(HL)^{2+}$, $Zn_2L_2OH^+$, $Cd(HL)^{2+}$, and CdL^+ . The other oximes form also $Zn(HL)L^+$, ZnL_2 , $Cd(HL)L^+$, and CdL_2 . $Cd(HL)_2^{2+}$ reaches only with pyridine-2-carboxamidoxime and $Zn(HL)_2^{2+}$ also with 1-(2-pyridinyl)ethanone oxime measurable concentrations. Pyridine-2-carboxamidoxime forms also $Zn_4(L-H)_2L_2^{2+}$ and $Cd_4(L-H)_2L_2^{2+}$.

The stability constants of the mono complexes $M(HL)^{2+}$ increase with few exceptions in the order 6-methylpyridine-2-aldoxime < pyridine-2-acetamidoxime < pyridine-2-aldoxime < 1-(2-pyridinyl)ethanone oxime < pyridine-2-carboxamidoxime < pyridine-2,6-dicarboxamidoxime and $Cd < Zn < Co < Ni < Cu$.

PREFACE

The experimental work of this thesis was carried out in the Laboratory of Inorganic Chemistry at University of Helsinki.

I am most grateful to my supervisors Emeritus Professor Heikki Saarinen for the guidance at the beginning of the work and to Professor Timo Repo for the completion of the work.

I am also grateful for Doctors Helena Hyvönen, Marjatta Orama, and Pirkko Tilus for the obtaining advice in the processing of the titration results and use of the modern data processing programs. To Dr. Helena Hyvönen I am grateful also for the many advice in the final stages of the work.

Crystallization of the complexes formed was difficult. For only one complex was the crystal structure determined. For this, I am grateful to Dr. Ilpo Mutikainen.

However, the main difficulty of this work was the oxidation of the divalent cobalt ion in its deprotonated complexes to trivalent. One would think that deprotonation of the oxime group would shorten the bond between it and the metal ion. However, studies around the world show that this is certainly not the case. In the deprotonated bis-oxime complexes, the oxime and oximate groups are generally *cis* oriented forming an intramolecular hydrogen bridge. But deprotonation of their oxime group causes isomerization of the complex by *trans* orientation of the oximate groups due to the repulsive forces between the negatively charges. Also in the crystalline non-deprotonated bis-complexes, the oxime groups are (generally) *trans* oriented due to the repulsive forces between the oxime protons.

I wish to thank the reviewers of the manuscript, Professor Konstantin Popov and Professor Mika Sillanpää, for their valuable comments my work.

Helsinki, November 2020

Markku Salonen

LIST OF PUBLICATIONS

- I M. Salonen, H. Saarinen, and M. Orama, Formation of Zinc(II) and Cadmium(II) Complexes with Pyridine Oxime Ligands in Aqueous Solution, *J. Coord. Chem.* **56** (2003) 1041.
- II M. Salonen, H. Saarinen, and M. Orama, Formation of Cobalt(II) Complexes with Five Pyridine Oximes in Aqueous Solution, *J. Coord. Chem.* **58** (2005) 317.
- III M. Salonen, H. Saarinen, and I. Mutikainen, Equilibrium and Structural Studies of Copper(II) and Nickel(II) Complexes with Pyridine-2,6-diamidoxime in Aqueous Solution, *J. Coord. Chem.* **61** (2008) 1462.
- IV M. Salonen, Formation of Zinc(II) and Cadmium(II) Complexes with Pyridine-2-carboxamidoxime and Pyridine-2-acetamidoxime, *J. Coord. Chem.* **63** (2010) 3127.
- V E. Lankinen, J. Paajanen, M. Salonen, and H. Hyvönen, Complexation of Pyrazine-2-carboxamidoxime with Cu(II), Ni(II), Zn(II), and Cd(II) Ions in Aqueous Solution, *J. Coord. Chem.* **68** (2015) 3498.

For publication **I** the author performed all experimental work and partly the processing of the results, designed the experimental work for cadmium (II) complexes, and wrote the manuscript.

For **II**, the author designed and performed all experimental work, the processing of the results, and wrote the manuscript.

For **III**, the author designed and performed the experimental work of the titrations in aqueous solution, the processing of the results, and wrote the manuscript.

For **IV**, the author designed and performed all experimental work, the processing of the results, and wrote the manuscript.

For **V**, the author wrote most of the text in the Results and Discussion section. Especially the interpretation of the results is the author's output. “

CONTENTS

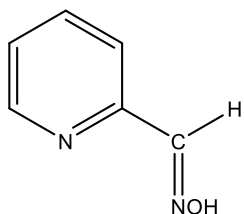
| | page |
|-----------------------------------------------------|------|
| Abstract | 3 |
| Preface | 4 |
| List of original publications | 5 |
| Abbreviations | 7 |
| 1. Introduction | 8 |
| 2. Experimental | 9 |
| 2.1. Reagents and solutions | 9 |
| 2.2. Potentiometric measurements | 10 |
| 2.3. Mathematical treatments of data | 11 |
| 2.4. Evaluation of the equilibrium model | 13 |
| 3. Results and discussion | 15 |
| 3.1. Pyridine-2-aldoxime complexes | 15 |
| 3.2. 6-methylpyridine-2-aldoxime complexes | 34 |
| 3.3. 1-(2-pyridinyl)ethanone oxime complexes | 43 |
| 3.4. Pyridine-2-carboxamidoxime complexes | 51 |
| 3.5 Pyridine-2-amdioxime complexes | 66 |
| 3.6. Pyridine-2,6-dicarboxamidoxime complexes | 70 |
| 4. Summary and conclusions | 80 |
| References | 85 |

ABBREVIATIONS

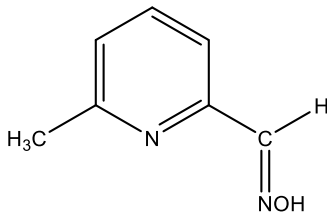
| | |
|----------------------------------------------------|----------------------------------------------------------------------|
| acac ⁻ | acetylacetonate ion (acetylacetone = Hacac) |
| ao ⁻ | 2-aminoamidoximate ion (2-aminoamidoxime = Hao) |
| ap ⁻ | 3-aminopropanamidoximate ion (3-aminopropanamidoxime = Hap) |
| bipy | 2,2'-bipyridine |
| C _H , C _M and C _L | the total concentration of hydrogen ion, metal ion and ligand |
| dea ⁻ | 2-(<i>N</i> -diethylamino)acetamidoximate ion |
| dma ⁻ | 2-(<i>N</i> -dimethylamino)acetamidoximate ion |
| dmf | dimethylformamide |
| dmg ⁻ | dimethylglyoximate ion (dimethylglyoxime = Hdmg) |
| dmp ⁻ | 3-(<i>N</i> -dimethylamino)propanamidoximate ion |
| emf | electromotive force |
| en | ethylenediamine |
| <i>h</i> | the concentration of the free hydrogen ion (= [H ⁺]) |
| Hoad ⁻ | oxamide dioximate ion (oxamide dioxime = H ₂ oad) |
| <i>I</i> | ionic strength |
| Im | imidazole |
| M | mol dm ⁻³ |
| mM | mmol dm ⁻³ (= 10 ⁻³ mol dm ⁻³) |
| ma ⁻ | 2-(<i>N</i> -methylamino)acetamidoximate ion |
| Me | methyl —CH ₃ group |
| mp ⁻ | 3-(<i>N</i> -methylamino)propanamidoximate ion |
| M ^{z+} | metal ion (<i>z</i> = its charge number) |
| ox | oxime or oximate group |
| Ph | phenyl group |
| phen | 1,10-phenatroline |
| py | pyridine |
| pz | pyrazine |
| pza ⁻ | pyrazine-2-carboxamidoximate ion (pyrazine-2-carboxamidoxime = Hpza) |

1. INTRODUCTION

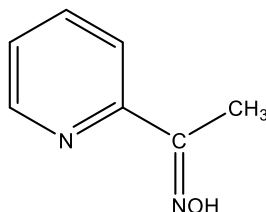
Equilibrium and structures of divalent copper, nickel, and zinc complexes with 2-aminoacetamidoxime,¹⁻⁴ 3-aminopropanamidoxime⁵⁻⁸ and their methyl and ethyl derivatives of type $RR'N(CH_2)_nC(NH_2)NOH$ has been studied in our laboratory in the last decades. Following this, the studies has been continued on the following pyridine-2-oximes.⁹⁻¹³



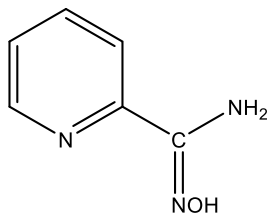
Pyridine-2-aldoxime



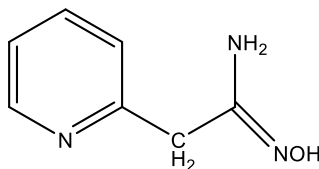
6-methylpyridine-2-aldoxime



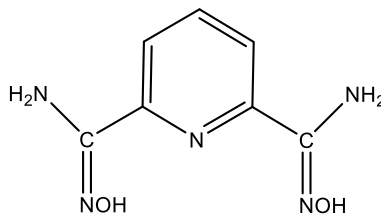
1-(2-pyridinyl)ethanone oxime



Pyridine-2-carboxamidoxime



Pyridine-2-acetamidoxime



Pyridine-2,6-carboxamidoxime

In this work the studies has been expanded to the complexation of divalent cobalt, zinc, and cadmium ions with the five pyridine-2-oximes and to the complexation of pyridine-2,6-dicarboxamidoxime.

These pyridine oximes coordinate to the divalent metal ions mainly through their pyridine and oxime nitrogen atom forming five- or, in the case of pyridine-2-acetamidoxime, six-membered chelate rings. The complexes formed can polymerize through the oxime oxygen atoms and the amidoxime complexes also through the amido group in the form $-NH^-$. The stability order of the most stable copper, nickel, zinc, and cadmium complexes of type $M(HL)_n^{2+}$ with $n = 1, 2$ or 3 is pyridine-2-carboxamidoxime > 1-(2-pyridinyl)ethanone oxime > pyridine-2-aldoxime.⁹⁻¹³ The stability of the pyridine-2-acetamidoxime complexes are weakened by their six-membered chelate rings. However, with divalent copper ion, the pyridine-2-acetamidoxime forms more stable complexes of $Cu(HL)^{2+}$ and $Cu(HL)_2^{2+}$ types than pyridine-2-aldoxime.⁹ It seems that the amide and methyl groups bonded to the oxime carbon atoms increase the stability of the complexes although they do not form any bond with the metal ion. The stability of the 6-methylpyridine-2-aldoxime complexes is decreased by the steric requirements of the 6-methyl group.¹⁰⁻¹³

The pyridine oximes are available reagents in analytical chemistry.^{14–19} Pyridine-2-aldoxime is also used to reactivate cholinesterase enzymes inhibited by organophosphorus compounds.^{20–22} The pyridine-2-aldoxime complexes CuL_2 and NiL_2 coordinate through two oximato bridges to alkaline earth metal 8-kinolates or 1-nitroso-2-naphtholates (MX_2) to form inhibitors against some bacteria.²²

2. EXPERIMENTAL

2.1. Reagents and solutions

The water used was purified by a Millipore Milli-Q water purifier, which purifies the water by reverse osmosis, filtrations by active carbon, cation and anion exchange and filtration of the organic compounds. The resistivity of the purified water was generally *ca.* 18 M Ω cm.

The copper, nickel, cobalt, and cadmium chloride solutions were prepared by dissolving the weighted amounts of solid p.a. grade CuCl_2 , NiCl_2 , CoCl_2 , and CdCl_2 hydrates in the purified water. The zinc chloride solution was prepared by using solid p.a. grade ZnO , HCl Titrisol ampoule, and a volumetric flask of 500 ml (Emil, Green line). The metal ion contents of the stock solutions were standardized by EDTA titration. The copper(II) ion concentration was also determined electrogravimetrically and the nickel(II) ion concentration by precipitation with dimethylglyoxime.

The 0.100 M HCl and NaOH solutions used in the potentiometric titrations were prepared by using Titrisol ampoules (Merck) and volumetric flasks of 1000 ml (Emil, Green line). Their exact concentrations were standardized by potentiometric titration of the HCl solution with the NaOH solution. The acid contents of the metal chloride solutions were determined by titration with 0.1 M NaOH solution after liberation of the hydrogen ions by cation exchange.

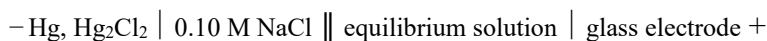
Pyridine-2-aldoxime (99+ % Aldrich, gold label) was taken to use without further purification. Pyridine-2-carboxamidoxime, pyridine-2-acetamidoxime, 1-(2-pyridinyl)ethanone oxime and 6-methylpyridine-2-aldoxime were prepared in our laboratory according to methods described in earlier papers.^{9,10} Pyridine-2,6-dicarboxamidoxime was synthesized by refluxing a suspension of 6.28 g hydroxylamine hydrochloride, 3.62 g NaOH, and 5.0 g 2,6-dicyanopyridine (97 %, Aldrich) in 1 : 1 ethanol/water solution according to the method described by Banks and Brookes.²³ The white crystalline product was poorly soluble in water and common organic solvents. It was recrystallized from an aqueous HCl solution as dihydrochloride. The recrystallized product was dissolved in deionized water, and the exact hydrochloride (HCl) concentration of the prepared solution (0.112 M) was determined by NaOH titration.

2.2. Potentiometric measurements

The investigation was carried out as a series of potentiometric titrations in aqueous 0.1 M NaCl solutions at 25.0 °C. Because of the poor solubility of some of the most interesting complexes in perchlorate solutions, NaCl, the main salt in natural waters, was chosen as inert salt instead the more common NaClO₄.

The titration system consisted of an autoburette (Metrohm Herisau Dosimat E 535), a magnetic stirrer (Metrohm Herisau E 649), a closed titration vessel and a digital potentiometer Radiometer PHM 52 connected to a sensitive REC61 servograph recorder. A water thermostat (B. Braun Melsungen AG, Thermomix 1430) to 25.0 ± 0.1 °C and nitrogen gas was passed through the solutions tempered in the titration vessel. The potentiometer was equipped to a Beckman glass electrode E 40495 and a calomel reference electrode with J-shaped liquid junction.

The free hydrogen concentration (h) was determined by measuring the emf of the cell:



Assuming the activity coefficients to be constant, the emf (E) of the cell at 25.0 °C can be written as

$$E = E_0 + 59.16 \log h + E_j \quad (1)$$

The liquid junction potential E_j can be expressed as

$$E_j = j_H h + j_{OH} K_w h^{-1}, \quad (2)$$

where j_H and j_{OH} are the liquid junction potential coefficients of the hydrogen and hydroxide ions and K_w is the ionic product of the water:

$$K_w = [\text{H}^+][\text{OH}^-] \quad (3)$$

According Näsänen *et al.*^{24,25} the dependence of K_w on the ionic strength of NaClO₄ solution at 25.0 °C can be expressed as

$$\text{p}K_w = 13.996 - 1.018I^{1/2}/(1 + 1.0I^{1/2}) + 0.26I, \quad (4)$$

when the value of $\text{p}K_w$ at zero ionic strength is taken to be 13.996.²⁶ The calculated $\text{p}K_w = 13.783$ in 0.10 M NaClO₄ solution is in a good agreement with the experimental results $\text{p}K_w = 13.775 \pm 0.001$ in 0.1 M Na(Cl) solution at 25.0 °C determined by Sjöberg *et al.*²⁷ The difference between NaCl and NaClO₄ solutions increases in the increase of the ionic strength; for example, at 25 °C in 1 M NaCl and NaClO₄ solutions $\text{p}K_w = 13.73$ and 13.77, but it is, 14.03 and 14.17, respectively, in 3 M solutions.²⁵

E_0 and j_H were determined before each titration by adding exactly known 0.1 M HCl solution to 0.100 M NaCl solution. The observed j_H values were generally in agreement with the experimental

results, $j_H = -511.5 \pm 4.9$ and $j_{OH} = 238.7 \pm 1.5 \text{ mV M}^{-1}$ in 0.1 M NaCl) solutions at 25.0 °C, and with the following equations:

$$j_H = (-49.7 \pm 0.5)I^{-1} \text{ mV M}^{-1} \quad (5)$$

$$j_{OH} = (21.4 \pm 0.8)I^{-1} \text{ mV M}^{-1} \quad (6)$$

determined in the ionic strength range $I = 0.05\text{--}2 \text{ M NaCl}$ at 25.0 °C by Sjöberg *et al.*²⁷ In the pH range < 10 the term $j_{OH}K_w h^{-1}$ of equation (2) is negligible ($< 0.05 \text{ mV}$) in the relation to the accuracy of the potentiometer ($\pm 0.1 \text{ mV}$). In the higher pH range, it was possible to study only a few solutions. In the calculations the experimental $j_{OH} = 238 \text{ mV M}^{-1}$ was used.

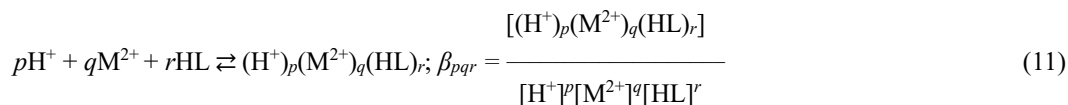
After the determination of E_0 , the composition of the solutions was in general 50.00 ml 0.100 M NaCl + 7.00 ml 0.1 M HCl. Then, the necessary amounts of metal chloride solution and solid oxime was added to the acid solution and its initial pH was adjusted with the HCl solution. The solution prepared in this way was titrated with an exactly known 0.1 M NaOH solution. The available concentration and pH ($= -\log h$) ranges were defined by the formation of a precipitate or very slow attainment of equilibrium.

2.3. Mathematical treatment of the data

In evaluating the equilibrium constants, the binary two-component equilibria (7–10) were considered:



The acid strengths of the oxime –NOH groups are very weak, and thus the values of the corresponding $p\beta_{-101}$ (pK_a) values in reaction (9) are not very accurate. This is the reason to choose the ligand as a component in the form of the uncharged oxime (HL) in evaluating the stability constants of a three-component (H^+ , M^{2+} and HL) system:



In the evaluation of the three-component experimental data, the binary complex models were considered as known. The protonation constants of the ligands are given with the results of the

correspondent ligand. The binary hydrolytic equilibrium constants of cobalt(II), which were used ($\log \beta_{-110} = -9.85$ and $\log \beta_{-210} = -19.02$), were extrapolated from those determined in 0.25–3 M NaClO₄ solutions to ionic strength 0.1 M by Debye–Hückel-type equations established by Baes and Mesmer.²⁸ Similarly, the hydrolytic equilibrium constants of zinc(II) ($\log \beta_{-110} = -9.15$ and $\log \beta_{-120} = -8.89$) were extrapolated from those determined in 2–3 M NaCl, and $\log \beta_{-120} = -9.13$ and $\log \beta_{-440} = -32.37$ for cadmium(II) from those determined in 3 M LiClO₄ solutions. In NaClO₄ solution at $I = 0.1$ M the $\log \beta_{-110}$ value²⁹ of Cd²⁺ is -10.01 and the stability constant of CdCl⁺ $\log K_1 = 1.59 \pm 0.30$.^{30,31} In 0.1 M Na(Cl) solution, the hydrolysis of Cd²⁺ ion is lower because the proportion of CdCl⁺ is considerable, but its hydrolysis and the proportion of CdClOH are insignificant in the pH range 9–10,³¹ where $[\text{OH}^-] \ll [\text{Cl}^-]$. The used $\log \beta_{-110}$ value of Cd²⁺ ion $= -11.8$ was calculated from that of -11.6 in KCl solution of $I = 0.1$ M at 30 °C determined by Chaberek *et al.*³² by using the hydrolytic enthalpy $\Delta H_{-110} = +54.8$ kJ mol⁻¹ determined by Arnek and Kakowicz.³³ The side reactions of the divalent metal ions of the first transition series with the chloride ion are smaller. For example, in NaClO₄ solution at $I = 1.0$ M the $\log K_1$ values of CoCl⁺, NiCl⁺, and CuCl⁺, are 0.18, 0.16, and 0.13, respectively.^{30,34} The $\log K_1$ value of ZnCl⁺ is 0.32 in fresh water ($I = 0.0015$ M), -0.25 in seawater ($I = 0.67$ M),³⁵ and -0.097 at $I = 1.0$ M.³⁰ It can be estimated to be about -0.1 at $I = 0.1$ M.³⁶ Because HCl is a very strong acid, it is completely in the form of Cl⁻ in the pH range 1–14. The coordination of the chloride ion to a metal ion does not affect the pH of the solution, so the glass electrode cannot distinguish chloro complexes from the free aqua ions or the mixed chloro oxime complexes from the oxime complexes. Thus, the possible chloro complexes have been ignored. The total concentrations of acid (C_H), metal ion (C_M) and ligand (C_L) are therefore:

$$C_H = 2[\text{H}_3\text{L}^{2+}] + [\text{H}_2\text{L}^+] - [\text{L}^-] + [\text{H}^+] - [\text{OH}^-] + \sum p[(\text{H}^+)_p(\text{M}^{2+})_q(\text{HL})_r] = C_{\text{HCl}} - C_{\text{NaOH}} \quad (12)$$

$$C_M = [\text{M}^{2+}] + \sum q[(\text{H}^+)_p(\text{M}^{2+})_q(\text{HL})_r] \quad (13)$$

$$C_L = [\text{H}_3\text{L}^{2+}] + [\text{H}_2\text{L}^+] + [\text{HL}] + [\text{L}^-] + \sum r[(\text{H}^+)_p(\text{M}^{2+})_q(\text{HL})_r] \quad (14)$$

The mathematical analysis of data were performed with the least-squares computer program SUPERQUAD.³⁷ The program calculates the concentrations of the known and proposed species in every titration points by using equations (1)–(14). The pqr triplets and corresponding equilibrium constants that best fit the experimental data were determined by minimizing the error sum:

$$U = \sum w_i (E_i^{\text{obs}} - E_i^{\text{calc}})^2 \quad (15)$$

The weighting factor w_i is determined by the equation

$$w_i = 1/(\sigma_E^2 + \delta E_i / \delta V_i) \sigma_V^2, \quad (16)$$

where $\sigma_E (= \pm 0.1 \text{ mV})$ and $\sigma_V (= \pm 0.02 \text{ ml})$ are the estimated uncertainties in the electrode and titrant (NaOH) volume readings, and $\delta E_i / \delta V_i$ is the slope of the titration curve.

2.4. Evaluation of the equilibrium model

The SUPERQUAD program calculates χ^2 and the sample standard deviation s for every model, indicating the fit of the model with the experimental data.

The Bjerrum-plots,^{38,39} Z_{HL} vs. $\log [\text{HL}]$, where Z_{HL} denotes the ratio of the coordinated ligands to the total metal ion concentration, can be an aid in the evaluation. In the low pH ranges, most of the oxime complexes are in the form of $\text{M}(\text{HL})_r^{2+}$. Then in the equation (12) the term $\Sigma p[(\text{H}^+)_p(\text{M}^{2+})_q(\text{HL})_r]$ ($= \Sigma p[\text{M}(\text{HL})_r^{2+}]$) = 0 with $p = 0$, and according equation (14) $Z_{\text{HL}} = \Sigma r[\text{M}(\text{HL})_r^{2+}] / C_{\text{M}}$. Reorganization of the contracted equation (12) gives:

$$2[\text{H}_3\text{L}^{2+}] + [\text{H}_2\text{L}^+] - [\text{L}^-] = C_{\text{HCl}} - C_{\text{NaOH}} - h + K_{\text{w}}h^{-1} \quad (17)$$

Substituting the concentrations $[\text{H}_3\text{L}^{2+}]$ and $[\text{H}_2\text{L}^+]$ calculated according the equations (7) and (8) and $[\text{L}^-] = 0$ to equation (17) gives:

$$[\text{HL}] = \frac{C_{\text{HCl}} - C_{\text{NaOH}} - h + K_{\text{w}}h^{-1}}{2\beta_{201}h^2 + \beta_{101}h} \quad (18)$$

and to equation (14) gives:

$$Z_{\text{HL}} = \frac{C_{\text{L}} - (\beta_{201}h^2 + \beta_{101}h + 1)[\text{HL}]}{C_{\text{M}}} \quad (19)$$

Assuming that only mononuclear complexes in the form $\text{M}(\text{HL})_r^{2+}$ are present, the Bjerrum-plots Z_{HL} vs. $\log [\text{HL}]$ coincide regardless of the concentrations C_{M} and C_{L} as well as of the ratio $C_{\text{L}}/C_{\text{M}}$. If deprotonated or polynuclear complexes are formed, the equation (17) is no longer valid ($p \neq 0$) and Z_{HL} no longer indicates the average number of ligands HL ($= r$) in the complexes $(\text{H}^+)_p(\text{M}^{2+})_q(\text{HL})_r$.^{*} The Z_{HL} curves are diverged.

If all the complexes are binary mononuclear of type ML_r^{2-r} ($p = -r$), the Bjerrum-plots and the total concentration of hydrogen ion ($C_{\text{H}} + C_{\text{L}}$) can be calculated over the zero level L^- , M^{2+} and H_2O :

$$C_{\text{H}} + C_{\text{L}} = 3[\text{H}_3\text{L}^{2+}] + 2[\text{H}_2\text{L}^+] + [\text{HL}] + [\text{H}^+] - [\text{OH}^-] = C_{\text{HCl}} + C_{\text{L}} - C_{\text{NaOH}} \quad (20)$$

^{*}This is the reason to replace the symbol \bar{n} , the average of n for example in the complexes $\text{M}(\text{HL})_n^{2+}$ (\bar{n}_{HL}) or ML_n^{2-n} (\bar{n}_{L}), commonly used in the literature, with a different symbol Z (Z_{HL} or Z_{L}).

(C_H has been calculated over the zero level HL, M^{2+} , and H_2O). Substituting the equations

$$[H_3L^{2+}] = \beta_{201}[H^+]^3[L^-]/\beta_{-101}, [H_2L^+] = \beta_{101}[H^+]^2[L^-]/\beta_{-101} \text{ and } [HL] = [H^+][L^-]/\beta_{-101} \quad (21)$$

to equations (20) and (14) gives $[L^-]$ and $Z_L = \Sigma r[ML_r^{2-r}]/C_M$:

$$[L^-] = \frac{C_{HCl} + C_L - C_{NaOH} - h + K_w h}{(3\beta_{201}h^3 + 2\beta_{101}h^2 + h)/\beta_{-101}} \quad (22)$$

$$Z_L = \frac{C_L - (\beta_{201}h^3/\beta_{-101} + \beta_{101}h^2/\beta_{-101} + h/\beta_{-101} + 1)[L^-]}{C_M} \quad (23)$$

Z_L indicates the average of r in the complexes ML_r^{2-r} , when only binary mononuclear complexes in the form ML_r^{2-r} are present. Then the Z_L curves vs. $\log [L^-]$ are independent on the concentrations C_M and C_L as well as of the ratio C_L/C_M . The possible dependence on these factors can indicate polymerization or protolysis of the complexes to forms $M_qL_r(OH)_s^{2q-r-s}$ ($s \geq 0$). In the presence of such complexes the equation (20) is no longer valid, because $\Sigma r[(H^+)_p(M^{2+})_q(HL)_r] \neq \Sigma r[ML_r^{2-r}]$.

The experimental result can also be visualized by calculating the Z_H values of the titration points vs. pH. Z_H is defined as the average number of OH^- ions reacted per ligand (HL):

$$Z_H = (h - C_H - K_w h^{-1})/C_L \quad (24)$$

When C_H is calculated over the zero level HL, H_2O , and M^{2+} according the equations (12), (14) and (24):

$$Z_H = \frac{[L^-] - [H_2L^+] - 2[H_3L^{2+}] - \Sigma p[(H^+)_p(M^{2+})_q(HL)_r]}{[L^-] + [HL] + [H_2L^+] + [H_3L^{2+}] + \Sigma r[(H^+)_p(M^{2+})_q(HL)_r]} \quad (25)$$

Also the Z_H values of the free ligand can be calculated according equation (25) by substituting $[(H^+)_p(M^{2+})_q(HL)_r] = 0$. Substituting $[H_3L^{2+}] = \beta_{201}[HL][H^+]^2$, $[H_2L^+] = \beta_{101}[HL][H^+]$ and $[L^-] = \beta_{-101}[HL][H^+]^{-1}$ calculated according the equations (8), (9) and (10) to equation (25) gives:

$$Z_H = \frac{\beta_{-101}h^{-1} - \beta_{101}h - 2\beta_{201}h^2}{\beta_{-101}h^{-1} + 1 + \beta_{101}h + \beta_{201}h^2} \quad (26)$$

Thus, the Z_H curve of the free ligand vs. pH is independent on the total ligand concentration (C_L). It can be considered as a "bottom line" for the solutions, where the ligand forms complexes. When complexes are formed, the increase of the Z_H curves of the solutions in the increase of pH depends on the concentrations of the formed complexes according the equation (25). If the metal ion is in some pH range nearly completely as one complex $(H^+)_p(M^{2+})_q(HL)_r$, the Z_H curves of the solutions can have

plateau (slow increase) or a inflection point. If the plateau or the inflection point is in a pH range, where $h \ll -C_H \gg K_w h^{-1}$ ($C_H < 0$, when the HCl added to the solution is completely neutralized) and $[H_3L^{2+}]$, $[H_2L^+]$ and $[L^-] \approx 0$, equations (12), (13) and (14) are contracted to the following forms:

$$C_H = p[(H^+)_p(M^{2+})_q(HL)_r] \quad (27)$$

$$C_M = q[(H^+)_p(M^{2+})_q(HL)_r] \quad (28)$$

$$C_L = [HL] + r[(H^+)_p(M^{2+})_q(HL)_r] \quad (29)$$

In these conditions $[(H^+)_p(M^{2+})_q(HL)_r] = C_H/p = C_M/q$ and according the Z_H curves:

$$p:q = C_H:C_M \text{ and } C_H = -Z_H C_L \quad (30)$$

By means of the ratio $p:q$ the pqr combination of the complex $(H^+)_p(M^{2+})_q(HL)_r$ can be estimated. For example, if $p:q = -3:2$, possible pqr combinations are among other things -322 , -323 and -644 . With the SUPERQUAD program the stability constants of the correspondent complexes can be estimated and the reliability of the given equilibrium model can be estimated by means of the χ^2 and s values.

3. RESULTS AND DISCUSSION

3.1. Pyridine-2-aldoxime complexes

At the end of the 1950s, pyridine-2-aldoxime was shown by Hartkamp¹⁴⁻¹⁶ to be a practical reagent in the spectrophotometric analytics of transition metals. In the following years, its complexation equilibria with transition metal ions interested many scientists.⁴⁰⁻⁴⁶ At the time, modern computer programs were unknown and the stepwise stability constants of the complexes ML_r^{2-r} were red directly or by extrapolation in the Bjerrum plots Z_L vs. $-\log [L^-]$ of the titrated solution. The complexes was generally supposed to be mainly of types ML^+ , ML_2 and ML_3^- , so their stability constants (β_r or K_r) were calculated conventionally over the zero level of hydrogen ions L^- , H_2O and M^{2+} according the equations:



However, in 1961, C. H. and C. F. Liu⁴⁰ published the acidity constants of the complex $Cu(HL)_2^{2+}$ $pK_{a1} = 2.77$ and $pK_{a2} = 6.70$ in aqueous solution at 25 °C. In the following year, Kirson⁴¹ found that the copper(II) complexes polymerize in solutions, where $C_M = C_L$, in the pH range 5–8, so that the

complexation relieves 1.3–1.7 protons per copper(II) ion. By virtue of this observation he proposed the structure of the polymer to be $[\text{HL}-\text{Cu}-\text{O}-\text{Cu}-\text{L}\cdot 2\text{H}_2\text{O}]^+$,^{*} where the ligands HL and L^- should be contacted by an intramolecular hydrogen bridge. It should decompose in the increase of pH to two complexes of $\text{CuL}(\text{OH})\cdot\text{H}_2\text{O}$. At the same time, Hanania and Irvine⁴² determined the acidity constants of complex $\text{Fe}(\text{HL})_3^{2+}$ and the conventional stability constant of FeL_3^- (β_3) in many ionic strengths of 0.001–0.05 M NaCl and NaClO_4 solutions at 17.5–33.5 °C with spectrophotometric studies.

The protonation of the pyridine ring is in pyridine-2-aldoxime ($\log \beta_{101} = 3.56$ at low ionic strength⁴⁷ and 3.590 in 0.1 M NaCl solution¹¹) markedly weaker than in the unsubstituted pyridine ($\log \beta_{101} = 5.25$ at 0 ionic strength⁴⁸ and 5.33 ± 0.01 in NaClO_4 solution at 0.1 M ionic strength).⁴⁹ This is due to the short distance of the electron-withdrawing oxime group from the pyridine ring. The oxime dissociation ($\text{p}K_a = 10.17$) is slightly stronger than in benzaldoxime (10.7) at low ionic strength.⁵⁰

In default modern data programs, the protonation of the complexes ML^+ , ML_2 and ML_3^- was supposed generally to be insignificant and was ignored.^{43–45} The polymerization of the complexes was prevented by using small metal ion concentrations and great ligand excesses.^{45,46} In our laboratory, these problems have been solved by the SUPERQUAD program. By means of this, the stability constants has been determined for pyridine-2-aldoxime complexes of the divalent nickel¹⁰ and copper.¹¹ In this work the series has been continued to the divalent cobalt, zinc and cadmium ions. Series of solutions with different metal ion and ligand concentrations were titrated with an exactly known 0.1 M NaOH solution.

The cobalt(II) complexes are mainly octahedral, although the d^7 electron structure favors high spin tetrahedral coordination with two fully occupied lower e and three half-occupied higher energy t_2 orbitals ($e^4t_2^3$). The octahedral ligand field splitting (Δ_o) is stronger than the tetrahedral one ($\Delta_t = -4/9 \Delta_o$). Therefore, the high spin cobalt(II) complexes are mainly octahedral complexes with $t_{2g}^5e_g^2$ electron structure, but tetrahedral complexes are also known with several ligands. For example, in aqueous solution, there are always some tetrahedral aqua ions $[\text{Co}(\text{H}_2\text{O})_4]^{2+}$ in equilibrium with the octahedral high spin ones $[\text{Co}(\text{H}_2\text{O})_6]^{2+}$.⁵¹

The octahedral cobalt(II) complexes have a low spin state ($t_{2g}^6e_g$) generally, when the energy level difference between t_{2g} and e_g orbitals is $\Delta_o \geq 15\,000\text{ cm}^{-1}$ ($\approx 180\text{ kJ/mole}$).⁵¹ Due to the uneven electron occupation in the e_g orbitals, the octahedral low spin cobalt(II) complexes are Jahn–Teller distorted. Because the only e_g electron is easily lose, the octahedral low spin cobalt(II) complexes are

^{*} Also Orama *et al.*¹¹ have noted that the complexation in a solution with $C_M = C_L = 5\text{ mM}$ relieves 1.3–1.7 (more accurately 1.33–1.67) protons per copper(II) ion in the pH range 5–8. SUPERQUAD calculations have indicated two trimers $\text{Cu}_3\text{L}_3\text{OH}^{2+}$ and $\text{Cu}_3\text{L}_3\text{O}^+$ (or $\text{Cu}_3\text{L}_3(\text{OH})_2^+$) instead of $[\text{HL}-\text{Cu}-\text{O}-\text{Cu}-\text{L}\cdot 2\text{H}_2\text{O}]^+$ and $\text{CuL}(\text{OH})\cdot\text{H}_2\text{O}$.

easily oxidized to the corresponding cobalt(III) complexes. Almost all the cobalt(III) complexes are octahedral with low spin state (t_{2g}^6).⁵¹ Because both of their e_g orbitals are empty and all their t_{2g} orbitals are occupied,⁵² the cobalt(III) complexes are chemically very inert. Their ligand exchange reactions are very slow, and the attainments of equilibria usually take many months.

The increase of pH enhances the amount of low spin cobalt(II) complexes and the oxidation of the cobalt(II) complexes. The oxygen dissolved from the air to the reaction mixture probably act as oxidant. Although nitrogen gas was passed through the solution during all titrations, the complete elimination of oxygen should need a great excess pressure of nitrogen. During and after the NaOH addition, very high local concentrations of OH^- ion and low spin cobalt(II) complexes (CoL_2) can be formed a moment before the complete mixing of the solution. The low spin cobalt(II) complexes can also be oxidized by the oxygen molecules coming with the NaOH to the reaction mixture very quickly to cobalt(III) complexes (no nitrogen was passed through the NaOH solution). Overnight, the solutions could perhaps change a little to browner, but the yellow color was continued. The solutions left to evaporate, but only powder and NaCl crystals were precipitated. Attempts to crystallize complexes for X ray determination of their structures were unsuccessful.

Seven solutions with initial $C_L = 4.86\text{--}8.64$ mM were titrated with 0.1 M NaOH using very strong nitrogen flow and strong magnetic mixing. Five solutions with initial $C_M = 1.82\text{--}8.54$ mM could be titrated to pH 3.8–4.2, but two solutions with very low metal ion concentration ($C_M = 0.182\text{--}0.359$ mM) could be titrated to pH 10–11. The oxidation of low spin cobalt(II) complexes appeared to be strongest in the pH range 5–8, where only 0.02 ml titrant at a time could be added, but oxidation was not marked in the pH range 9–11.

In all solutions, the initial pink color weakened during the titration and gradually changed to an intense yellow. Hartkamp¹⁶ reported a similar observation in that solution of cobalt(II) obtain an intense yellow color. Bolton and Ellin⁴⁴ have noted that the solutions are yellow in low pH ranges and yellow-orange in the high pH ranges. In this work, only the most dilute cobalt(II) solution ($C_M = 0.182$ mM and $C_L = 5.68$ mM) became browner and more yellow-orange towards the end of titration. The yellow color returned at $\text{pH} \approx 3$ by adding of 0.1 M HCl solution to samples of the solution. The other dilute cobalt(II) solution ($C_M = 0.359$ mM and $C_L = 5.63$ mM) kept its yellow color until the end of the titration in the pH range 10–11. This solution was finally titrated by using the addition of only 0.02–0.05 ml NaOH in the pH range 5–8. In this way, the momentary great local OH^- ion concentrations and the oxidation of low spin cobalt(II) complexes were avoided where possible. Overnight, the solutions acquired a brownish tinge but the basic yellow color persisted.

The Z_H curves of only the two most dilute cobalt(II) solutions (Figure 1) exceed the zero level in the pH range 4–5, probing the formation of some deprotonated complexes. The complexations in

these solutions are best described by their Z_L curves (Figure 2) over the zero level L^- , Co^{2+} and H_2O . The Z_L curve of the solution ($C_M = 0.359$ mM, $C_L = 5.63$ mM) hardly exceeds the value 2.0. Its decrease at the end of the titration points to hydrolysis or polymerization of some complexes. Also, Bolton and Ellin⁴⁴ and Burger *et al.*⁴⁵ have found that the Z_L curves of the cobalt(II) solutions have the limiting value 2.0. Burger *et al.*⁴⁵ confirmed the composition of ML_2 for the cobalt(II), copper(II) and zinc(II) complexes from chloroform extracts with elemental analyses (C, H, N and metal). Electrophoretic measurements have shown that these complexes are uncharged but the formed iron(II) and nickel(II) complexes are negatively charged (ML_3^-).⁴⁵ The Z_L curve of the most dilute cobalt(II) solution ($C_M = 0.182$ mM, $C_L = 5.68$ mM) at the end of titration is clearly higher than the latter curve, which can be due to the fact that a remarkable part of the cobalt(II) complexes should have been oxidized. Therefore, the curve of this solution is marked with a dashed line.

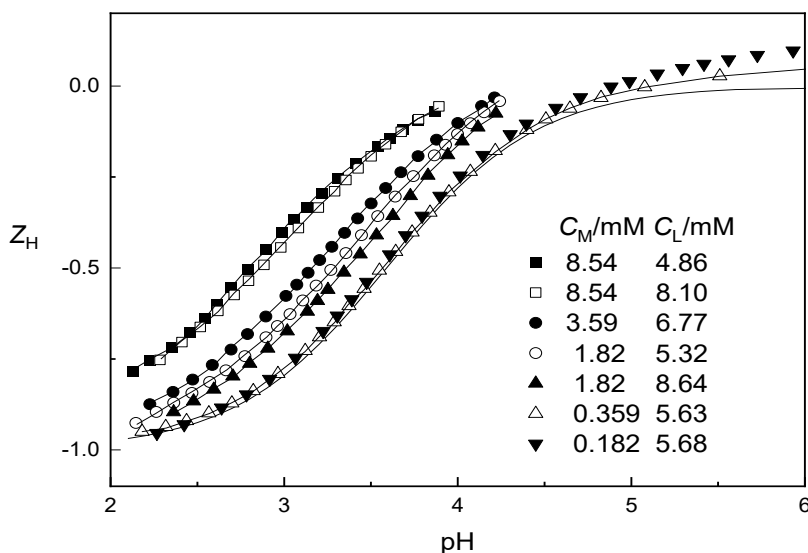


Figure 1. Part of the experimental data plotted as Z_H curves vs. pH for cobalt(II) complex formation with pyridine-2-aldoxime HL. The full lines have been calculated using sets of proposed stability constants in Table 1. The lowest line refers to the ligand alone.

In the calculation of the stability constants of the complexes with the SUPERQUAD program, the pH range of the most dilute cobalt(II) solution was limited for the apparent oxidations under 5.6. The inaccuracies of the NaOH additions and the potential were assumed $\sigma_V = \pm 0.02$ ml and $\sigma_E = \pm 0.1$ mV. The pH range of the other dilute cobalt(II) solution was limited to 8.66, where the cobalt(II) ion was

already completely CoL_2 . The SUPERQUAD program rejected the stability constants β_{-111} , β_{013} , β_{-213} and β_{-313} also by using wider pH ranges. No polynuclear complexes could be observed. The stability constants of Co(HL)^{2+} , Co(HL)_2^{2+} , Co(HL)L^+ , CoL_2 and $\text{Co(HL)}_2\text{L}^+$ are given in Table 1 with the previously determined stability constants of another pyridine-2-aldoxime complexes. The distribution curves of two solutions are given in Figure 3. The computer program SPE⁵³ was used in these calculations.

$\text{Co(HL)}_2\text{L}^+$ appears in the pH range 3.0–3.5 (Figure 3), but its parent complex Co(HL)_3^{2+} never reaches measurable concentrations. This means for Co(HL)_3^{2+} $\text{p}K_{a1} \leq 3.0$ –3.5 and $\log\beta_{013} \leq 6.0$ –6.5. With the increase of pH $\text{Co(HL)}_2\text{L}^+$ is completely displaced by CoL_2 and the deprotonated complexes Co(HL)L_2 and CoL_3^- never reach measurable concentrations. Burger *et al.*⁴⁵ have proved with qualitative NMR measurements⁵⁴ that the pyridine-2-aldoxime complex CoL_2 is less paramagnetic than the aqua Co^{2+} ion, FeL_3^- is completely diamagnetic, and NiL_3^- is equally paramagnetic than the aqua Ni^{2+} ion in 10^{-2} M aqueous solution (at $\text{pH} \approx 8$). The results show that CoL_2 and FeL_3^- are low spin but NiL_3^- is high spin and octahedral. Krause and Busch⁵⁵ prepared and characterized several solid nickel(II), palladium(II), and platinum(II) complexes with pyridine-2-aldoxime. All of the solid nickel(II) complexes, including $[\text{Ni(HL)}_3]\text{I}_2$, $[\text{Ni(HL)}_2\text{Cl}_2]$, $[\text{Ni(HL)L}]\text{I}$, and $[\text{NiL}_2]$, are paramagnetic with magnetic moments 3.01–3.56 BM. The palladium(II) and platinum(II) complexes $[\text{Pd(HL)L}]\text{Cl}$, $[\text{PdL}_2]$, and $[\text{PtL}_2]$ are square-planar and diamagnetic. Pd(HL)_2^{2+} is a strong diprotic acid.⁵⁵

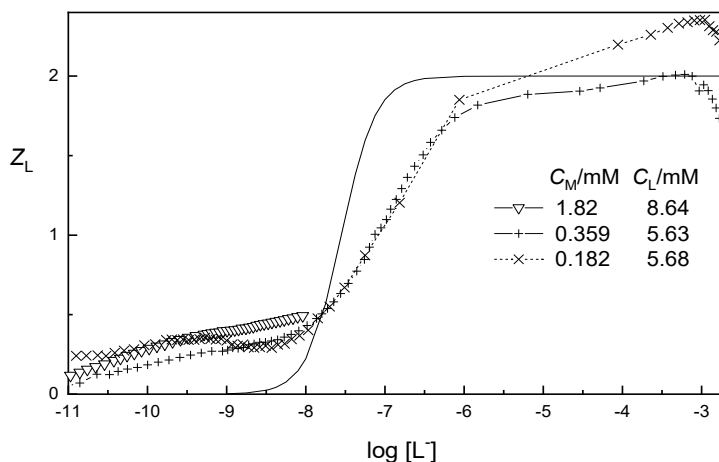


Figure 2. Part of the experimental data plotted as Z_L curves vs. $\log [L^-]$ for cobalt(II) complex formation with pyridine-2-aldoximate ion L^- and the curve calculated according the stability constant $\log \beta_2 = 15.1$ of the complex CoL_2 (—).

Table 1. Proposed formulas and stability constants of pyridine-2-aldoxime complexes relating to reaction $pH^+ + qM^{2+} + rHL \rightleftharpoons (H^+)_p(M^{2+})_q(HL)_r$ at 25 °C.^a

| Proposed | | | | $\log \beta_{pqr} \pm 3\sigma$ | | | | | |
|-----------------------------|----------|----------|-------------------------------------------------------------------------------------------------------|--------------------------------|------------|---------------------|------------|-------------|-------------|
| <i>p</i> | <i>q</i> | <i>r</i> | formula | M = Fe ^b | M = Co | M = Ni ^c | M = Cu | M = Zn | M = Cd |
| 0 | 1 | 1 | M(HL) ²⁺ | | 2.85±0.02 | 4.19±0.02 | 3.93±0.09 | 1.90±0.02 | 2.02±0.02 |
| 0 | 1 | 2 | M(HL) ₂ ²⁺ | | 5.04±0.07 | 7.62±0.02 | 7.48±0.09 | | |
| 0 | 1 | 3 | M(HL) ₃ ²⁺ | 6 | | 10.42±0.02 | | | |
| -1 | 1 | 1 | ML ⁺ | | | | 0.90±0.09 | -4.81±0.29 | -5.26±0.12 |
| -1 | 1 | 2 | M(HL)L ⁺ | | 0.43±0.29 | 2.80±0.05 | 5.43±0.04 | -2.50±0.24 | -2.97±0.11 |
| -2 | 1 | 2 | ML ₂ | | -4.92±0.23 | -3.68±0.06 | -1.53±0.04 | -9.44±0.04 | -10.93±0.03 |
| -1 | 1 | 3 | M(HL) ₂ L ⁺ | 5.02 | 3.14±0.18 | 5.58±0.04 | | | |
| -2 | 1 | 3 | M(HL)L ₂ | 1.57 | | -0.70±0.05 | | | |
| -3 | 1 | 3 | ML ₃ ⁻ | -5.45 | | -8.42±0.04 | | -17.09±0.18 | -18.35±0.13 |
| -2 | 2 | 2 | M ₂ L ₂ ²⁺ | | | | | -6.76±0.27 | -8.02±0.17 |
| -3 | 2 | 2 | M ₂ L ₂ OH ⁺ | | | | | -13.30±0.04 | -16.66±0.08 |
| -4 | 2 | 2 | M ₂ L ₂ (OH) ₂ | | | | | -22.66±0.20 | |
| -4 | 3 | 3 | M ₃ L ₃ OH ²⁺ | | | | 5.57±0.12 | | |
| -5 | 3 | 3 | M ₃ L ₃ O ⁺ (or M ₃ L ₃ (OH) ₂) | | | | -0.97±0.12 | | |
| Number of points/titrations | | | | | 297/7 | 145/9 | 360/12 | 413/8 | 465/8 |
| χ^2 | | | | | 39.5 | 47 | 48.6 | 53.3 | 45.3 |
| <i>s</i> | | | | | 1.59 | 2.1 | 2.75 | 2.42 | 1.89 |
| Ref. | | | | 30 | II | 10 | 11 | I | I |

^a In aqueous 0.1 M Na(Cl) solution unless advised to the contrary. The protonation and acidity constants of the ligand HL in the used solutions are given in Table 2. ^b At ionic strength 0.045 M (NaCl or NaClO₄), where the conventional stability constant of FeL₃⁻ $\log \beta_3 = 24.85 \pm 0.09$ according to the equation (31), the acidity constant of the free ligand HL $p\beta_{-101} = 10.10$ and those of Fe(HL)₃²⁺ $pK_{a1} \approx 1$, $pK_{a2} = 3.45$ and $pK_{a3} = 7.02$. The listed stability constants were calculated according the following equations: $\log \beta_{-313} = \log \beta_3 - 3p\beta_{-101}$, $\log \beta_{-213} = \log \beta_{-313} + pK_{a3}$, $\log \beta_{-113} = \log \beta_{-213} + pK_{a2}$ and $\log \beta_{013} = \log \beta_{-113} + pK_{a1}$. ^c In aqueous 1.0 M Na(Cl) solution.

The octahedral low spin cobalt(II) complexes are Jahn–Teller distorted due to the uneven e_g electron occupation ($t_{2g}^6 e_g$). Therefore, in CoL₂, both of the oximato ligands are located in the *xy* plane and the possible aqua ligands in the *z* axis. It is possible that CoL₂ is at least partly square planar or square-pyramidal in aqueous solution. The comparable dimethylglyoxime complex Co(dmg)₂ is square-planar in solid state, but is able to form halide and pseudohalide mixed complexes Co(Hdmg)(dmg)X_{*n*}^{1-*n*} (*n* = 1 or 2) with increasing acidity $I^- < Br^- < Cl^- < SCN^-$ ($pK_a \approx 6.2$) < Co(Hdmg)(dmg)⁺ ($pK_a \approx 4.4$) < SeCN⁻ in aqueous solution.^{56,57} Their stability constants calculated according the equation $\beta_n^X = [Co(Hdmg)(dmg)X_n^{1-n}][Co(Hdmg)(dmg)]^{-1}[X^-]^{-n}$ (without modern data programs) increase with increasing concentration of the present alkali metal ion and in the order

$\text{Rb}^+ < \text{K}^+ < \text{Na}^+ < \text{Li}^+$, with reducing water activity (a). For example, the stability constant ($\log \beta_2^X$) of $\text{Co}(\text{Hdmg})(\text{dmg})\text{Cl}_2^-$ is 0.12 ± 0.04 in RbCl solution ($a = 0.90$), 0.4 ± 0.1 in NaCl solution ($a = 0.885$), and 0.9 ± 0.1 in LiCl solution ($a = 0.86$).⁵⁶ In potassium halide (KX) solution the stability of

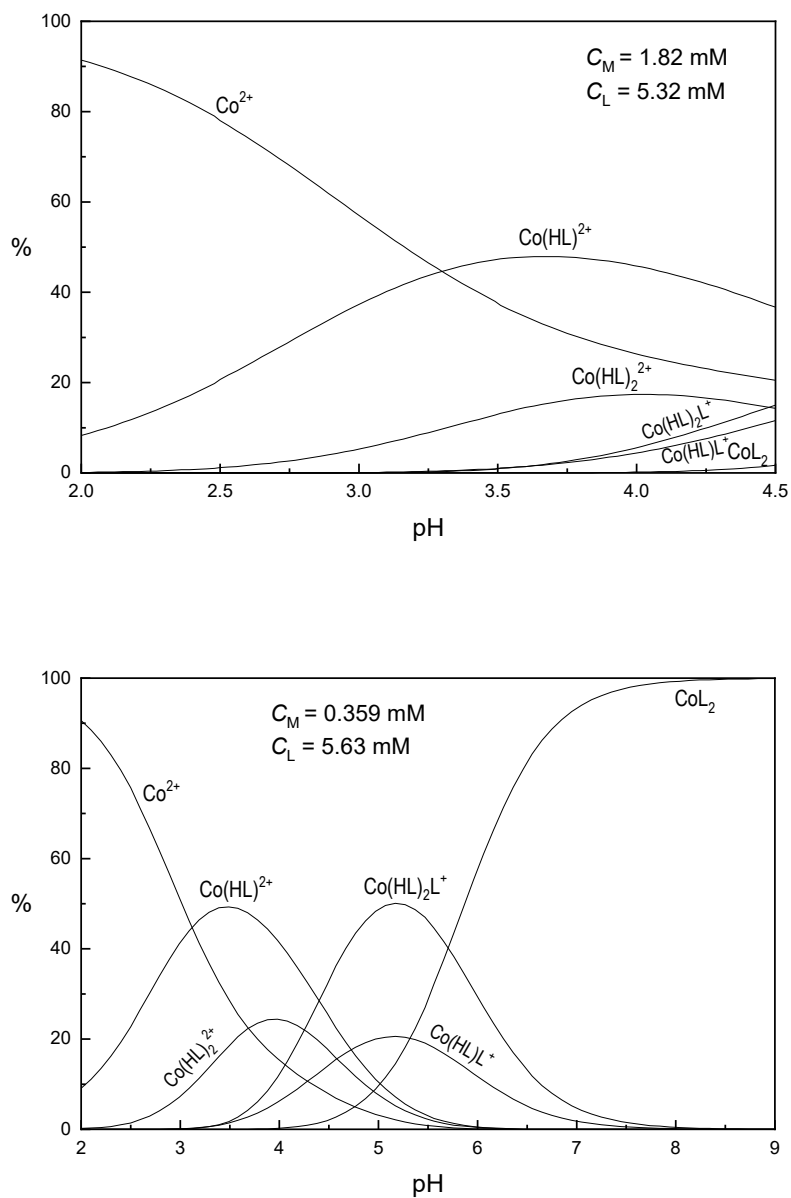


Figure 3. Examples of the concentration distribution of cobalt(II) species with pyridine-2-aldoxime.

Table 2. Conventional stability constants^a of deprotonated pyridine-2-aldoxime complexes compared with β_{011} , β_{012} (see Table 1) and stepwise protonation constants^b of the ligand L^- in aqueous solution at 25 °C.

| M^{2+} | $\log \beta_{011}$ | $\log \beta_{012}$ | $\log \beta_1$ | $\log \beta_{11}^c$ | $\log \beta_2$ | $\log \beta_3$ | Medium ^d | Method ^e | Ref. |
|-----------|--------------------|--------------------|----------------|---------------------|----------------|----------------|-----------------------------|---------------------|------|
| H^+ | 3.56 | | 10.17 | | | | <0.001 M | sp | 47 |
| | 3.52 | | 10.10 | | | | 0.045 M (NaCl) ^f | sp | 42 |
| | 3.590 | | 10.01 | | | | 0.1 M Na(Cl) | gl | 11 |
| | 3.4 | | 10.0 | | | | 0.3 M NaClO ₄ | sp | 45 |
| | 3.865 | | 9.922 | | | | 1.0 M Na(Cl) | gl | 10 |
| Mn^{2+} | | | 5.2±0.2 | | 9.1±0.2 | | 0.3 M (NaClO ₄) | gl | 45 |
| Fe^{2+} | | | | | | 24.85±0.09 | 0.045 M (NaCl) ^f | sp | 42 |
| | | | 8.4 | | 16.1 | 21.2 | <0.01 M | gl | 43 |
| | | | 9.4 | | 17.4 | 22.5 | 0.1 M (KNO ₃) | gl ^g | 44 |
| Fe^{3+} | | | 11.4 | | 21.7 | 29.1 | 0.1 M (KNO ₃) | gl ^g | 44 |
| Co^{2+} | 2.85 | 5.04 | | 10.44 | 15.1 | | 0.1 M Na(Cl) | gl | 11 |
| | | | 8.8±0.1 | | 17.6±0.1 | | 0.3 M (NaClO ₄) | gl | 45 |
| | | | 8.6±0.2 | | 17.2±0.2 | | 0.3 M NaClO ₄ | sp | 45 |
| | | | 9.6 | | 18.3 | | 0.1 M (KNO ₃) | gl ^g | 44 |
| Ni^{2+} | 4.19 | 7.62 | | 12.72 | 16.16 | 21.35 | 1.0 M Na(Cl) | gl | 10 |
| | | | 9.4±0.2 | | 16.5 | 22.0±0.4 | 0.3 M (NaClO ₄) | gl | 45 |
| | | | 8.1 | | 14.2 | 21.2 | 0.1 M (KNO ₃) | gl ^g | 44 |
| Cu^+ | | | | | 14.48 | | ? | pol ^h | 40 |
| | | 11.05 | | | 14.4 | | 0.5 M (NaNO ₃) | pol ⁱ | 46 |
| Cu^{2+} | 3.93 | 7.48 | 10.91 | 15.44 | 18.49 | | 0.1 M Na(Cl) | gl | 11 |
| | | 8.1 | | 15.3 | 18.68 | | ? | pol ^{h,j} | 40 |
| | | 8.3 | | 15.85 | 18.6 | | 0.5 M (NaNO ₃) | pol ⁱ | 46 |
| | | | 10.8 | | 16.8 | | 0.1 M (KNO ₃) | gl ^g | 44 |
| | | | 8.9 | | 14.55 | | <0.02 M | gl | 41 |
| Zn^{2+} | 1.90 | | 5.2±0.3 | 7.51 | 10.58 | 12.94 | 0.1 M Na(Cl) | gl | 1 |
| | | | 5.8±0.1 | | 11.1±0.1 | | 0.3 M (NaClO ₄) | gl | 45 |
| | | | 5.5 | | 10.8 | | 0.1 M (KNO ₃) | gl ^g | 44 |
| Cd^{2+} | 2.02 | | 4.75 | 7.04 | 9.09 | 11.68 | 0.1 M Na(Cl) | gl | 1 |
| | | | 5.2 | | 9.6 | | 0.1 M (KNO ₃) | gl ^g | 44 |
| Hg^{2+} | | | 6.5 | | 12.2 | | 0.1 M (KNO ₃) | gl ^g | 44 |

^a $\log \beta_r = \log \beta_{-r1r} + r p\beta_{-101}$, where $p\beta_{-101}$ is the acidity constant of HL (= the stability constant $\log \beta_1$ of the complex ML with $M^+ = H^+$) in the correspondent medium. ^b Indicated as stability constants of complexes HL (see footnote a) and $H(HL)^+$ ($\log \beta_{011} = \log \beta_{101}$ of H_2L^+). ^c The conventional stability constant of $M(HL)L^+$ ($= \log \beta_{-112} + p\beta_{-101}$). ^d Or its ionic strength (the background electrolyte in parentheses). ^e gl = glass electrode, sp = spectrophotometry, pol = polarography. ^f Or NaClO₄. ^g At 24(±0.5) °C. ^h The given $\log \beta_2$ has been determined polarographically in 0.2 M phosphate buffer solution at pH 12. ⁱ At 20 °C. ^j The acidity constants of HL ($p\beta_{-101} = 10.04$) and $Cu(HL)_2^{2+}$ ($pK_{a1} = 2.77$ and $pK_{a2} = 6.70$) have been determined with glass electrode in dilute aqueous solution (≤ 0.01 M $CuCl_2$). By using these values, the given $\log \beta_{012} = \log \beta_2 - 2p\beta_{-101} + pK_{a1} + pK_{a2}$ and $\log \beta_{11} = \log \beta_2 - p\beta_{-101} + pK_{a2}$ have been calculated.

the mixed complexes increases in the order $\text{Cl}^- < \text{Br}^-$ ($\log \beta_2^X = 0.60 \pm 0.10$) $< \text{I}^-$ (4.0 ± 0.1) $< \text{SCN}^-$ (7.8 ± 0.3) $< \text{Co}(\text{dmg})_2(\text{SeCN})_2^{2-}$ (8.0 ± 0.2). The size and the polarizability of the anions, the π acceptor capability of the ligands and the softness of the Lewis bases⁵⁸ increase in the same order. Among the corresponding iron(II) complexes, the stability constants could be determined only for $\text{Fe}(\text{dmg})_2\text{SCN}^-$ ($\log \beta_1^X = 0.35 \pm 0.05$), $\text{Fe}(\text{dmg})_2(\text{SCN})_2^{2-}$ ($\log \beta_2^X = 1.30 \pm 0.10$), and $\text{Fe}(\text{dmg})_2(\text{SeCN})_2^{2-}$ ($\log \beta_2^X = 3.43 \pm 0.07$, $K_2^X \gg K_1^X$). Qualitative NMR measurements⁵⁴ indicate that $\text{Co}(\text{dmg})_2$, $\text{Fe}(\text{dmg})_2$, and all the mixed complexes are low spin in aqueous solution.⁵⁶ The monohalide mixed complexes are softer Lewis acids and better π donors than $\text{Co}(\text{dmg})_2$ and $\text{Fe}(\text{dmg})_2$. For this reason, the stepwise stability order of the mixed complexes is reversed: $K_1^X < K_2^X$, when K_1^X is small or the water activity is high. The decrease of the water activity in increasing background electrolyte concentration increases the stability of the monohalide mixed complexes in particular. For example, the stepwise stability constants of the mixed iodide cobalt(II) complexes $\text{Co}(\text{Hdmg})(\text{dmg})\text{I}_n^{1-n}$ are in 1 M NaClO_4 solution ($a = 0.966$) $\log K_1^X = 1.38$ and $\log K_2^X = 1.98$, in 4 M NaClO_4 solution ($a = 0.849$) $\log K_1^X = \log K_2^X = 2.40$, and in 6 M NaClO_4 solution ($a = 0.763$) $\log K_1^X = 3.86$ and $\log K_2^X = 2.46$.⁵⁷ Apparently, the decrease of the water activity facilitates the dissociation of the aqua ligands and the coordination of a halide ligand to the z axis of $\text{Co}(\text{dmg})_2$. Jahn–Teller distortion weakens the stability of the dihalide mixed complexes. The coordination of a halide or SCN^- ion enhances the softness of the central ion as Lewis acid and leads to protonation of the mixed cobalt(II) complexes, because the uncharged dimethylglyoxime (Hdmg) is a softer Lewis base than the negatively charged dimethylglyoximate ion (dmg^-). The iron(II) ion is a clearly harder Lewis acid and the iron(II) mixed complexes are much less stable and not protonated.

The low spin iron(II) and cobalt(II) ions are markedly smaller (ionic radii 0.61 and 0.65 Å, respectively) than the high spin nickel(II) ion (0.690 Å).⁵⁹ The smaller size of the metal ion strengthens the metal–ligand bonds, which weakens the O–H bonds in the oxime groups. Thus, the pyridine-2-aldoxime complexes $\text{Co}(\text{HL})_3^{2+}$ ($\text{p}K_{a1} \leq 3.0\text{--}3.5$), $\text{Fe}(\text{HL})_3^{2+}$, $\text{Fe}(\text{HL})_2\text{L}^+$, and $\text{Fe}(\text{HL})\text{L}_2$ are much stronger acids than the corresponding nickel(II) complexes (Table 1). It is also clear that $\text{Co}(\text{HL})_2\text{L}^+$, $\text{Fe}(\text{HL})_2\text{L}^+$ and $\text{Fe}(\text{HL})\text{L}_2$ are low spin. $\text{Fe}(\text{HL})_3^{2+}$ ($\log \beta_{013} \approx 6$), $\text{Co}(\text{HL})_3^{2+}$ ($\leq 6.0\text{--}6.5$), and $\text{Ni}(\text{HL})_3^{2+}$ (10.42) follow Irving–Williams⁶⁰ stability order, and stepwise stability order of the cobalt(II) complexes is normal: $K_1 > K_2 > K_3$. At least $\text{Co}(\text{HL})_3^{2+}$, $\text{Co}(\text{HL})_2^{2+}$, $\text{Fe}(\text{HL})_2^{2+}$, and $\text{Fe}(\text{HL})_2^{2+}$ are high spin. In $\text{Co}(\text{HL})_3^{2+}$, the low spin state is possible, if the Jahn–Teller distortion cancels the stability enhancement by spin pairing. The stability constants of the octahedral high spin iron(II) complexes ($t_{2g}^4 e_g^2$) difficult to determine, because they are easily oxidized to octahedral high spin iron(III) complexes, where all the d orbitals are equally occupied ($t_{2g}^3 e_g^2$).

The formation of zinc(II) complexes was possible to research with sufficient ligand excess in the pH range 9–10, but with low $\text{C}_L:\text{C}_M$ ratios (≤ 1.1), a precipitate was formed already in the pH range

7.0–7.5. The Z_H curves with $C_L:C_M = 2-4$ (Figure 4) revealed a weak inflection point at *ca.* $C_H \approx -1.7 C_M$. Although this may suggest the presence of a trinuclear species with $p:q = -5:3$, such as $Zn_3L_3O^+$ or $Zn_3L_3(OH)_2^+$, SUPERQUAD calculations led to much better χ^2 and s for a set of mono- and binuclear complexes $Zn(HL)^{2+}$, $Zn(HL)L^+$, ZnL_2 , $Zn_2L_2^{2+}$, $Zn_2L_2OH^+$, and $Zn_2L_2(OH)_2$ than for any single tri- or tetranuclear species. The summation of -322 and -212 gives the same $p:q$ ratio of $-5:3$. The analysis, based on 413 titration points from eight titrations, terminated at $\chi^2 = 53.3$ and $s = 2.42$. This can be considered to provide a fairly good explanation of the data (s values lower than 3 are generally regarded as acceptable for comparable systems).⁶¹ The proposed complexes with their stability constants are given in Table 1. Distribution curves of the complexes are in Figure 5.

Zinc(II) ion has d^{10} electronic structure, which allows no ligand field stabilization energy. The complexes $Zn(HL)^{2+}$, $Zn(HL)L^+$, and ZnL_2 are clearly less stable than the corresponding cobalt(II) complexes. The aqua Zn^{2+} ion is precipitated in the pH range 7–8 as zinc hydroxide $Zn(OH)_2$. The pK_s value of the amorphous $Zn(OH)_2$ at 25 °C is in 0.2 M KNO_3 and $NaClO_4$ solutions 14.70 ± 0.03 and at zero ionic strength 15.52 ± 0.03 .⁶²

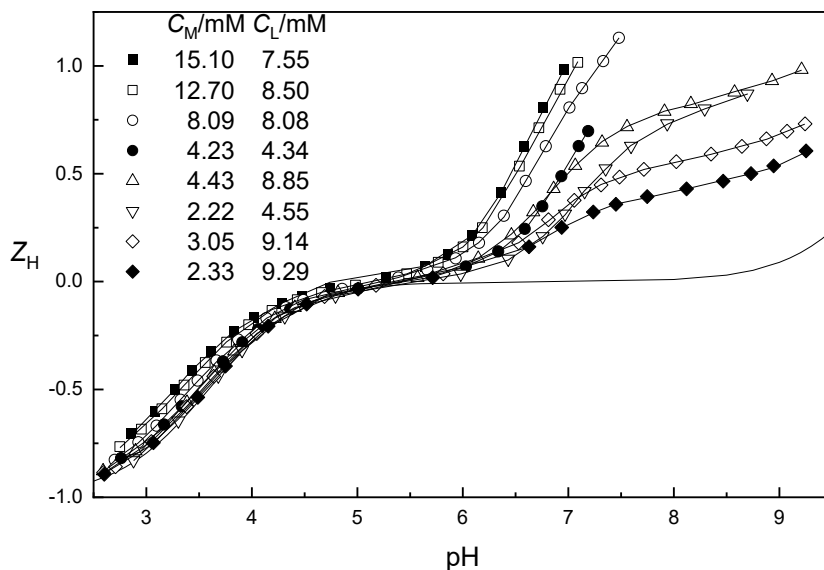


Figure 4. Part of the experimental data plotted as Z_H curves vs. pH for zinc(II) complex formation with pyridine-2-aldoxime HL. The full lines have been calculated using sets of proposed stability constants in Table 1. The lowest line refers to the ligand alone.

Cadmium(II) hydroxide $Cd(OH)_2$ is more soluble⁶³ than $Zn(OH)_2$ and allows titrating the solutions of low $C_L:C_M$ ratios to pH range 8.0–8.5 and in the presence of twofold ligand excess to pH range 9–

10. The inflection points of the Z_H curves (Figure 6) in the pH range 7–10 are clearly weaker than those of zinc(II) ion probing that the polymerization of cadmium(II) complexes is weaker than that of the zinc(II) complexes. Due to its larger ionic radius⁵⁹ (0.95 Å) and d^{10} electronic structure, the cadmium(II) ion is clearly a soft Lewis acid, which more readily binds uncharged nitrogen donors through π -bonds than negatively charged oxygen donors through electrostatic forces. The smaller zinc(II) ion (ionic radius⁵⁹ 0.740 Å) has more properties of hard Lewis acids, more readily binding negatively charged ligands through electrostatic forces.

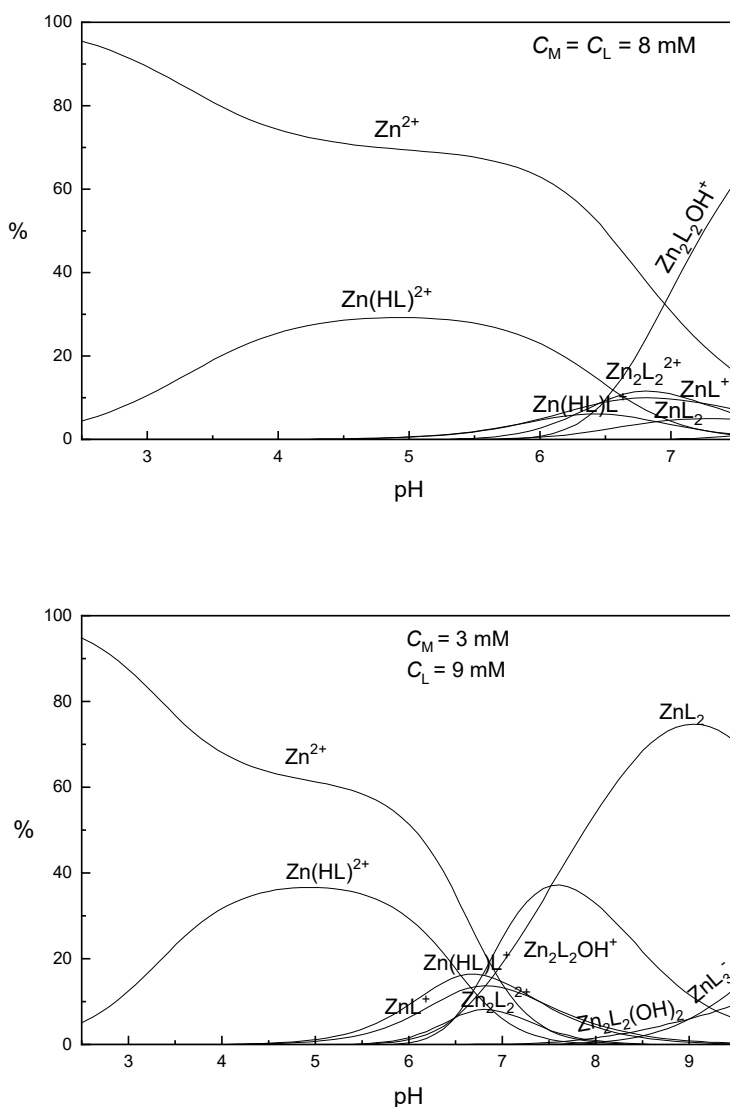


Figure 5. Examples of the concentration distribution of zinc(II) species with pyridine-2-aldoxime.

SUPERQUAD calculations show that $\text{Cd}(\text{HL})^{2+}$ ($\log \beta_{011} = 2.02$) is more stable than $\text{Zn}(\text{HL})^{2+}$ (1.90) but less stable than the other complexes of type $\text{M}(\text{HL})^{2+}$ formed by the metal ions of the first transition series (Table 2). The other cadmium(II) complexes are less stable and less acidic than the corresponding zinc(II) complexes (Table 1). Distribution curves of the cadmium(II) complexes are shown in Figure 7.

The stability constants calculated before the discovery of modern computer programs are listed in Table 2. These results are based to the supposition that pyridine-2-aldoxime should mainly form complexes according to equation (31). It is now known that the oximes form also complexes $\text{H}_p\text{M}(\text{HL})_r^{2+p}$, where $p \neq -r$. If such complexes are present in the solution, the equation (20) is no longer valid, and Z_L does not give the average of r in the present complexes of types ML_r^{2-r} .

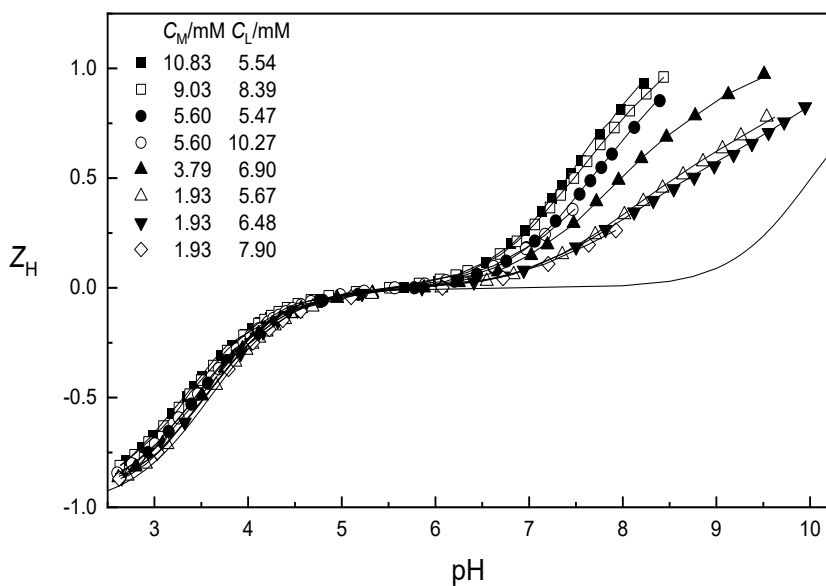


Figure 6. Part of the experimental data plotted as Z_H curves vs. pH for cadmium(II) complex formation with pyridine-2-aldoxime HL. The full lines have been calculated using sets of proposed stability constants in Table 1. The lowest line refers to the ligand alone.

The deprotonated mono complexes, ZnL^+ , CdL^+ , and CuL^+ coordinate a free uncharged pyridine-2-aldoxime ligand HL according the following reaction



clearly more strongly than their parent aqua ions do ($\beta_{-112}/\beta_{-111} > \beta_{011}$). The formed complexes

$M(HL)L^+$ are stabilized by intramolecular hydrogen bonding ($=N-O-H\cdots O-N=$) between the *cis* oriented oxime and oximate oxygen atoms and the resultant extra chelate ring observed in many other similar compounds.^{1,4,9,40,64-66}

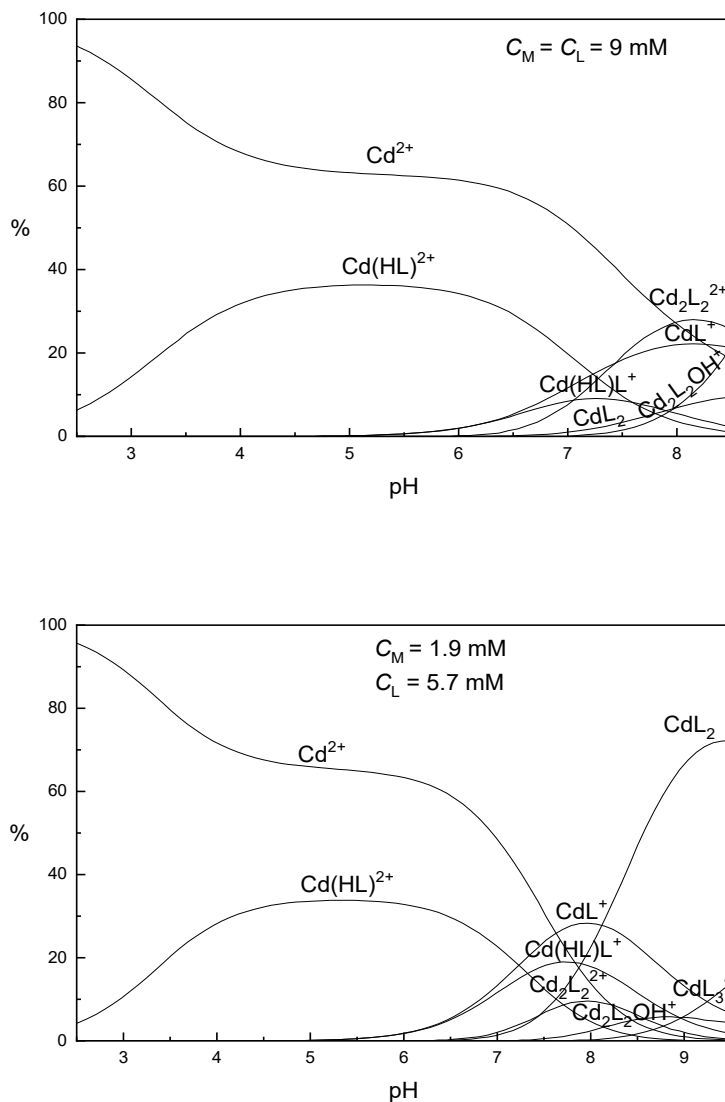


Figure 7. Examples of the concentration distribution of cadmium(II) species with pyridine-2-aldoxime.

C. F. and C. H. Liu⁶⁵ have observed both *cis* and *trans* oriented oximate groups in $[PtL_2] \cdot 2H_2O$. In 0.1 M HCl, *cis*- $[PtL_2] \cdot 2H_2O$ dissolves instantly but *trans*- $[PtL_2] \cdot 2H_2O$ only upon prolonged heating. Both of the dissolved *cis* and *trans* isomers can be isolated from the solution as bromide, chloride or

PtCl_4^{2-} salts of only *cis*-Pt(HL)L⁺ and from the neutralized solution only as *cis*-[PtL₂] \cdot 2H₂O. From these results, it seems that the intramolecular hydrogen bonding and the extra chelate ring tend to stabilize the *cis* configuration of Pt(HL)L⁺ and serve to isomerize *trans*-[PtL₂] \cdot 2H₂O to *cis* through the formation of the intermediate *cis*-Pt(HL)L⁺. However, *cis*-[PtL₂] \cdot 2H₂O is converted to *trans* by heating at 140 °C or by heating in 1 M HCl followed by neutralization of the solution.⁶⁵ The fact that the conversion of *cis*-[PtL₂] \cdot 2H₂O to *trans* requires more concentrated acid seems to indicate that both oximate groups may be protonated and that the resulting *cis*-Pt(HL)₂²⁺ loses the stabilizing influence of the extra chelate ring and rearranges to the *trans* configuration. The crystal structure of *trans*-[PtL₂] \cdot 2H₂O consists of linear chains of roughly square-planar PtL₂ units, which are hydrogen bonded through the oximate oxygen atom to water molecules.⁶⁷

In [PdL₂] \cdot 2H₂O only *trans* oriented oximate groups have been found.⁶⁶ At room temperature, it dissolves instantly in 0.1 M HCl, from which it has been isolated as PdCl₄²⁻, Cl⁻, and NO₃⁻ salts of *cis*-Pd(HL)L⁺. From the neutralized solution *cis*-Pd(HL)L⁺ is isolated very quickly as *trans*-[PdL₂] \cdot 2H₂O.⁶⁶ The palladium(II) complexes are labile and their isomerization and substitution reactions are rapid, but the platinum(II) complexes are inert and their isomerization and substitution reactions are very slow.⁵² For example, in aqueous solution at 25 °C, the first order water exchange constant k_{ex} of Pt(H₂O)₄²⁺ is $3.9 \cdot 10^{-4} \text{ s}^{-1}$,⁶⁸ but that of Pd(H₂O)₄²⁺ is 560 s^{-1} ,⁶⁹ and those of Fe²⁺, Co²⁺, Ni²⁺, Cu²⁺, Zn²⁺, and Cd²⁺ aqua ions are 10^4 – 10^{10} s^{-1} .⁷⁰ Also, these metal ions form labile complexes in aqueous solution.⁵²

In the crystalline [M(HL)₂(OOCCH₃)₂] complexes, where M = Ni,⁷¹ Zn,⁷² or Cd,⁷³ the acetate ligands are monodentately coordinated in the angles: O–Ni–O 89.56°,⁷¹ O–Zn–O 92.39°,⁷² and O–Cd–O 95.55°.⁷³ The oxime groups are *trans* oriented in the angles N_{ox}–Ni–N_{ox} 166.55°, N_{ox}–Zn–N_{ox} 158.75°, and N_{ox}–Cd–N_{ox} 155.72° forming intramolecular hydrogen bridges with their adjacent uncoordinated acetate oxygens N–O–H \cdots OOCCH₃. The H \cdots O distance are 1.65–1.69 Å and the O \cdots O distances are 2.463–2.545 Å.^{71–73}

In the crystalline Ni(HL)₂Cl₂, the oxime groups are *trans* oriented in the N–Ni–N angle of 171.73° and the pyridine nitrogens *cis* oriented in the N–Ni–N angle of 95.26°. The Cl–Ni–Cl angle is 92.83°.⁷⁴ The oxime hydrogens form weak intramolecular hydrogen bridges with their adjacent chloride ligands (the H \cdots Cl distances are 2.10 and 2.50 Å). The lengths of the Ni–NOH bonds are 2.039 and 2.048 Å. A similar structure in aqueous Ni(HL)₂(H₂O)₂²⁺ allows the formation of Ni(HL)₃²⁺ with *mer* oriented oxime groups. The crystalline octahedral tris complex Ni(HL)₂ \cdot 6½H₂O with *mer* oriented oxime and oximate groups is dimeric; the two parts of the molecule being together at the oxime ends by two hydrogen bridges N–O–H \cdots O–N.¹⁰ The non-bridged N–O⁻ bonds (1.339 Å) are shorter than the bridged N–O⁻ bonds (1.354 Å), which are shorter than the N–OH bonds

(1.380 Å). The deprotonation of the oxime group NOH of ligand HL to negatively charged oximate NO⁻ group shortens clearly the N—O bonds and would also increase the electrostatic attraction forces between the metal ion and the NO group. Despite this, both the bridged Ni—NO⁻ (2.100 Å) and the non-bridged Ni—NO⁻ bonds (2.077 Å) are longer than the Ni—NOH bonds (2.062 Å). The bridged and non-bridged Ni—NO⁻ bonds are *trans* oriented at N—Ni—N angle of 170.9°, ¹⁰ and the structural *trans* effects⁷⁵ of the oximate groups weaken (lengthen) the Ni—N bonds *trans* to them. Apparently, the hydrogen bonding and protonation weaken the structural *trans* effect of the —NO⁻ group. In aqueous solution, Ni(HL)L₂ is probably not dimeric and the oxime and oximate groups are hydrogen bonded with their adjacent water molecules. The Ni—N bonds are obviously not as long in the solution as in the solid state. The *trans* effects of the ligands or their coordination groups are in solution kinetic and labilize the M—N bonds that are *trans* to them. In octahedral complexes of divalent metal ions, the substitution reactions are generally dissociatively activated, and there is often a close correlation between the structural and kinetic *trans* effects.⁷⁵

As in the crystalline Ni(HL)₂Cl₂ the oxime groups are apparently *trans* oriented also in the aqueous Ni(HL)₂(H₂O)₂²⁺ and Co(HL)₂(H₂O)₂²⁺. The dissociation of only one aqua ligand allows the rearrangements of HL ligands to a plane with *cis* oriented oxime groups and the deprotonation of the complexes to Ni(HL)L⁺ and Co(HL)L⁺ in the pH range 3–6 (Figure 3) stabilized by the intramolecular hydrogen bonding O—H···⁻O and the extra chelate ring. The about equal acidity constants of Co(HL)₂²⁺ (pK_{a1} = 4.61) and Ni(HL)₂²⁺ (4.82) calculated as stability differences log (β₀₁₂/β₋₁₁₂) prove that Co(HL)L⁺ is high spin. When *cis*-Co(HL)L⁺ is deprotonated to *cis*-CoL₂, the repulsion forces between the adjacent negatively charged oximate oxygens very quickly cause its isomerization via tetrahedral CoL₂ to square planar or octahedral low spin *trans*-CoL₂. The formation of CoL₂ is also possible through deprotonation of *trans*-Co(HL)₂²⁺ via *trans*-Co(HL)L⁺ in the pH range 4–5, where CoL₂ appears (Figure 3). The SUPERQUAD program is unable to distinguish between isomers of the same *pqr* combination. It calculates for Co(HL)L⁺ only one stability constant according to equation (11) using the concentration [Co(HL)L⁺] = Σ[*cis*-Co(HL)L⁺] + Σ[*trans*-Co(HL)L⁺]. However, *trans*-Co(HL)L⁺ is undoubtedly much less stable and a stronger acid than its *cis* isomer and probably a stronger acid than its parent complex *trans*-Co(HL)₂²⁺ (K_{a2} > K_{a1} or pK_{a2} < pK_{a1}), since they are both high spin but CoL₂ is low spin. CoL⁺ and NiL⁺ have not been observed. Both Co(HL)₂²⁺ and Ni(HL)₂²⁺ disappear in the pH range 5.5–6.0 (Figure 3 and ref. 10). If their pK_a values are 6–7, CoL⁺ and NiL⁺ never reach measurable concentrations. Thus, the formations of Co(HL)L⁺ and Ni(HL)L⁺ according reaction (33) are very small.

The tetrahedral aqueous Co(HL)₂²⁺ is able to form Co(HL)₃²⁺ with both *mer* and *fac* oriented oxime groups. Co(HL)₃²⁺ deprotonates immediately to low spin Jahn–Teller distorted Co(HL)₂L⁺.

The intramolecular hydrogen bonding $\text{O}-\text{H}\cdots\text{O}^-\cdots\text{H}-\text{O}$ may be stronger between *fac* oriented oxime and oximate groups than *mer* oriented groups. The crystalline $[\text{Zn}(\text{HL})_2\text{L}]_2[\text{ZnI}_4]$ consists of two distorted octahedral $[\text{Zn}(\text{HL})_2\text{L}]^+$ cationic parts and one distorted tetrahedral $[\text{ZnI}_4]^{2-}$ anionic part.⁷⁶ In both of the cations, the oxime and oximate groups are *fac* oriented forming intramolecular hydrogen bridges $\text{O}-\text{H}\cdots\text{O}^-\cdots\text{H}-\text{O}$. In one of the cations the $\text{H}\cdots\text{O}$ distances are 1.64 and 1.92 Å, and in the other 1.71 and 1.76 Å. The $\text{O}^-\cdots\text{O}$ distances are 2.535 and 2.556 Å in the former cation and 2.544 and 2.566 Å in the latter one.⁷⁶

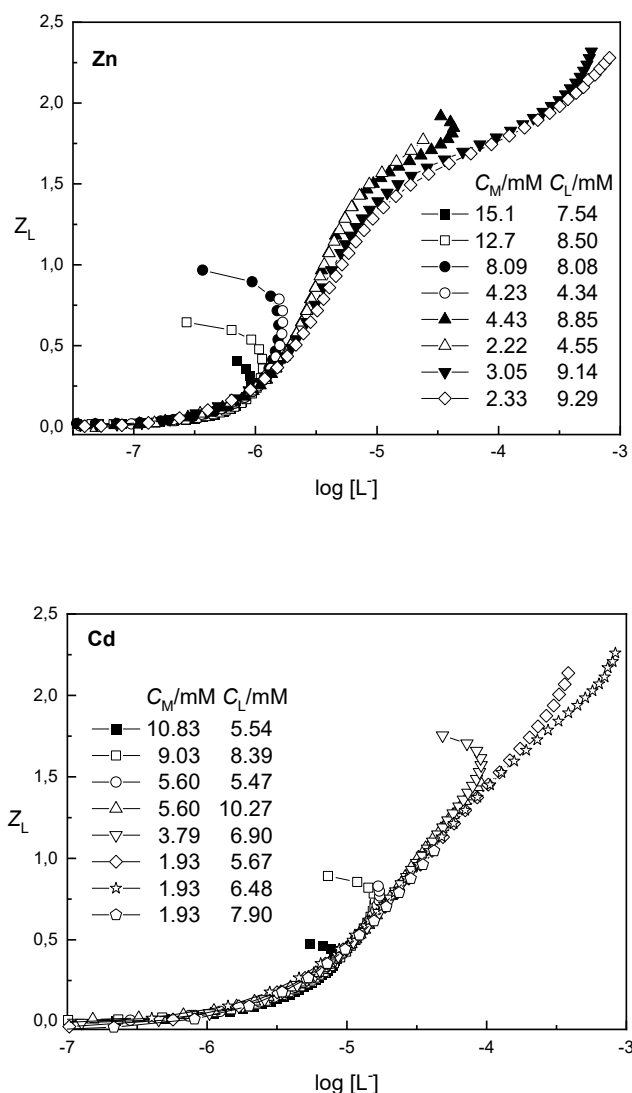


Figure 8. Experimental data plotted as Z_L curves vs. $\log [\text{L}^-]$ for zinc(II) and cadmium(II) complex formation with pyridine-2-aldoximate ion L^- .

The oximate groups are *fac* oriented also in the crystalline complexes $[\text{NiL}_3\text{ML}_3\text{Ni}]\text{ClO}_4$, where the central M^{3+} ion (Mn^{3+} or Cr^{3+}) is surrounded by six oximate oxygen atoms of the two *fac*- NiL_3^- units.⁷⁷ Also in the polymeric $\{[(\text{NiL}_3\text{NaL}_3\text{Ni})\text{Na}_2\text{OH}(\text{H}_2\text{O})]\text{Py}(\text{H}_2\text{O})_2\}_n$ the central Na^+ ion of each $(\text{NiL}_3)\text{Na}$ moiety is surrounded by six oximate oxygen atoms of the two *fac*- NiL_3^- units, but two oximate bridges of each NiL_3^- unit are branched to bind the two terminal Na^+ ions.⁷⁸ The $(\text{NiL}_3)\text{Na}$ moieties are linked together via the terminal Na^+ centers by one aqua and one hydroxo ligand, resulting in a one-dimensional chain structure.⁷⁸ The crystalline complex $[\text{Ni}_3(\text{HL})\text{L}_5]\text{ClO}_4$ consists of two NiL_2 units and one $\text{Ni}(\text{HL})\text{L}$ unit. In only one of the NiL_2 unit, the oximate groups are *trans* oriented and linked via oximate bridges to the other nickel(II) ions. In the other NiL_2 unit and in the $\text{Ni}(\text{HL})\text{L}$ unit one oximate ligand forms branched bridges to the other nickel(II) ions completing their octahedral coordination spheres. The other oximate NO^- and the NOH group are non-bridging and form an intramolecular hydrogen bridge ($\text{O}-\text{H}\cdots\text{O}$). The $\text{N}_{\text{ox}}-\text{Ni}-\text{N}_{\text{ox}}$ angles are 175.24, 109.94, and 108.32°.⁷⁷ In $[\text{NiL}_2\text{Py}_2]\text{Py}\cdot 3\text{H}_2\text{O}$ crystallized from pyridine (Py) the pyridine ligands, oximate nitrogens, and the pyridine nitrogens of the ligands L^- are mutually *trans* oriented with $\text{Py}-\text{Ni}-\text{Py}$, $\text{N}_{\text{ox}}-\text{Ni}-\text{N}_{\text{ox}}$, and $\text{N}_{\text{py}}-\text{Ni}-\text{N}_{\text{py}}$ angles of 180.0°.⁷⁸ The NiL_2Py_2 units are linked together through hydrogen bridges between the oximate oxygens and the lattice water molecules forming a hydrogen bonded one-dimensional chain structure.⁷⁸ The coordinated pyridine ligand has no free electron pair to form hydrogen bridges.

The further deprotonation of $\text{Co}(\text{HL})_2\text{L}^+$ to $\text{Co}(\text{HL})\text{L}_2$ causes repulsion forces between the adjacent oximate groups. If the oxime and oximate groups are *mer* oriented, the Jahn–Teller distorted $\text{Co}-\text{NOH}$ bond is apparently not sufficiently strong on the z axis of $\text{Co}(\text{HL})\text{L}_2$. Thus, the ligand HL loses and the remaining CoL_2 isomerizes so that both of the ligands L^- are in the xy plane of CoL_2 with *trans* oriented oximate groups.

$\text{Zn}(\text{HL})_2^{2+}$ does not reach measurable concentrations. The statistic ratios of the stepwise stability constants $K_1:K_2:K_3$ of octahedral complexes for a bidentate ligand are 12:(5/2):(4/15).⁷⁹ If both $\text{Zn}(\text{HL})^{2+}$ ($\log \beta_{011} = 1.90$ or $\beta_{011} = 79.4$) and $\text{Zn}(\text{HL})_2^{2+}$ are octahedral, the stepwise stability constant of $\text{Zn}(\text{HL})_2^{2+}$ would be $K_2 = 16.5$ or $\log K_2 = 1.22$, $\log \beta_{012} = 3.12$, and its $\text{p}K_{\text{a}1} = 5.62$. Apparently, the stability constants of $\text{Zn}(\text{HL})_2^{2+}$ are smaller, and its *cis* isomers decompose at least partly due to the repulsion forces between the positively charged adjacent oxime protons. Thus, the proportion of $\text{Zn}(\text{HL})_2^{2+}$ remains so small that it cannot be observed.

The stability constants of ZnL^+ ($\log \beta_{-111} = -4.81 \pm 0.29$) and $\text{Zn}(\text{HL})\text{L}^+$ ($\log \beta_{-112} = -2.50 \pm 0.24$) are very inaccurate, because the complexes occur in the same pH range (Figure 5). However, it is reasonable to assume that the stepwise stability constant of $\text{Zn}(\text{HL})\text{L}^+$ $\log (\beta_{-112}/\beta_{-111}) = 2.3 \pm 0.3 > \log \beta_{011} = 1.90 \pm 0.02$, because $\text{Zn}(\text{HL})\text{L}^+$ is mainly formed via the coordination of HL to ZnL^+ with

cis orientation of the oxime and oximate groups and stabilized by the intramolecular hydrogen bonding $\text{O—H}\cdots\text{O}$. Its *trans* isomer is much less stable. If the stability constant of $\text{trans-Zn(HL)}_2^{2+}$ $\log \beta_{012} \approx 2.8$ ($K_2 \approx 8.3$, $\log K_2 \approx 0.9$), and its acidity constants $K_{a1} > K_{a2}$ ($\text{p}K_{a1} < \text{p}K_{a2}$) in its deprotonation via $\text{trans-Zn(HL)L}^+ \rightarrow \text{ZnL}_2$ ($\log \beta_{-212} = -9.44$), its $\text{p}K_{a1} \leq 6.1$, $\text{p}K_{a2} \geq 6.1$, and the stability constant of trans-Zn(HL)L^+ would be $\log \beta_{-112} \leq -3.3$. Thus, the proportion of trans-Zn(HL)L^+ remains very small. It seems that the conventional stepwise stability constant of ZnL_2 $\log K_2 = 5.4 > \log K_1 = 5.2 (\pm 0.3)$.

The complex formation according to reactions (31) and (32) is very small in the pH range 5–9, where the free ligand is almost wholly in the form HL ($\text{p}K_a = 10.01$). ZnL^+ is formed through deprotonation of Zn(HL)_2^{2+} and ZnL_2 mainly via coordination of HL to ZnL^+ with *trans* orientation and following deprotonation of the formed trans-Zn(HL)L^+ . ZnL_2 is also formed upon deprotonation of cis-Zn(HL)L^+ , but the repulsion forces between the negative charges of the adjacent oximate oxygens very quickly cause isomerization of the formed cis-ZnL_2 to trans-ZnL_2 and possibly its partial decomposition to ZnL^+ and the free HL. CdL^+ , Cd(HL)L^+ , and CdL_2 are formed in similar way than ZnL^+ , Zn(HL)L^+ , and ZnL_2 . However, the stepwise stability order of CdL^+ and CdL_2 is normal $K_1 > K_2$. Apparently, trans-Cd(HL)L^+ is only a slightly more potent acid than Cd(HL)_2^{2+} ($\text{p}K_a = 7.28$).

The SUPERQUAD program calculates stability constants also for ZnL_3^- and CdL_3^- not observed earlier. The Z_L curves (Figure 8) with $C_L:C_M = 3-4$ exceed the value of $Z_L = 2.0$ between the $\log [L^-]$ values -3.5 and -3.0 showing the existence of ZnL_3^- and CdL_3^- . The Z_L curve of zinc(II) ion published by Burger *et al.*⁴⁵ ends at $\log [L^-] \approx -3.5$ and it seems to reach the limiting value $Z_L = 2.0$ at $\log [L^-] \approx -4.0$. The Z_L curves of zinc(II) and cadmium(II) ions published by Bolton and Ellin⁴⁴ end already between the Z_L values $1.7-1.9$, where the $\log [L^-]$ values are between -5 and -4 .

The distribution curves (Figures 5 and 7) show that both ZnL_3^- and CdL_3^- appear in the pH range 8.0–8.5. Apparently, they are also formed via the coordination of HL to ZnL_2 and CdL_2 , respectively, and the coordination requires the oximate groups to be perpendicularly *trans* oriented in their parent complexes ZnL_2 and CdL_2 . The formed Zn(HL)L_2 and Cd(HL)L_2 deprotonate without reaching measurable concentrations. Due to the repulsion forces between the *mer* oriented oximeters groups the conventional stepwise stability constants of ZnL_3^- ($\log K_3 = 2.36 \pm 0.22$) and CdL_3^- (2.59 ± 0.16) are small. For the same reason, the stepwise stability constants of *cis*- ML_2 complexes are also small. NiL_3^- ($\log K_3 = 5.19$) is stabilized by the ligand field splitting, but *cis*- NiL_2 probably isomerizes quickly to *trans*- NiL_2 . The detection of *cis*- $[\text{PtL}_2] \cdot 2\text{H}_2\text{O}$ is allowed only by its very slow isomerization.

In $[\text{Zn(HL)}_2(\text{OSMe}_2)_2][\text{BF}_4]$ crystallized from a mixture of dimethyl sulfoxide (Me_2SO), dimethylformamide (dmf), and methanol, the oxime groups are *trans* oriented in $\text{N}_{\text{ox}}-\text{Zn}-\text{N}_{\text{ox}}$ angle of 158.75° and the $\text{O}-\text{Zn}-\text{O}$ angle between the dimethyl sulfoxide ligands is 91.47° . The oxime

groups bind the $[\text{BF}_4]^-$ anions with hydrogen bonds $\text{O}-\text{H}\cdots\text{F}$.⁷² In $[\text{Zn}(\text{HL})_2(\text{NCS})_2]$ crystallized from a mixture of methanol and dmf, the pyridine nitrogens are *trans* oriented in $\text{N}-\text{Zn}-\text{N}$ angle of 162.1° . The $\text{N}_{\text{ox}}-\text{Zn}-\text{N}_{\text{ox}}$ angle is 82.6° and the $\text{N}-\text{Zn}-\text{N}$ angle between the thiocyanate ions is 94.7° . The intermolecular hydrogen bonds $\text{O}-\text{H}\cdots\text{S}$ between the oxime groups and the terminal sulfur atom of NCS^- link the complex molecules to form infinite layers.⁷²

$\text{Zn}_2\text{L}_2^{2+}$ is probably formed by dimerization of ZnL^+ via two oximato $-\text{NO}^-$ bridges forming a six-membered $(\text{ZnNO})_2$ ring. The dimer is deprotonated with $\text{pK}_a = 6.54$ to $\text{Zn}_2\text{L}_2\text{OH}^+$ by forming a hydroxo $-\text{OH}^-$ bridge beside the $(\text{ZnNO})_2$ ring. In the increase of pH, $\text{Zn}_2\text{L}_2\text{OH}^+$ is further deprotonated to $\text{Zn}_2\text{L}_2(\text{OH})_2$, but only one $-\text{OH}^-$ bridge can exist at the same time between the zinc(II) atoms, if their coordination spheres are still octahedral. The bending of the $(\text{ZnNO})_2$ ring breaks easily the hydroxo bridge and causes a collision of two adjacent aqua ligands on the opposite site of the broken hydroxo bridge. One of the two aqua ligands is then released as oxonium H_3O^+ ion and the other deprotonated to OH^- ligand, which forms a new hydroxo bridge. Soon, the formed hydroxo bridge is broken and the former hydroxo ligand is again bridged. The two hydroxo ligands of $\text{Zn}_2\text{L}_2(\text{OH})_2$ form alternatively short-lived hydroxo bridges between the zinc(II) atoms.

CdL^+ dimerizes in a similar way to $\text{Cd}_2\text{L}_2^{2+}$, which deprotonates with $\text{pK}_a = 8.64$ to $\text{Cd}_2\text{L}_2\text{OH}^+$ by forming a hydroxo bridge beside the $(\text{CdNO})_2$ ring. Due to the larger size of cadmium(II) ion, $\text{Cd}_2\text{L}_2^{2+}$ ($\log \beta_{-222} = -8.02$) and $\text{Cd}_2\text{L}_2\text{OH}^+$ ($\log \beta_{-322} = -16.66$) are less stable and weaker acids than $\text{Zn}_2\text{L}_2^{2+}$ (-6.76) and $\text{Zn}_2\text{L}_2\text{OH}^+$ (-13.30 , $\text{pK}_a = 9.36$). $\text{Cd}_2\text{L}_2(\text{OH})_2$ cannot be detected in the pH range 9–10.

The octahedral copper(II) complexes are Jahn–Teller distorted because of their $t_{2g}^6 e_g^3$ electron structure with three electrons in their two e_g orbitals. In the complexes $\text{Cu}(\text{HL})_2^{2+}$ and CuL_2 , the ligands HL and L^- lie in the xy plane of the complex with *trans* oriented oxime and oximate groups. Jahn–Teller distortion prevents the coordination of the ligands HL or L^- on the z axis of $\text{Cu}(\text{HL})_2^{2+}$ and CuL_2 , which is required for the formation of tris complexes with bidentate ligands.

$\text{Cu}(\text{HL})\text{L}^+$ is mainly formed via coordination of HL to CuL^+ with *cis* orientation of the oxime and oximate groups and stabilized by the intramolecular hydrogen bonding $\text{O}-\text{H}\cdots\text{O}$. Its stepwise stability constant $\log (\beta_{-112}/\beta_{-111}) = 4.53 > \log \beta_{011} = 3.93$.¹¹ Its *trans* isomer is much less stable. The stability constant of CuL_2 $\log \beta_{-212} = -1.53$.¹¹ If the stepwise stability constant of *trans*- $\text{Cu}(\text{HL})\text{L}^+$ $\log (\beta_{-112}/\beta_{-111}) \leq \log (\beta_{012}/\beta_{011}) = 3.55$, its stability and acidity constants are $\log \beta_{-112} \leq 4.45$ and $\text{pK}_a \leq 5.98$. The acidity constant of its parent complex *trans*- $\text{Cu}(\text{HL})_2^{2+}$ ($\log \beta_{012} = 7.48$) is then $\text{pK}_{a1} \geq 3.03$. The proportion of *trans*- $\text{Cu}(\text{HL})\text{L}^+$ remains small in solutions with $C_M = 5$ mM and $C_L = 10$ mM (Figure 2 in ref 11).

Instead of dimerization CuL^+ trimerizes and hydrolyzes to $\text{Cu}_3\text{L}_3\text{OH}^{2+}$ ($\text{pK}_a = 6.57$) and $\text{Cu}_3\text{L}_3\text{O}^+$ (or $\text{Cu}_3\text{L}_3(\text{OH})_2^+$).¹¹ The binuclear $\text{Cu}_2\text{L}_2\text{OH}^+$ structure with octahedral coordination environments

would be highly unstable because of Jahn–Teller distortion. The trimers are main species at low $C_L:C_M$ ratios (1:1) in the pH range 4–8, but in the presence of sufficient ligand excess ($C_L:C_M \geq 2$) their proportions are small and the main species are $Cu(HL)L^+$ and CuL_2 in the pH range 3–9. The trinuclear $Cu_3O(H)$ core is held together by three peripheral oximate bridges.^{11,80} The oxygen atom in the core is located above the Cu_3 plane and thus exhibits a roughly tetrahedral coordination sphere.^{80,81} The polymerization reactions require deprotonation of mono complexes in their oxime groups.

In the crystalline $[CuL_3CrT](ClO_4)_2$, where T is 1,4,7-trimethyl-1,4,7-triazacyclononane, the coordination sphere around the Cu center is strongly distorted.⁸² The geometry of the Cu center may be envisaged as pseudo-trigonal-bipyramidal with a non-bonded pyridine nitrogen (at a distance of 2.490 Å from the Cu center, while the other Cu–N distances are 1.983–2.205 Å. In the crystalline $[CuL_3CrFeT](ClO_4)_2$ the two oximate ligands deviate significantly from the z axis of the copper(II) ion: the $N_{ox}-Cu-N_{py}$ angle is 154.3°.⁸³

It must be noted in Table 2 that the most stable bis complex formed by the uncharged pyridine-2-aldoxime is $Cu(HL)_2^+$ ($\log \beta_{012} = 11.05$).⁴⁶ The uncharged pyridine-2-aldoxime is a soft Lewis base and prefers to bind to the univalent copper ion, which is a much softer Lewis acid than for example divalent cadmium ion. Also, the negatively charged pyridine-2-aldoximate ion (L^-) is a rather soft Lewis base; CuL_2^- ($\log \beta_2 = 14.4$) is more stable than ZnL_2 (10.58) and CdL_2 (9.09) but less stable than the ligand field stabilized CoL_2 , NiL_2 , and CuL_2 . It is generally very difficult to determine stability constants of copper(I) complexes, because they are easily oxidized by air oxygen.

3.2. 6-Methylpyridine-2-aldoxime complexes

In 1960, Hartkamp¹⁶ noted that 6-methylpyridine-2-aldoxime is a very selective reagent for spectrophotometric determinations of little amounts of copper (1–10 µg/ml) in presence of large excess of many another metals (for example in presence of 50 µg/ml Ni or 2500–5000 µg/ml Zn). 6-methylpyridine-2-aldoxime forms much less stable complexes with divalent transition metal ions than pyridine-2-aldoxime does, but both ligands form brownish orange copper(I) chelates with approximately equal intensity. The best pH range for the determination of copper with 6-methylpyridine-2-aldoxime is 4.5–6.5, where the formation of $Cu(HL)_2^+$ is complete. In the pH range 6.5–8.5, $Cu(HL)_2^+$ is deprotonated to $Cu(HL)L$ and in the further increase of pH to CuL_2^- , which is also selective in alkaline solution ($pH \geq 12$). These complexes are probably tetrahedral in aqueous solution, because copper(I) ion is a soft Lewis acid and water a hard Lewis base.⁶¹ All the copper(II) complexes formed by 6-methylpyridine-2-aldoxime are reduced rapidly to copper(I) complexes by

hydroxylamine also in cold solution. In the presence of air, the solutions of 6-methylpyridine-2-aldoxime complexes $\text{Cu}(\text{HL})_2^+$ and CuL_2^- are stable at least 24 hours but all the copper(I) complexes formed by pyridine-2-aldoxime,¹⁶ pyridine⁸⁴ and 2-, 3- and 4-picoline⁸⁵ are rapidly oxidized to copper(II) complexes. It is clear that the 6-methyl groups give steric screenings from the air oxidation of the central copper(I) ion in $\text{Cu}(\text{HL})_2^+$, $\text{Cu}(\text{HL})\text{L}$, and CuL_2^- but weaken the stabilities of octahedral complexes. A similar weakening effect of the 6- or 2-methyl groups on the complex stability has been observed in comparable instances, with methylated pyridine^{49,84,85} and 2-picolinate ligands.⁸⁶ With large metal ions like Ca^{2+} , Sr^{2+} , Ba^{2+} , Ag^+ , and Hg^{2+} , the increased basicity of the ligand due to the presence of methyl group may actually lead to the stabilization of the complexes. Such are the cases, for example, with 6-methyl-2-picolinate ligand⁸⁶ and with tetrahedral copper(I) complexes of 2-picoline.^{84,85} Apparently, the 6-methylpyridine-2-aldoxime complexes $\text{Cu}(\text{HL})_2^+$ and CuL_2^- are somewhat more stable than the corresponding pyridine-2-aldoxime complexes, although the stability constants of last complexes ($\log \beta_{012} = 11.05$ and $\log \beta_2 = 14.4$) in NaNO_3 solution ($I = 0.5 \text{ M}$) at 20°C observed by Petitfaux⁴⁶ are, according SPE calculation, also sufficiently large for the complete complex formation in the pH ranges 4.5–6.5 and ≥ 12 , respectively.

Orama *et al.*^{10,11} have determined the protonation and acidity constants of 6-methylpyridine-2-aldoxime and the stability constants of its copper(II) and nickel(II) complexes in aqueous 0.1 M NaCl solution at 25°C . In this work, the studies have been extended to its complex formation with cobalt(II), zinc(II), and cadmium(II) ions.

The 6-methyl groups screen also the formed low spin cobalt(II) complexes from oxidation, but the attainments of equilibria became slow already in the pH range 5–6, if the nitrogen current or the magnetic mixing were insufficient. By using a sufficiently strong nitrogen current and magnetic mixing, the titration could be continued to pH range 8–10. Then, the NaOH additions less than 0.1 ml were not ever necessary in the pH range 5–8, as in the case of pyridine-2-aldoxime.

The pink color of the cobalt(II) ion disappeared in the solutions in the initial stages of the titrations, and the solutions gradually developed a weak yellowish brown color. Hartkamp¹⁶ also observed the same color after the addition of 6-methylpyridine-2-aldoxime to cobalt(II) salt solutions. In this work, the color was strengthened in the pH range 6–8, and the solutions often had a reddish tone in the end of the titrations (in the pH range 8–11). When the nitrogen current was stopped, the solutions darkened fairly quickly and their pH values first raised something (contrary to the pyridine-2-aldoxime complex solutions) but soon started again fall. The evaporations of also these solutions left only powdery precipitate, which could not be used to determination of the structure of the complexes with X-ray diffraction.

The dispersion of the Z_{H} curves (Figure 9) is only weak in the pH range 4–6, where $Z_{\text{H}} \leq 0$, indicating the stability constants of the complexes of the type $\text{Co}(\text{HL})_r^{2+}$ are very small. The Z_{H} curves

with $C_L/C_M = 2-5$ (Figure 9) have a plateau in the pH range 7–9 and an inflection point at $C_H \approx -2C_M$ indicating that the major species should be CoL_2 , $\text{Co}_2\text{L}_2(\text{OH})_2$ or $\text{Co}_2\text{L}_3\text{OH}$, where $p = -2q$. The increases of the Z_H curves with low $C_L/C_M (\leq 1)$ over to level $Z_H = 1$ also indicates the existence of complexes, where $p < -r$. The SUPERQUAD program calculated the stability constants for complexes $\text{Co}(\text{HL})^{2+}$, CoL^+ , CoL_2 , $\text{Co}_2\text{L}_2\text{OH}^+$, Co_2L_3^+ , and $\text{Co}_2\text{L}_3\text{OH}$ but rejected the pqr combinations –012, –112, –312, –313, –222, –422, –433 and –533. The stability constants are given in Table 3. Examples of the distribution curves are given in Figure 10.

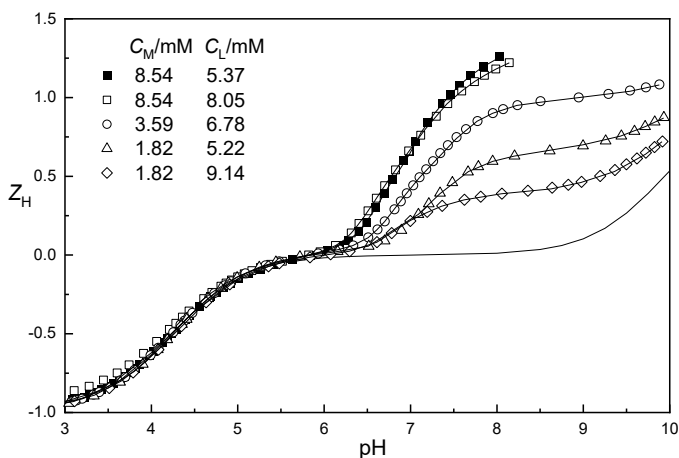


Figure 9. Part of the experimental data plotted as Z_H curves vs. pH for cobalt(II) complex formation with 6-methylpyridine-2-aldoxime HL. The full lines have been calculated using sets of proposed stability constants in Table 3. The lowest line refers to the ligand alone.

The conventional stability constants of CoL^+ and CoL_2 are $\log \beta_1 = 4.27$ and $\log \beta_2 = 10.11$ ($\log K_2 = 5.86$). The inverse stability order $K_2 \gg K_1$ and the weak acidity of $\text{Co}(\text{HL})^{2+}$ ($\text{p}K_a = 6.86$) prove that both $\text{Co}(\text{HL})^{2+}$ and CoL^+ are high spin but CoL_2 is low spin. Due to Jahn–Teller distortion, both of the ligands L^- would be expected to lie in the xy plane of CoL_2 with *trans* oriented oximate groups. However, Kumar *et al.*⁸⁷ have proved that 6-methylpyridine-2-aldoxime is a gravimetric reagent for the estimation of uranium(VI) ion as UO_2L_2 , but unable to form any insoluble compound with palladium(II) ion. Uranium(VI) ion (0.73 \AA) is sufficiently large⁵⁹ to bind the two ligands L^- in the equatorial plane of the linear uranyl ion UO_2^{2+} .⁵¹ But palladium(II) ion, which almost invariably forms square-planar low spin complexes,⁵¹ is too small (0.64 \AA) to bind two 6-methylpyridine-2-aldoximate ligands in its xy plane. The low spin cobalt(II) ion (0.65 \AA) is also too small for their planar coordination. Only one of the ligands L^- may lie in the xy plane of CoL_2 , but not both. If CoL_2 is octahedral and Jahn–Teller distorted, the uncharged $\text{Co}-\text{N}_{\text{py}}$ bond is probably too weak to lie on its z

axis. The $\text{Co}-\text{NO}^-$ bond is stronger to lie there, and the oximate groups are able to intramolecular hydrogen bonding with the aqua ligand of the xy plane ($\text{NO}^- \cdots \text{H}-\text{O}-\text{H} \cdots \text{ON}^-$). The intramolecular hydrogen bonding, along with the Jahn–Teller distortion, probably causes a significant deviation from the z axis of CoL_2 for the $\text{Co}-\text{NO}^-$ bond. Thus, CoL_2 ($\log \beta_{-212} = -9.77$) is much less stable than NiL_2 (-7.43).

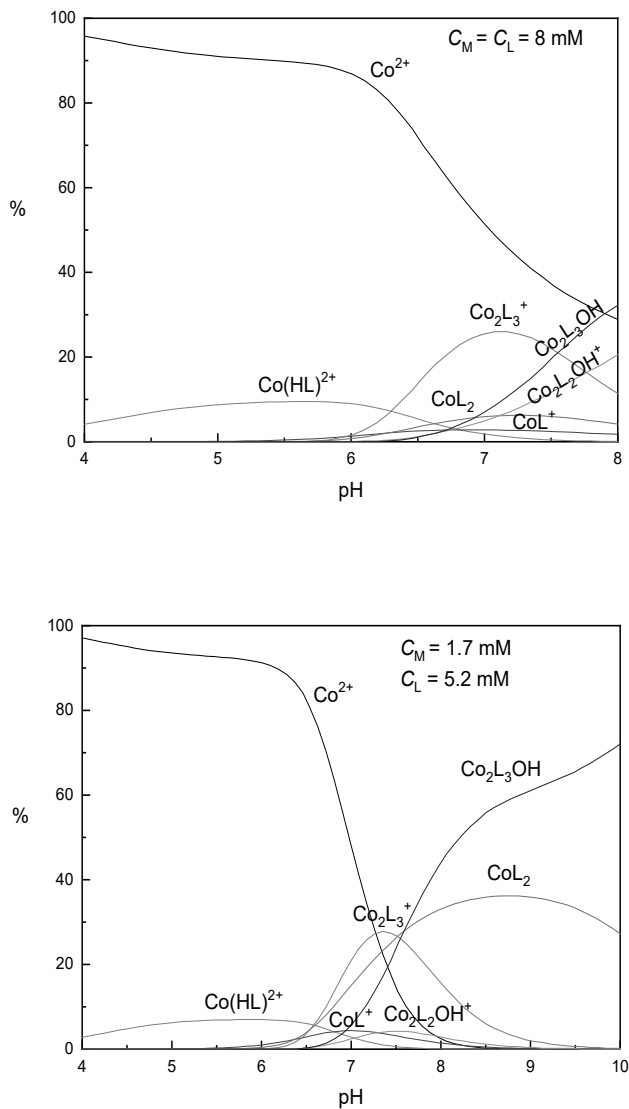


Figure 10. Examples of the concentration distribution of cobalt(II) species vs. pH with 6-methylpyridine-2-aldoxime.

Table 3. Proposed formulas and stability constants ^a of 6-methylpyridine-2-aldoxime complexes relating to the reaction $pH^+ + qM^{2+} + rHL \rightleftharpoons (H^+)_p(M^{2+})_q(HL)_r$ in aqueous 0.1 M Na(Cl) solution at 25 °C.

| <i>p</i> | <i>q</i> | <i>r</i> | Proposed formula | $\log \beta_{pqr} \pm 3\sigma$ | | | | |
|-----------------------------|----------|----------|--------------------------------------------------------------|--------------------------------|-------------|------------|-------------|-------------|
| | | | | M = Co | M = Ni | M = Cu | M = Zn | M = Cd |
| 0 | 1 | 1 | M(HL) ₂ ²⁺ | 1.19±0.17 | 1.94±0.06 | 2.87±0.04 | | |
| 0 | 1 | 2 | M(HL) ₂ ²⁺ | | 3.86±0.04 | 5.29±0.20 | | |
| -1 | 1 | 1 | ML ⁺ | -5.67±0.29 | | | | -5.71±0.03 |
| -1 | 1 | 2 | M(HL)L ⁺ | | | 1.97±0.07 | | |
| -2 | 1 | 2 | ML ₂ | -9.77±0.09 | -7.43±0.09 | -3.68±0.12 | | -11.49±0.03 |
| -2 | 2 | 2 | M ₂ L ₂ ²⁺ | | | | -8.24±0.24 | |
| -3 | 2 | 2 | M ₂ L ₂ OH ⁺ | -14.81±0.10 | | | -14.55±0.03 | -17.37±0.06 |
| -4 | 2 | 2 | M ₂ L ₂ (OH) ₂ | | | | -22.84±0.09 | |
| -3 | 2 | 3 | M ₂ L ₃ ⁺ | -11.47±0.09 | -7.28±0.04 | | | |
| -4 | 2 | 3 | M ₂ L ₃ OH | -19.08±0.03 | | | | |
| -4 | 3 | 3 | M ₃ L ₃ OH ²⁺ | | | 1.05±0.03 | | |
| -5 | 3 | 3 | M ₃ L ₃ (OH) ₂ ⁺ | | -20.11±0.06 | | | |
| Number of points/titrations | | | | 227/5 | 366/8 | 306/8 | 164/8 | 253/8 |
| χ^2 | | | | 14.8 | 20 | 34.9 | 53.6 | 32.9 |
| <i>s</i> | | | | 1.84 | 3.3 | 2.27 | 3.18 | 2.72 |
| Ref. | | | | II | 12 | 11 | I | I |

^a Calculated by using the following protonation and acidity constants of the free ligand HL: $\log \beta_{101} = 4.258 (\pm 0.008)$ and $\log \beta_{-101} = -9.94 (\pm 0.08)$ (ref. 11).

In Ni(HL)₂²⁺, the ligands HL are perpendicularly coordinated with *trans* oriented oxime group. This is evidenced by the fact that the stepwise stability difference $\log (K_1:K_2)$ between Ni(HL)₂²⁺ ($\log K_1 = 1.94$) and Ni(HL)₂²⁺ ($\log K_2 = 1.92$) is only 0.02. The hydrophobic 6-methyl (—CH₃) groups expel water molecules from the coordination spheres of the complexes. This stabilizes the bis complexes by slowing their aquation reactions back to the mono complex. The structure of Ni(HL)₂²⁺ with perpendicularly *trans* oriented oximes remains the same when it deprotonates through Ni(HL)L⁺ to NiL₂. Apparently, the difference between the acidity constants of Ni(HL)₂²⁺ (K_{a1} and K_{a2}) is due to the intramolecular hydrogen bonding by the oximate oxygens with their adjacent aqua ligands in NiL₂ (NO⁻...H₂O—) so small that Ni(HL)L⁺ has not reached measurable concentrations (Table 3).¹²

Also, the stability difference $\log (K_1:K_2)$ between Cu(HL)₂²⁺ ($\log K_1 = 2.87$) and Cu(HL)₂²⁺ ($\log K_2 = 2.42$) is smaller (0.45) than the statistic difference of octahedral mono and bis complexes for a bidentate ligand $\log (K_1:K_2) = \log (12:2.5) = 0.68$.^{11,79} This and the acidity constants of Cu(HL)₂²⁺, $pK_{a1} = 3.32$, $pK_{a2} = 5.65$,¹¹ which fit within the limits estimated above (p. 33) for the acidity constants of the corresponding pyridine-2-aldoxime complex *trans*-Cu(HL)₂²⁺ ($pK_{a1} \geq 3.03$, $pK_{a2} \leq 5.98$),

indicate that the ligands HL/L^- lie in the xy planes of $\text{Cu}(\text{HL})_2^{2+}$, $\text{Cu}(\text{HL})\text{L}^+$, and CuL_2 with *trans* oriented oxime or oximate groups. The difference between the values of $\text{p}K_{\text{a}1}$ and $\text{p}K_{\text{a}2}$ is large, because the Jahn–Teller distortion hinders the intramolecular hydrogen bonding between the oximate groups and the aqua ligands. The steric requirements by the 6-methyl and oxime/oximate groups in the xy plane diminish the stabilities of the bis complexes. $\text{Cu}_3\text{L}_3\text{OH}^{2+}$ is the main species in the pH range 4–7 also in the presence of twofold ligand excess.¹¹

In the binuclear complexes Co_2L_3^+ and $\text{Co}_2\text{L}_3\text{OH}$ one of the cobalt(II) ions (in octahedral CoN_4O_2 or partly in square-pyramidal CoN_4O environment) is low spin and the other one surrounded by two nitrogen and four oxygen atoms (in CoN_2O_4 environment) is high spin. Co_2L_3^+ is probably formed through combination of CoL_2 and CoL^+ together via three oximate bridges with *fac* orientation to both cobalt(II) ions. Two of the oximate bridges bind the low spin cobalt(II) ion in its xy plane and the third oximate bridge is Jahn–Teller distorted. The deprotonation Co_2L_3^+ to $\text{Co}_2\text{L}_3\text{OH}$ in the pH range 7–9 requires the formation of a hydroxo $-\text{OH}-$ bridge and breaking of an oximate $-\text{NO}-\text{Co}$ bond, if the coordination spheres of the forming $\text{Co}_2\text{L}_3\text{OH}$ are still octahedral. The Jahn–Teller distorted oximate bridge of Co_2L_3^+ is weak and easily broken; after bending of the remaining $(\text{CoNO})_2$ ring, the hydroxo $-\text{OH}-$ bridge is formed on the opposite side of the opened oximate $-\text{NO}-$ group.

$\text{Co}_2\text{L}_2\text{OH}^+$ is apparently formed through dimerization of CoL^+ via two oximate bridges and deprotonation of the formed $\text{Co}_2\text{L}_2^{2+}$ ($\text{p}K_{\text{a}} < 7.0$) by forming a hydroxo bridge beside the $(\text{CoNO})_2$ ring. Both of the cobalt(II) ions of $\text{Co}_2\text{L}_2\text{OH}^+$ are in CoN_2O_4 environments probably high spin. Due to the third Jahn–Teller distorted oximate bridge, Co_2L_3^+ ($\text{p}K_{\text{a}} = 7.61$) is a weaker acid than $\text{Co}_2\text{L}_2^{2+}$. The proportion of $\text{Co}_2\text{L}_2\text{OH}^+$ reaches about 20 % of C_{M} in solutions with $C_{\text{M}} \approx C_{\text{L}}$. In the presence of threefold ligand excess, $\text{Co}_2\text{L}_3\text{OH}$ displaces CoL_2 as main species in the pH range 6–8 (Figure 10).

The structure of Ni_2L_3^+ is likely to be different to that of Co_2L_3^+ , because one of the pyridine nitrogens can lie on the z axis of the nickel(II) ion of the NiN_4O_2 environment. The perpendicularly *trans* oriented oximate groups allow NiL_2 to form insoluble polymers via oximate and hydroxo bridges starting with $\text{Ni}_3\text{L}_4(\text{OH})_2$. In all solutions with $C_{\text{L}} \geq 1.5 C_{\text{M}}$, a precipitate or very slow attainment of equilibrium appears already in the pH range 6.5–7.5.¹² A light green crystalline complex $[\text{Ni}_9\text{L}_{10}(\text{OH})_6(\text{H}_2\text{O})_6](\text{ClO}_4)_2 \cdot 10\text{H}_2\text{O}$ has been isolated as perchlorate from solution, where $C_{\text{L}} = C_{\text{M}}$ and $\text{pH} = 8$.^{12,88} This metallacrown⁸⁹ structure contains an octahedral NiO_6 central core, two NiL_2 units (two different NiN_4O_2 environments), and NiL units (two different NiN_2O_4 environments). Both of the NiL_2 units form with their adjacent NiL units two $\text{Ni}_3\text{L}_4(\text{OH})_2$ units, where each nickel(II) atom is linked together via an oximate and a hydroxo bridge. The two $\text{Ni}_3\text{L}_4(\text{OH})_2$ units are linked to the remaining nickel(II) atoms via several bi- or trifurcated oximate and hydroxo bridges.^{12,88} In 0.1 M $\text{Na}(\text{Cl})$ solutions with $C_{\text{L}} \approx C_{\text{M}}$, the proportion of NiL_2 is so small that the titrations can be continued to pH range 8–9.¹² The main species is Ni_2L_3^+ (50–60 % of C_{M}) in the pH range 6.0–7.5 and

$\text{Ni}_3\text{L}_3(\text{OH})_2^+$ in the higher pH range.¹² Ni_2L_3^+ disappears in the pH range 8–9 without deprotonation to $\text{Ni}_2\text{L}_3\text{OH}$, although the proportion of Ni_2L_3^+ at pH = 8 is still about 20 % of C_M . Apparently, the nickel(II) ions of Ni_2L_3^+ are linked together via three oximato bridges with *fac* orientation to both nickel(II) ions. If Ni_2L_3^+ is formed through combination of *trans*- NiL_2 to a mono complex, two oximato bridges are easily formed. The unbridged $\text{Ni}-\text{NO}^-$ bond is easily broken and after the following rotation of the ligand L⁻ about 90° around its $\text{Ni}-\text{N}_{\text{py}}$ the third oximato bridge is formed. $\text{Ni}(\text{HL})^{2+}$ disappears in the pH range 6.5–7.0 without deprotonation to NiL^+ .¹²

It must be noted that also pyrazine-2-carboxamidoxime (Hpza) forms $\text{Co}_2(\text{pza})_3^+$ ($\log \beta_{-323} = -13.53$) and $\text{Ni}_2(\text{pza})_3^+$ (-9.06) in 0.1 M NaCl solution.^V Only $\text{Co}_2(\text{pza})_3^+$ ($\text{p}K_a = 9.34$) is deprotonated to $\text{Co}_2(\text{pza})_3\text{OH}$ ($\log \beta_{-423} = -22.87$), but $\text{Ni}_2(\text{pza})_3^+$ is displaced in the pH range 8–10 by $\text{Ni}(\text{Hpza})(\text{pza})_2$ ($\log \beta_{-213} = -6.02$) and $\text{Ni}(\text{pza})_3^-$ ($\log \beta_{-313} = -16.12$). $\text{Ni}_2(\text{pza})_3\text{OH}$ is not formed, although the proportion of $\text{Ni}_2(\text{pza})_3^+$ is about 55 % of C_M at pH = 8 and still about 15 % at pH = 10 in solution of $C_M = 1$ mM and $C_L = 3$ mM. In $\text{Co}_2(\text{pza})_3^+$ one of the cobalt(II) ions is low spin and the other is high spin. Thus, one of the three oximato bridges is Jahn–Teller distorted and easily broken, but all the three oximato bridges in $\text{Ni}_2(\text{pza})_3^+$ are about equally strong. $\text{Co}_2(\text{pza})_3^+$ ($\text{p}K_a = 9.34$) is a still weaker acid than the 6-methylpyridine-2-aldoxime complex Co_2L_3^+ , but also the free pyrazine-2-carboxamidoxime Hpza ($\text{p}K_a = 11.17$) is a weaker acid than the free 6-methylpyridine-2-aldoxime HL (9.94). Thus, the basicity of the oximato $-\text{NO}^-$ group is stronger in the free pyrazine-2-carboxamidoximate pza^- ion and the $-\text{NO}-\text{Co}$ (high spin) bond is stronger in $\text{Co}_2(\text{pza})_3^+$ than in Co_2L_3^+ .

The research of the zinc(II) complex formation to pH range 8–9 also required at least twofold ligand excess with this ligand. A weak inflection point is observable on the titration curves at $C_H:C_M \approx 1.85$ and $\text{pH} \approx 8.5$ –8.6. In the solution with low $C_L:C_M$ ratios (≤ 1.1) $\text{Zn}(\text{OH})_2$ was precipitated in the pH range 7.0–7.5. The Z_H curves of the solutions are close together before they exceed the zero level at pH range 6–7 (Figure 11). The SUPERQUAD program calculated stability constants only for $\text{Zn}_2\text{L}_2^{2+}$, $\text{Zn}_2\text{L}_2\text{OH}^+$, and $\text{Zn}_2\text{L}_2(\text{OH})_2$ ($\chi^2 = 48.8$, $s = 3.13$; 171 data points from eight titrations). The sample standard deviation s is somewhat high but still indicates a quite satisfactory explanation of the data. The mononuclear species $\text{Zn}(\text{HL})^{2+}$ and ZnL^+ never reach measurable concentrations, and the proportion of $\text{Zn}_2\text{L}_2^{2+}$ remains in all the solutions small (5–7 % of C_M). $\text{Zn}_2\text{L}_2\text{OH}^+$ is the major species in the pH range 7–8 (Figure 12). It is even more stable ($\log \beta_{-322} = -14.55 \pm 0.04$) than $\text{Co}_2\text{L}_2\text{OH}^+$ (-14.81 ± 0.10). According to the spectrochemical series of ligands, the d -orbital splitting increases in the order $\text{I}^- < \text{Br}^- < \text{Cl}^- < \text{F}^- < \text{OH}^- < \text{C}_2\text{H}_4^{2-} \approx \text{H}_2\text{O} < \text{NCS}^- < \text{py} \approx \text{NH}_3 < \text{en} < \text{bipy} < \text{phen} < \text{NO}_2^- < \text{CN}^-$.^{28,51,79} Water provides a relatively weak and hydroxide ion a slightly weaker ligand field.²⁸ As the deprotonation/hydrolysis of the aqua ion weakens the d -orbital splitting around the central metal ion, the acidity of the following aqua ions in aqueous solution decreases in the

strengthening of the ligand field in the order Fe^{2+} ($\log \beta_{-110} = -9.5$ at $I \approx 0$) $>$ Co^{2+} (-9.65) $>$ Ni^{2+} (-9.86) $<$ Zn^{2+} (-8.96).²⁸ So $\text{Co}_2\text{L}_2^{2+}$ is probably a weaker acid than $\text{Zn}_2\text{L}_2^{2+}$ ($\text{p}K_a = 6.31$).

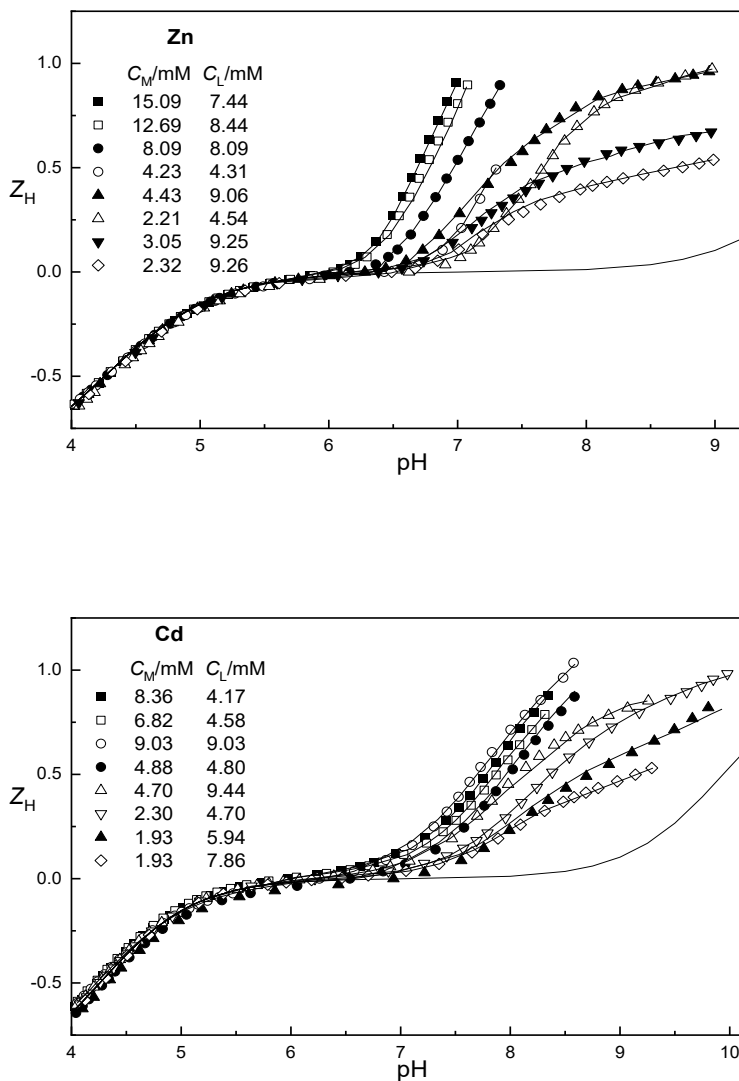


Figure 11. Part of the experimental data plotted as Z_H curves vs. pH for zinc(II) and cadmium(II) complex formation with 6-methylpyridine-2-aldoxime HL. The full lines have been calculated using sets of proposed stability constants in Table 3. The lowest line refers to the ligand alone.

The formation of cadmium(II) complexes could be researched to pH range 8.0–8.5, and by using at least twofold ligand excess to pH range 9–10. On the titration curves in the pH range 8.8–9.3, a weak inflection point is observable at $C_H:C_M = 1.69$ –1.86. This refers to complexes with $p:r = 1.5$ and

2, but the wide pH range proves that the latter complex ($p:r = 2$) is not formed through deprotonation of the former (1.5). The Z_H curves (Figure 11) of the solutions exceed the zero level at somewhat higher pH range 6–7 than the Z_H curves of the zinc(II) solutions. The SUPERQUAD program calculated stability constants only for CdL^+ , CdL_2 , and $Cd_2L_2OH^+$ ($\chi^2 = 32.9$, $s = 2.72$; 263 data points from eight titrations). Due to the large size of cadmium (II) ion, the polymerization of CdL^+ is weak. The proportion of $Cd_2L_2OH^+$ remains small (Figure 12) and CdL_2 is the main species in the pH range 8.5–10.0. The stepwise stability difference $\log(K_1:K_2)$ between CdL^+ ($\log K_1 = 4.23$) and CdL_2 ($\log K_2$

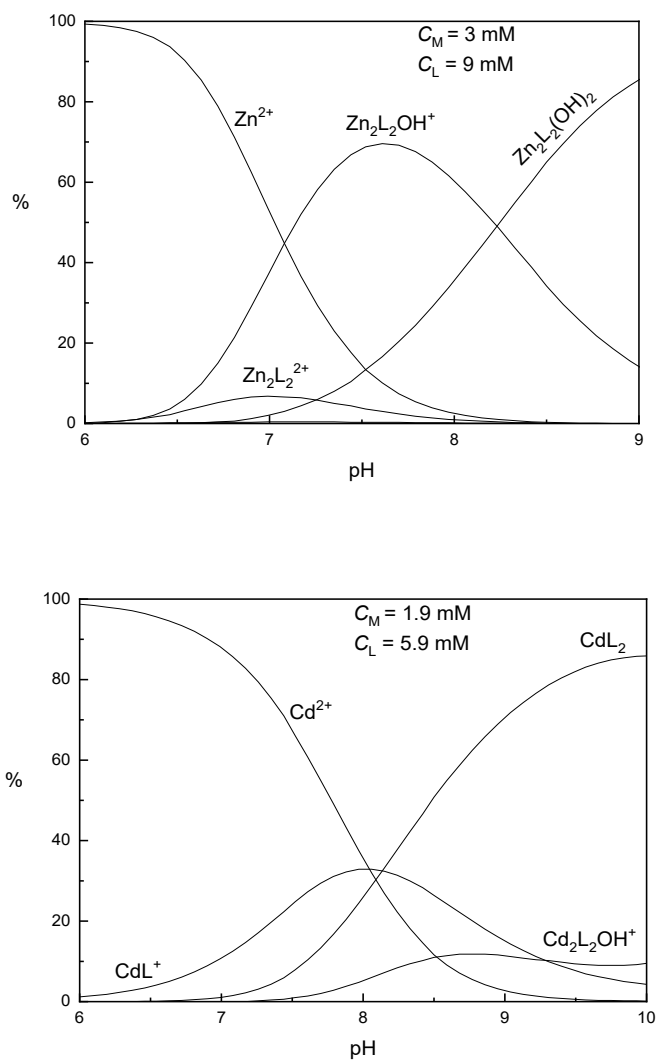


Figure 12. Examples of the concentration distribution of zinc(II) and cadmium(II) species vs. pH with 6-methylpyridine-2-aldoxime solutions.

= 4.17, $\log \beta_2 = 8.39$) is 0.06, proving that also the oximate groups of CdL_2 are perpendicularly *trans* oriented forming intramolecular hydrogen bridges with the adjacent aqua ligands ($\text{NO}^- \cdots \text{H}_2\text{O} -$).

The complex formation of 6-methylpyridine-2-aldoxime in the pH range 4.5–6.5 is very weak with Zn^{2+} and Cd^{2+} ions (Figure 12) but not insignificant with Co^{2+} (Figure 10) and Ni^{2+} ions.¹² The known copper concentration of 5.00 $\mu\text{g/ml}$ determined at pH = 5 as $\text{Cu}(\text{HL})_2^+$ gives 4.95 $\mu\text{g/ml}$ Cu in the presence of 5000 $\mu\text{g/ml}$ Zn^{2+} or 1000 $\mu\text{g/ml}$ Cd^{2+} .¹⁶ The same copper concentration gives 5.26 $\mu\text{g/ml}$ Cu in the presence of 50 $\mu\text{g/ml}$ Co^{2+} and 5.20 $\mu\text{g/ml}$ Cu in the presence of 500 $\mu\text{g/ml}$ Ni^{2+} , if the solution contains tartaric acid 5 mg/ml.¹⁶ For the determination of copper in alloys of aluminum, zinc, antimony or tin, the measurement in alkaline appears advantageous. The known copper concentration of 5.00 $\mu\text{g/ml}$ determined at pH = 12 as gives CuL_2^- give exactly 5.00 $\mu\text{g/ml}$ Cu in the presence of 2500 $\mu\text{g/ml}$ Zn^{2+} .¹⁶ This proves that $\text{ZnL}_2(\text{OH})_2$ hydrolyzes completely in very alkaline solution but CuL_2^- is stable still at pH = 12.

3.3. 1-(2-Pyridinyl)ethanone oxime complexes

1-(2-pyridinyl)ethanone oxime is a derivative of pyridine-2-aldoxime, where the aldoxime hydrogen is replaced by a methyl $-\text{CH}_3$ group. It is also a derivative of acetaldoxime (predicted $\text{pK}_a = 11.82 \pm 0.10$),⁹⁰ where the aldoxime hydrogen is replaced by pyridine ring. It belongs to ketoximes. Other derivatives of acetaldoxime are acetophenone oxime ($\text{pK}_a = 11.48$),⁹¹ where the aldoxime hydrogen is replaced by a benzene ring, and acetoxime (at 24.9 °C $\text{pK}_a = 12.42$ at $I = 0$ and 12.20 at $I = 0.10 \text{ M}$).⁹² The electron-withdrawing pyridine and benzene rings decrease but the additional methyl group in acetoxime increases the electron density on the oxime group. Thus, the oxime dissociation is stronger in 1-(2-pyridinyl)ethanone oxime ($\text{pK}_a = 10.87$ in 0.1 M NaCl solution) than in acetaldoxime but weaker than in pyridine-2-aldoxime (10.00).¹¹ The increased electron density strengthens the $\text{NO}-\text{H}$ bond and in the protonated ligand H_2L^+ also the heterocyclic $\text{N}-\text{H}^+$ bond. So the protonation is in 1-(2-pyridinyl)ethanone oxime ($\log \beta_{101} = 3.968$) is stronger than in pyridine-2-aldoxime (3.590).

The complex formation equilibria of 1-(2-pyridinyl)ethanone oxime with divalent copper¹¹ and nickel¹² ions in aqueous 0.1 M NaCl solution at 25 °C have been studied earlier. In this work, the studied were continued to cobalt(II), zinc(II), and cadmium(II) ions.

In all the solutions, the pink color of the cobalt(II) ion changed with the first addition of NaOH, making the solutions yellowish or brownish. During titration, the solutions darkened to yellow-brown, and the attainments of equilibria became slow already in the pH range 2.7–2.9. This indicates the formation of low spin cobalt(II) complexes in such low pH ranges in the solutions and their at least

partial oxidation to cobalt(III) complexes. The dispersion of the Z_H curves (Figure 13) indicates that the complex formation should be strong already in the pH range 1.7–2.0. The low and narrow pH range is very unfavorable for determination of stability constants. The SUPERQUAD program calculated among the five complexes $\text{Co}(\text{HL})^{2+}$, $\text{Co}(\text{HL})_2^{2+}$, $\text{Co}(\text{HL})_3^{2+}$, $\text{Co}(\text{HL})\text{L}^+$ and $\text{Co}(\text{HL})_2\text{L}^+$ the stability constants generally only for the complexes $\text{Co}(\text{HL})^{2+}$, $\text{Co}(\text{HL})_3^{2+}$ and $\text{Co}(\text{HL})\text{L}^+$. This model is very unreliable because of the unusual stepwise stability order: $K_3 > K_1 > K_2$. Although the tris complex $\text{Co}(\text{HL})_3^{2+}$ were low spin, its stability should be weakened by Jahn–Teller distortion. It is also very improbable that the smaller-sized low spin tris complex $\text{Co}(\text{HL})_3^{2+}$ were a weaker acid by 2–3 log units than the high spin bis complex $\text{Co}(\text{HL})_2^{2+}$. Removing $\text{Co}(\text{HL})_3^{2+}$ led to further rejection of $\text{Co}(\text{HL})_2\text{L}^+$ and to calculation of the stability constants of the complexes $\text{Co}(\text{HL})^{2+}$, $\text{Co}(\text{HL})_2^{2+}$ and $\text{Co}(\text{HL})\text{L}^+$. The lowest limits of the pH ranges of the solutions could be set to 1.80, because the Z_H curves (Figure 13) of the solutions increases regularly. In this way, the program calculated the stability constant given in Table 4 with $\chi^2 = 12.58$ and $s = 2.94$. The sample standard deviation s is somewhat large, because of the low and narrow pH range, but still indicates a satisfactory explanation of the data. An example of the concentration distribution of the species is given in Figure 14.

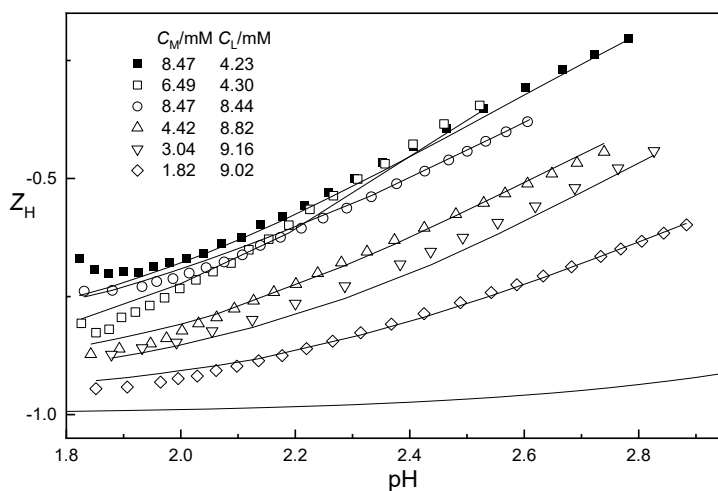


Figure 13. Part of the experimental data plotted as Z_H curves vs. pH for cobalt(II) complex formation with 1-(2-pyridinyl)ethanone oxime HL. The full lines have been calculated using sets of proposed stability constants in Table 4. The lowest line refers to the ligand alone.

Table 4. Proposed formulas and stability constants ^a of 1-(2-pyridinyl)ethanone oxime complexes relating to the reaction $p\text{H}^+ + q\text{M}^{2+} + r\text{HL} \rightleftharpoons (\text{H}^+)_p(\text{M}^{2+})_q(\text{HL})_r$ in aqueous 0.1 M Na(Cl) solution at 25 °C.

| <i>p</i> | <i>q</i> | <i>r</i> | Proposed formula | $\log \beta_{pqr} \pm 3\sigma$ | | | | |
|-----------------------------|----------|----------|-----------------------------------------------------------------------------------------------------------------|--------------------------------|------------|------------|-------------|-------------|
| | | | | M = Co | M = Ni | M = Cu | M = Zn | M = Cd |
| 0 | 1 | 1 | M(HL) ²⁺ | 3.74±0.09 | 4.98±0.03 | 5.63±0.06 | 2.723±0.015 | 2.370±0.015 |
| 0 | 1 | 2 | M(HL) ₂ ²⁺ | 7.0 ±0.3 | 9.39±0.04 | | 4.30±0.15 | |
| 0 | 1 | 3 | M(HL) ₃ ²⁺ | | 12.88±0.04 | | | |
| -1 | 1 | 1 | ML ⁺ | | | | | -5.56±0.05 |
| -1 | 1 | 2 | M(HL)L ⁺ | 4.25±0.15 | 4.58±0.05 | 8.09±0.03 | -0.86±0.02 | -2.93±0.06 |
| -2 | 1 | 2 | ML ₂ | | -3.55±0.06 | -0.32±0.05 | -9.74±0.16 | -11.73±0.05 |
| -1 | 1 | 3 | M(HL) ₂ L ⁺ | | 7.28±0.06 | | | |
| -2 | 1 | 3 | M(HL)L ₂ | | -0.09±0.06 | | | |
| -3 | 1 | 3 | ML ₃ ⁺ | | -9.31±0.06 | | | |
| -2 | 2 | 2 | M ₂ L ₂ ²⁺ | | | | -5.88±0.07 | |
| -3 | 2 | 2 | M ₂ L ₂ OH ⁺ | | | | -12.72±0.03 | -17.43±0.11 |
| -4 | 2 | 2 | M ₂ L ₂ (OH) ₂ | | | | -20.70±0.03 | -27.26±0.24 |
| -3 | 2 | 3 | M ₂ L ₃ ⁺ | | -1.33±0.08 | | | |
| -4 | 3 | 3 | M ₃ L ₃ OH ²⁺ | | | 9.72±0.05 | | |
| -5 | 3 | 3 | M ₃ L ₃ O ⁺ (or M ₃ L ₃ (OH) ₂ ⁺) | | | 3.47±0.06 | | |
| Number of points/titrations | | | | 129/6 | 433/8 | 450/12 | 425/8 | 458/8 |
| χ^2 | | | | 10.7 | 35 | 34.6 | 25.2 | 32.6 |
| <i>s</i> | | | | 2.93 | 2.1 | 2.90 | 2.1 | 2.33 |
| Ref. | | | | II | 12 | 11 | I | I |

^a Calculated by using the following protonation and acidity constants of the free ligand HL: $\log \beta_{101} = 3.968 (\pm 0.003)$ and $\log \beta_{-101} = -10.87 (\pm 0.03)$ (ref. 11).

Co(HL)²⁺ and Co(HL)₂²⁺ are less stable than Ni(HL)²⁺ and Ni(HL)₂²⁺ (Table 4). This and the normal stepwise stability order $\log K_1 = 3.74 < \log K_2 \approx 3.3$ prove that both of the cobalt(II) complexes are high spin. But the formation of Co(HL)L⁺ already in the pH range 2.0–2.1 proves that it is low spin unlike the corresponding pyridine-2-aldoxime complex. The replacing of the aldoxime hydrogen atom by a methyl group strengthens the ligand field around the metal ion and the stability of the complex. In the crystalline distorted square-pyramidal [Cu(HL)LCI]·3H₂O the N–O[−] bond (1.333 Å) is shorter than the N–OH bond (1.359 Å), but the Cu–NO[−] bond (2.004 Å) is longer than the Cu–NOH bond (1.975 Å).⁹³ In the deep orange octahedral [Ni(HL)L(H₂O)₂][NO₃], the N–O[−] bond (1.362 Å) is shorter than the N–OH bond (1.381 Å) and also the Ni–NO[−] bond (2.031 Å) is shorter than the Ni–NOH bond (2.042 Å).⁹⁴ An intramolecular hydrogen bridge exists between the *cis* oriented oxime and oximate groups (O–H···O[−]) in both of the crystalline complexes^{93,94} and

undoubtedly also in the aqueous $\text{Co}(\text{HL})\text{L}^+$. The Ni—NOH distances are 2.039 Å in the crystalline $\text{Ni}(\text{HL})_2\text{Cl}_2$,⁷⁴ 2.036 and 2.051 Å in $\text{Ni}(\text{HL})_2\text{Br}_2$,⁹⁴ 2.059 and 2.069 Å in $[\text{Ni}(\text{HL})_2(\text{NO}_3)_2]$, and 2.0670 and 2.0793 Å in $[\text{Ni}(\text{HL})_2(\text{OOCPh})_2]$.⁹⁵ All four complexes are slightly distorted octahedral with *trans* oriented oxime groups at N—Ni—N angles of 165–170° and *cis* oriented monodentate ligands at angles of 85–94°. ^{74,94,95} Their crystal structures show intramolecular hydrogen bonding between the oxime hydrogen and their adjacent bound anion or the uncoordinated oxygen atom of the monodentate nitrate —ONO₂ and phenolate —OOCPh ligands. The NOH···Cl distances are 2.23 and 2.24 Å,⁷⁴ the NOH···Br distances are 2.36 and 2.50 Å,⁹⁴ the NOH···ONO₂ distances are 1.88 Å (O···O distances 2.677 and 2.686 Å), and the NOH···OOCPh (O···O) distances are 1.58 (2.4848) and 1.616 (2.5190) Å.⁹⁵ In the crystalline $[\text{Ni}(\text{HL})_3](\text{NO}_3)_2 \cdot \frac{1}{2}\text{H}_2\text{O}$ the oxime groups are *mer* oriented, the Ni—NOH distances are 2.0631–2.0866 Å, and the oxime hydrogen atoms form hydrogen bonds to the free nitrate anions.⁹⁵ $\text{Co}(\text{HL})_3^{2+}$ and $\text{Co}(\text{HL})_2\text{L}^+$ have probably a similar structure, but they do not reach measurable concentrations in the pH range 2.5–2.9. This is not possible, if $\log \beta_{013} = 9.0$ –9.5 ($\log K_3 = 2.0$ –2.5) and $\log \beta_{-113} \leq 6.0$. At least $\text{Co}(\text{HL})_2\text{L}^+$ would be low spin and Jahn–Teller distorted.

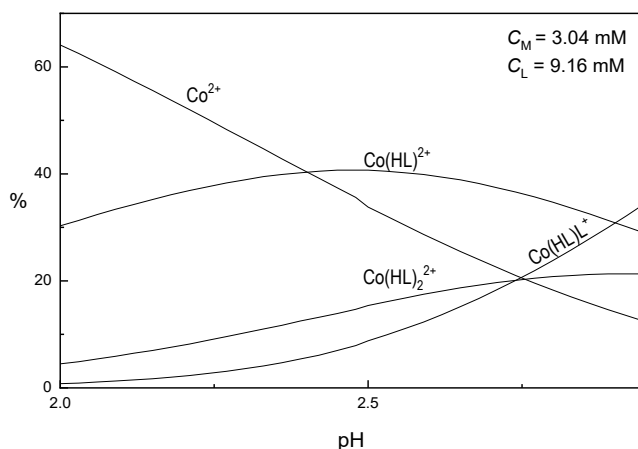


Figure 14. An example of the concentration distribution of the cobalt(II) species vs. pH with 1-(2-pyridinyl)ethanone oxime.

The zinc(II) solutions were in the presence of sufficient ligand excess still stable in the pH range 9–10. The Z_{H} curves (Figure 15) show complex formation already in the pH range 2–3. A weak inflection point appeared at $C_{\text{H}}:C_{\text{M}} = -1$ in the titration curves of solutions with $C_{\text{L}}:C_{\text{M}}$ ratios 3 and 4. SUPERQUAD calculations prove that the major species, $\text{Zn}(\text{HL})\text{L}^+$, reached maximum concentrations, 80–85 % of C_{M} , at $\text{pH} \approx 7.1$ around these two inflection points. In the further increase

of pH, $\text{Zn}_2\text{L}_2(\text{OH})_2$ displaces $\text{Zn}(\text{HL})\text{L}^+$ as major species. With cadmium(II), a colorless precipitate appeared in the $C_L:C_M = 4$ titration at pH *ca.* 9.0 and in the $C_L:C_M = 3$ titration at pH *ca.* 9.7. With the addition of more NaOH, the precipitates dissolved in the pH range 11.3–11.5. In backward titrations with HCl, the precipitates reappeared when the pH fell below 10.

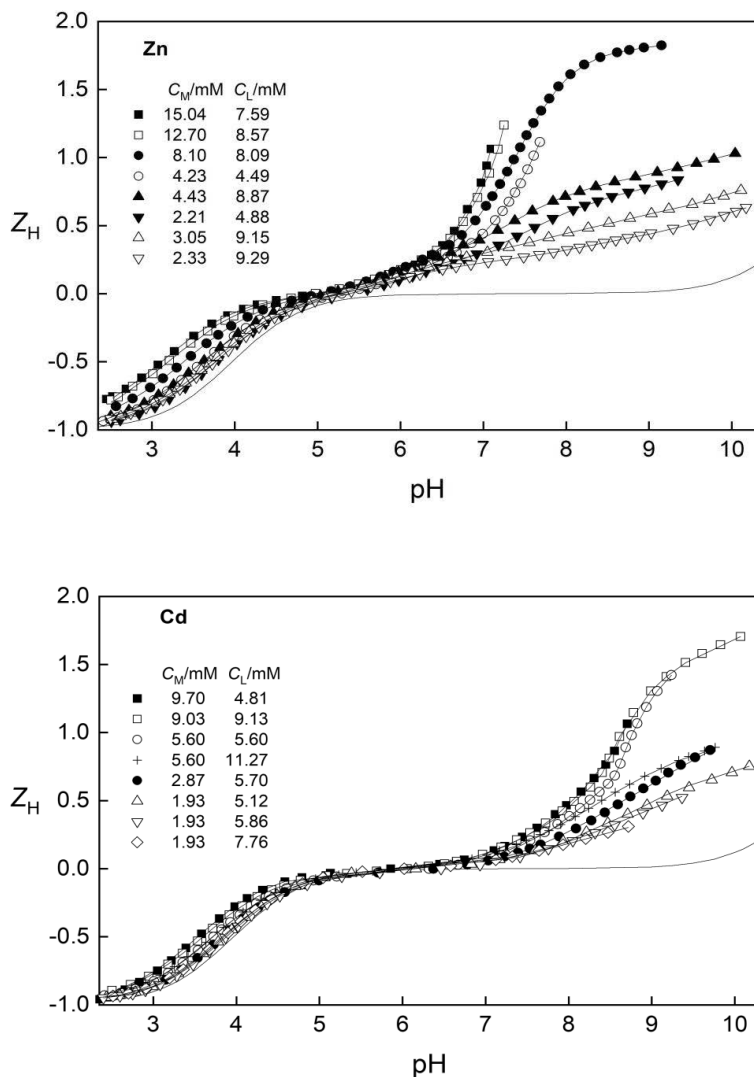


Figure 15. Part of the experimental data plotted as Z_H curves vs. pH for zinc(II) and cadmium(II) complex formation with 1-(2-pyridinyl)ethanone oxime HL. The full lines have been calculated using sets of proposed stability constants in Table 4. The lowest line refers to the ligand alone.

SUPERQUAD calculations gave the best χ^2 and s statistics for almost identical models of mono- and binuclear complexes for zinc(II) ($\chi^2 = 25.2$, $s = 2.10$; 425 data points from eight titrations) and

cadmium(II) ($\chi^2 = 30.0$, $s = 2.35$; 456 data points from eight titrations). The proposed complexes and their stability constants are given in Table 4. Examples of the concentration distributions of the zinc(II) and cadmium(II) species are given in Figures 16 and 17, respectively.

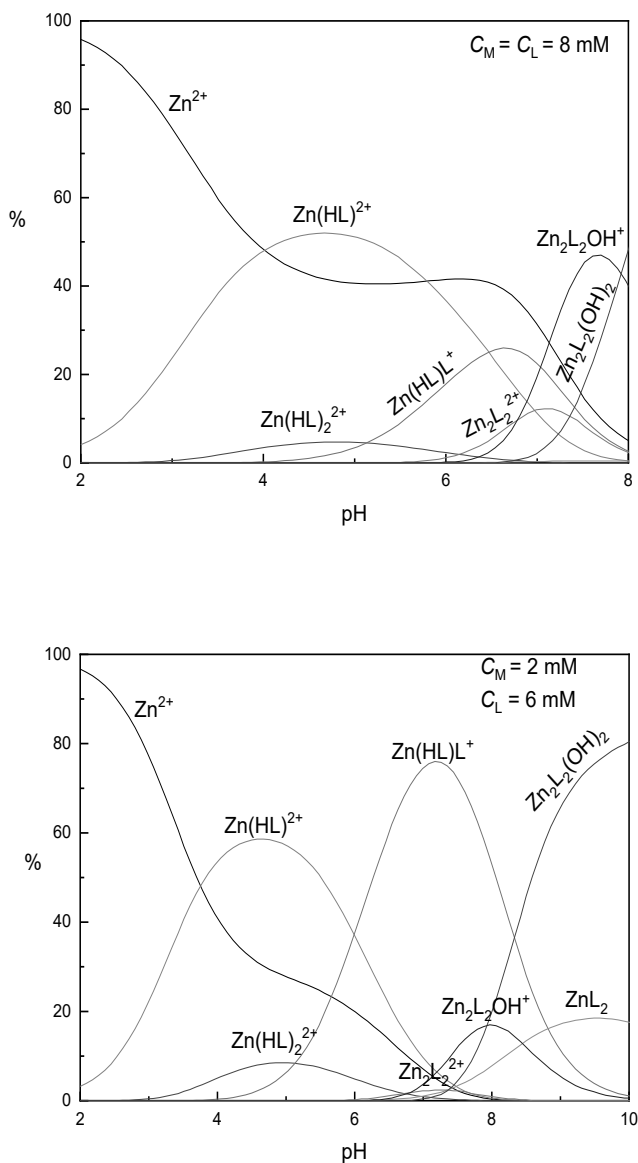


Figure 16. Examples of the concentration distribution of the zinc(II) species vs. pH with 1-(2-pyridinyl)ethanone oxime.

The 1-(2-pyridinyl)ethanone oxime complexes of type $\text{M}(\text{HL})_r^{2+}$ are clearly more stable but generally about 1–2 log units weaker acids than the corresponding pyridine-2-aldoxime complexes.

The increased electron density on the oxime NOH group by the methyl $-\text{CH}_3$ group strengthens the $\text{NO}-\text{H}$ bonds and also the $\text{N}-\text{M}^{2+}$ bonds. The values of the conventional stability constants calculated according to equation (31) show that the 1-(2-pyridinyl)ethanone oxime complexes ZnL_2 ($\log \beta_2 = 11.99$), CdL^+ ($\log \beta_1 = 5.31$), CdL_2 ($\log \beta_2 = 10.02$), and $\text{Cd}_2\text{L}_2\text{OH}^+$ ($\log \beta_{-322} + 2\text{p}\beta_{-101} = 4.30$) are in actual fact more stable than the corresponding pyridine-2-aldoxime complexes (10.58, 4.75, 9.09, and

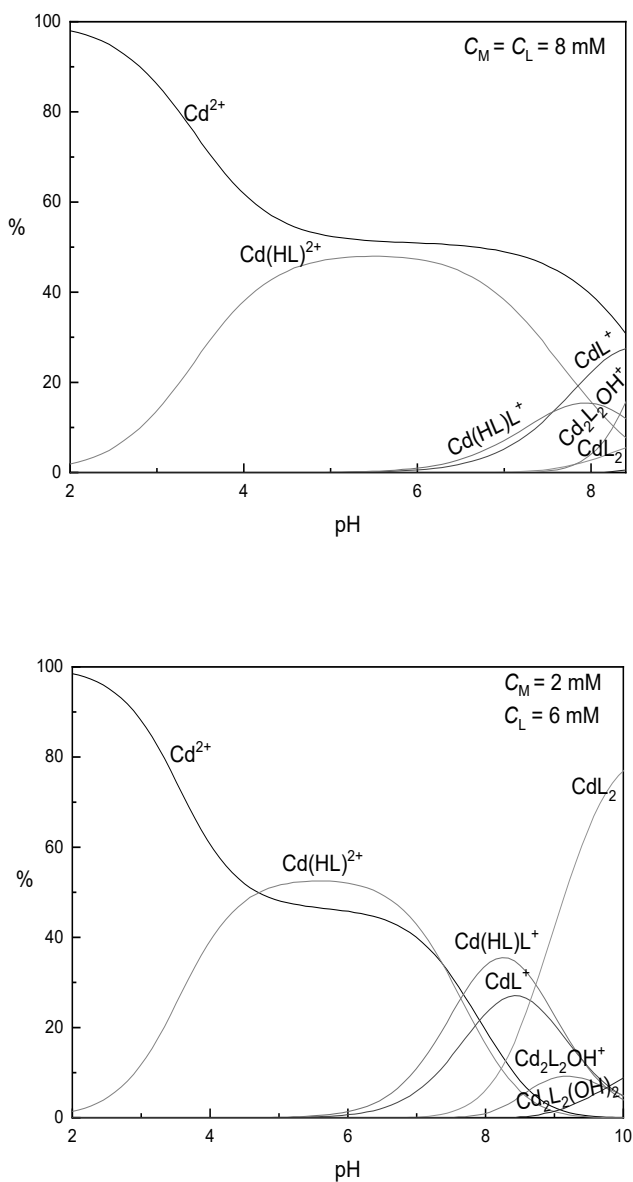


Figure 17. Examples of the concentration distribution of the cadmium(II) species vs. pH with 1-(2-pyridinyl)ethanone oxime.

3.36, respectively). In the crystalline roughly square-planar 1-(2-pyridinyl)ethanone oxime complex PtL_2 the oximate groups are *trans* oriented⁹⁶ and undoubtedly also in the aqueous ZnL_2 and CdL_2 .

Zn(HL)^{2+} disappear in the pH range 7.5–8.0 (Figure 16). If its $\text{pK}_a = 7.5\text{--}8.0$, the detection of ZnL^+ is very difficult with SUPERQUAD. ZnL^+ dimerizes easily via two oximate —NO— bridges to $\text{Zn}_2\text{L}_2^{2+}$, which hydrolyzes with the increase of pH to $\text{Zn}_2\text{L}_2\text{OH}^+$ and $\text{Zn}_2\text{L}_2(\text{OH})_2$. $\text{Zn}_2\text{L}_2(\text{OH})_2$ displaces the bis complexes Zn(HL)L^+ and ZnL_2 as main species in the pH range 8–9 (Figure 16) even in the presence of fourfold ligand excess.

The Cd—O bonds seem to be weaker than in the pyridine-2-aldoxime complexes, because the 1-(2-pyridinyl)ethanone oximate ion is a harder Lewis base and favors more hydrogen H^+ ion over cadmium(II) ion. Thus, the amounts of $\text{Cd}_2\text{L}_2\text{OH}^+$ and $\text{Cd}_2\text{L}_2(\text{OH})_2$ remain small. CdL^+ rather binds the free ligand HL with *cis* orientation of the oxime and oximate groups according reaction (33). The formed *cis*- Cd(HL)L^+ is stabilized by the intramolecular hydrogen bonding ($\text{O—H}\cdots\text{O}$), and its stepwise stability constant of $\text{Cd(HL)L}^+ \log(\beta_{-112}/\beta_{-111}) = 2.63 > \log \beta_{011} = 2.370$. The *trans* orientation of their oxime and oximate groups yields *trans*- Cd(HL)L^+ , which deprotonates in the pH range 7–10 to CdL_2 . In the pH range 9–10, CdL_2 is the main species in the presence of sufficient ligand excess (Figure 17).

The 1-(2-pyridinyl)ethanone oxime and 6-methylpyridine-2-aldoxime complexes $\text{Zn}_2\text{L}_2\text{OH}^+$ ($\text{pK}_a = 7.98$ and 8.29 , respectively) are unlike the corresponding pyridine-2-aldoxime complex ($\text{pK}_a = 9.36$) considerably more acidic than the aqua Zn^{2+} ion (9.15). Also the 1-(2-pyridinyl)ethanone oxime complex $\text{Cd}_2\text{L}_2\text{OH}^+$ ($\text{pK}_a = 9.83$) is more acidic than the aqua Cd^{2+} ion (11.8). This is surprising, because only one —OH— bridge can exit at the same time in $\text{Zn}_2\text{L}_2(\text{OH})_2$ and $\text{Cd}_2\text{L}_2(\text{OH})_2$, if the coordination spheres are still octahedral. The methyl —CH_3 groups accelerate the forward deprotonation reaction



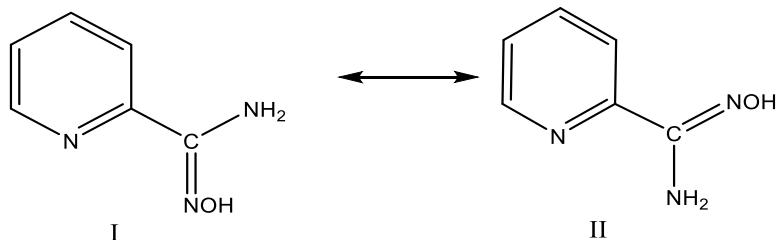
through increasing the bending vibrations of the $(\text{MNO})_2$ rings but retard the backward recombination reaction through expelling hydrogen/oxonium ($\text{H}^+/\text{H}_3\text{O}^+$) ions. The substitution of the hydrogen atoms of ammonia (NH_3) with methyl —CH_3 groups decreases the rate constant (k_R) of the recombination of proton (H^+) in aqueous solution at 25 °C from $4.3 \cdot 10^{10} \text{ M}^{-1} \text{ s}^{-1}$ with NH_3 , to $3.7 \cdot 10^{10}$, $3.1 \cdot 10^{10}$, and $2.5 \cdot 10^{10} \text{ M}^{-1} \text{ s}^{-1}$ with NH_2CH_3 , $\text{NH}(\text{CH}_3)_2$, and $\text{N}(\text{CH}_3)_3$, respectively.⁹⁷ In other recombination reactions of H^+ the rate constants (k_R) are in aqueous solution at 25 °C, for example, with OH^- $1.3 \cdot 10^{11}$, with HS^- $7.5 \cdot 10^{10}$, with *meta*-nitrophenol $4.2 \cdot 10^{10}$, with *para*-nitrophenol $3.6 \cdot 10^{10}$,⁹⁸ with UO_2OH^+ $1.65 \cdot 10^{10}$,⁹⁹ with CuOH^+ $1 \cdot 10^{10}$,¹⁰⁰ with $\text{Co}(\text{NH}_3)_5\text{OH}^{2+}$ $4.8 \cdot 10^9$,¹⁰¹ and with AlOH^{2+} $4.4 \cdot 10^9 \text{ M}^{-1} \text{ s}^{-1}$.¹⁰⁰ They seem to decrease by a factor 0.3–0.5 for each added positive charge unit to the reaction partner.¹⁰⁰ If the recombination rate constant k_R of $\text{H}^+/\text{H}_3\text{O}^+$ with the uncharged

pyridine-2-aldoxime and 1-(2-pyridinyl)ethanone oxime complexes $\text{Zn}_2\text{L}_2(\text{OH})_2$ are about 4×10^{10} and $2 \cdot 10^{10} \text{ M}^{-1} \text{ s}^{-1}$, respectively, the deprotonation rate constant k_D of their parent complexes $\text{Zn}_2\text{L}_2\text{OH}^+$ are about 15–20 and 200 s^{-1} , respectively.

3.4. Pyridine-2-carboxamidoxime complexes

Pyridine-2-carboxamidoxime or pyridine-2-amidoxime is a derivative of pyridine-2-aldoxime, where the aldoxime hydrogen is replaced by an amide $-\text{NH}_2$ group. Orama and Saarinen⁹ have determined its protonation and acidity constants and the stability constants of its copper(II) and nickel(II) complexes in aqueous 0.1 M Na(Cl) solution at 25 °C. In this work, the stability constants have been determined for cobalt(II), zinc(II), and cadmium(II) complexes.

The free pyridine-2-carboxamidoxime HL ($\text{pK}_a = 11.7$) is a clearly weaker acid⁹ than 1-(2-pyridinyl)ethanone oxime (10.87) and pyridine-2-aldoxime (10.00) in 0.1 M Na(Cl) solution.¹¹ Also acetamidoxime ($\text{pK}_a = 13.21$) and benzamidoxime (12.36) are in NaCl solution at 0.3 M ionic strength¹⁰² weaker acids than acetoxime ($\text{pK}_a = 12.42$ at 24.9 °C),⁹² acetophenone oxime (11.48),⁹¹ acetaldoxime (11.82),⁹⁰ and benzaldoxime (10.7) at low ionic strength.⁵⁰ The electron-withdrawing benzene or pyridine ring decreases but the delocalization of the lone electron pair of the amide nitrogen increases the electron density on the oxime NOH group more than the methyl $-\text{CH}_3$ group does. The increased electron density strengthens the $\text{NO}-\text{H}$ bond and also the $\text{N}-\text{H}^+$ bond in the protonated ligand H_2L^+ . However, the protonation is slightly weaker in pyridine-2-carboxamidoxime HL ($\log \beta_{101} = 3.798 \pm 0.006$) than in 1-(2-pyridinyl)ethanone oxime (3.968 ± 0.003). The free uncharged pyridine-2-carboxamidoxime HL exists in the crystalline state^{103,104} and according to IR data also in solution¹⁰⁵ as the *syn* isomer, and the amide $-\text{NH}_2$ group and the pyridine nitrogen atom are on the same side of the $\text{C}(2)-\text{C}_{\text{ox}}$ bond (conformation II below). This conformation is caused by the



electrostatic repulsion forces between the lone electron pairs of the oxime ($\text{H}_2\text{N}-\text{C}=\text{N}-\text{OH} \leftrightarrow \text{H}_2\text{N}^+=\text{C}-\text{N}^--\text{OH}$) and pyridine nitrogens and by the intramolecular hydrogen bonding between amide hydrogens and the pyridine nitrogen ($\text{N}-\text{H} \cdots \text{N}$). However, the complex formation of the ligand HL occurs through the pyridine and oxime nitrogens, which requires the rotation of the

amidoxime group about the C(2)—C_{ox} bond (to conformation I).¹⁰⁴ Apparently, the rotation also occurs, when the ligand HL protonates to H₂L⁺, because the conformation I allows a stronger intramolecular hydrogen bonding N—H⁺⋯N—OH between the pyridine and oxime nitrogens. 2-aminoacetamidoxime¹ (log β_{101} = 7.942) and its *N*-alkyl^{1,2,4} derivatives (7.214–8.260) protonate undoubtedly in their amino groups and, at low pH, their amidoxime groups also protonate with stepwise protonation constants log (β_{201}/β_{101}) = 1.351–2.467 in 1.0 M Na(ClO₄),¹ in 0.1 M Na(ClO₄),² or in 1.0 M Na(Cl) solution.⁴ However, no accurate value for the second protonation constant β_{201} has been determined for pyridine-2-carboxamidoxime.⁹ The reasons are the short distances between the amide, oxime, and pyridine nitrogens, and the repulsion forces between the protons and amide hydrogens. In addition, the pyridine ring is much more rigid than the 2-aminoacetamidoxime molecules. According ¹H NMR spectra acetamidoxime (log β_{101} = 5.78 at 0.0 M ionic strength) and according UV/VIS spectra also benzamidoxime (4.85) protonate in their oxime nitrogens (H⁺—NOH), not in their amide nitrogens.¹⁰²

The pink color of cobalt(II) ion was changed to yellowish or brownish already while adding the ligand to the solutions. Only one solution (C_M = 7.26 mM, C_L = 7.23 mM) was clearly pink in the beginning of titration. Also, it was changed to brownish already after the first addition of NaOH. When titrating and enhancing of pH, the solutions were darkened. The attainments of equilibria became very slow already at pH 3.67–4.73. In the end of titration, the solutions were yellowish or dark brown. On standing overnight, they became slightly darker and their yellowish tone weakened. No observed precipitate was formed from the solutions. No structure of the complexes could be determined with X-ray diffraction.

SUPERQUAD analysis showed only two deprotonated complexes Co(HL)L⁺ and Co(HL)₂L⁺ formed in addition to Co(HL)²⁺, Co(HL)₂²⁺, and Co(HL)₃²⁺. The fit to the experimental data was not good: χ^2 = 32.0 and s = 3.92 with σ_V = ±0.02 ml and σ_E = ±0.1 mV. The Z_H curves (Figure 18) did not exceed the zero level, showing that the deprotonated complexes were not formed in large amounts. The high Z_H values of the 1:1 titrations point to the presence of protonated complexes with H₂L⁺ as ligand. After the tests of many species, SUPERQUAD analysis showed that only protonated complex with *pqr* combination 123 and probable formula Co₂(HL)₂H₂L⁵⁺ showed satisfactory fit with experimental data. Because the stable pH ranges were very narrow, their lower limits in calculation of the stability constants were chosen to 1.80, where the weighting coefficients of the titration points were small (in general between ±3.0) in spite of the great liquid junction potential. The stability constants are given in Table 5. SUPERQUAD analysis rejected all the deprotonated polynuclear complexes. Examples of the concentration distribution of the species are in Figure 19.

The Co(HL)₂L⁺ complex was only observable in the presence of fivefold ligand excess, where its concentration was in maximum 12–13 % of C_M . This is the reason to the very great inaccuracy of

its stability constant $\log \beta_{-113} = 5.1 \pm 0.3$. The model of Table 5 without $\text{Co}(\text{HL})_2\text{L}^+$ gave $\chi^2 = 6.00$ and $s = 1.84$.

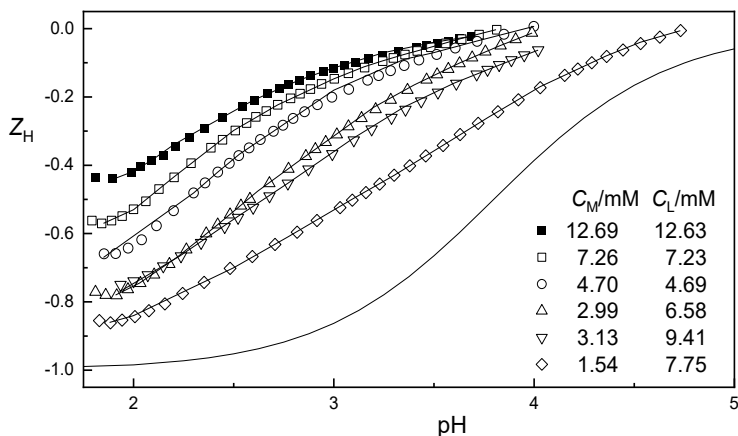


Figure 18. Part of the experimental data plotted as Z_H curves vs. pH for cobalt(II) complex formation with pyridine-2-carboxamidoxime HL. The full lines have been calculated using sets of proposed stability constants in Table 5. The lowest line refers to the ligand alone.

The slow attainment of equilibria already in the pH range 3.7–4.8 depending on the solution can be due to the slow reactions of the formed cobalt(III) complexes, and also the color changes for the solutions in the night. The brown color of the solutions formed during titrating never disappeared during backward titrating with HCl solution. This indicates that the oxidation reactions are irreversible. Because of the oxidation of the low spin cobalt complexes the stable pH range left very narrow. No polynuclear complexes except $\text{Co}_2(\text{HL})_2\text{H}_2\text{L}^{5+}$ could be observed yet in the pH range 4.0–4.8. The little χ^2 and s values, however, indicate that the amounts of the possible cobalt(III) complexes were yet small in the used pH ranges.

The zinc(II) solutions could be titrated to pH range 7.0–8.4, but the cadmium(II) solution with $C_L:C_M = 3-4$ could be titrated to pH range 9–10. In the $C_L:C_M = 5$ titration of cadmium(II) a precipitate appeared at pH = 9.3 also with this ligand. The Z_H curves (Figure 20) show complex formation for both of the metal ion already in the pH range 2–3. The model of mono and bis complexes with oximate and hydroxo bridged binuclear complexes $\text{Zn}_2\text{L}_2^{2+}$, $\text{Zn}_2\text{L}_2\text{OH}^+$, and $\text{Zn}_2\text{L}_2(\text{OH})_2$ observed with the previous ligands proved unsatisfactory ($\chi^2 = 44.6$ and $s = 2.99$). Addition of a tetranuclear species with the pqr combination –644 to the model gave a considerably better fit to the data. Some binuclear species $\text{Zn}_2\text{L}_2^{2+}$ or $\text{Zn}_2\text{L}_2\text{OH}^+$, but not $\text{Zn}_2\text{L}_2(\text{OH})_2$, also seem to be formed in the pH range 7–8. In

this pH range, the hydrolyzed species $\text{Zn}_2\text{L}_2\text{OH}^+$ is more probable. The cadmium(II) complexes are less stable and undergo less polymerization. The SUPERQUAD program calculated stability constants for CdL^+ and the pqr combination -644 but rejected the pqr combination -322 .

Table 5. Proposed formulas and stability constants of pyridine-2-carboxamidoxime complexes relating to the reaction $p\text{H}^+ + q\text{M}^{2+} + r\text{HL} \rightleftharpoons (\text{H}^+)_p(\text{M}^{2+})_q(\text{HL})_r$ in aqueous 0.1 M Na(Cl) solution at 25 °C.^a

| <i>p</i> | <i>q</i> | <i>r</i> | Proposed formula | $\log \beta_{pqr \pm 3\sigma}$ | | | |
|-----------------------------|----------|----------|--------------------------------------------------|--------------------------------|-------------|-------------|-------------|
| | | | | M = Co | M = Ni | M = Zn | M = Cd |
| 0 | 1 | 1 | $\text{M}(\text{HL})^{2+}$ | 3.94±0.04 | 4.93±0.10 | 3.03±0.02 | 2.53±0.01 |
| 0 | 1 | 2 | $\text{M}(\text{HL})_2^{2+}$ | 7.51±0.04 | 9.52 | 5.47±0.03 | 4.17±0.07 |
| 0 | 1 | 3 | $\text{M}(\text{HL})_3^{2+}$ | 10.44±0.06 | 13.92 | | |
| -1 | 1 | 1 | ML^+ | | | | -6.53±0.07 |
| -1 | 1 | 2 | $\text{M}(\text{HL})\text{L}^+$ | 2.44±0.21 | 1.76±0.18 | -2.33±0.08 | -4.28±0.15 |
| -2 | 1 | 2 | ML_2 | | -6.84±0.12 | -10.96±0.23 | -13.44±0.08 |
| -1 | 1 | 3 | $\text{M}(\text{HL})_2\text{L}^+$ | 5.1 ±0.3 | 5.69±0.09 | | |
| -2 | 1 | 3 | $\text{M}(\text{HL})\text{L}_2$ | | -3.99±0.09 | | |
| -3 | 1 | 3 | ML_3^- | | -14.84±0.09 | | |
| -3 | 2 | 2 | $\text{M}_2\text{L}_2\text{OH}^+$ | | | -14.32±0.22 | |
| -6 | 4 | 4 | $\text{M}_4\text{L}_2(\text{L}-\text{H})_2^{2+}$ | | | -24.96±0.13 | -34.48±0.17 |
| 1 | 2 | 3 | $\text{M}_2(\text{HL})_2\text{H}_2\text{L}^{5+}$ | 16.22±0.08 | | | |
| Number of points/titrations | | | | 202/6 | 407/7 | 379/8 | 400/8 |
| χ^2 | | | | 6.55 | 30.3 | 15.5 | 48.6 |
| <i>s</i> | | | | 1.73 | 1.7 | 2.15 | 1.44 |
| Ref. | | | | II | 9 | IV | IV |

^a The protonation and acidity constants of the free ligand (HL) and the stepwise stability and acidity constants of $\text{Cu}(\text{HL})_2^{2+}$ are given in Table 6.

SUPERQUAD calculations gave the best χ^2 and *s* statistics for almost identical models of mono- and binuclear complexes for zinc(II) ($\chi^2 = 15.5$, *s* = 2.15; 379 data points from eight titrations) and cadmium(II) ($\chi^2 = 48.6$, *s* = 1.44; 400 data points from eight titrations). The proposed complexes and their stability constants are given in Table 5. Examples of the concentration distributions of the zinc(II) and cadmium(II) species are given in Figure 21.

The pyridine-2-carboxamidoxime complexes of type $\text{M}(\text{HL})_2^{2+}$ and $\text{M}(\text{HL})_3^{2+}$ are generally slightly more stable, but about 2–3 $\text{p}K_{\text{a1}}$ units weaker acids than the corresponding 1-(2-pyridinyl)ethanone oxime complexes (Table 6). The delocalized lone electron pair of the amide nitrogen lengthens the N–OH distances and strengthens the NO–H and N– M^{2+} bonds more than the methyl –CH₃ group. The N–OH distances are in the free pyridine-2-carboxamidoxime HL 1.419–

1.420 Å,^{103,104} in other free amidoximes 1.415–1.438 Å,^{106–110} and in amidoxime complexes generally 1.395–1.426 Å,^{111–119} but in free aldoximes, ketoximes and in their complexes only 1.35–1.39 Å.^{64,93,94}

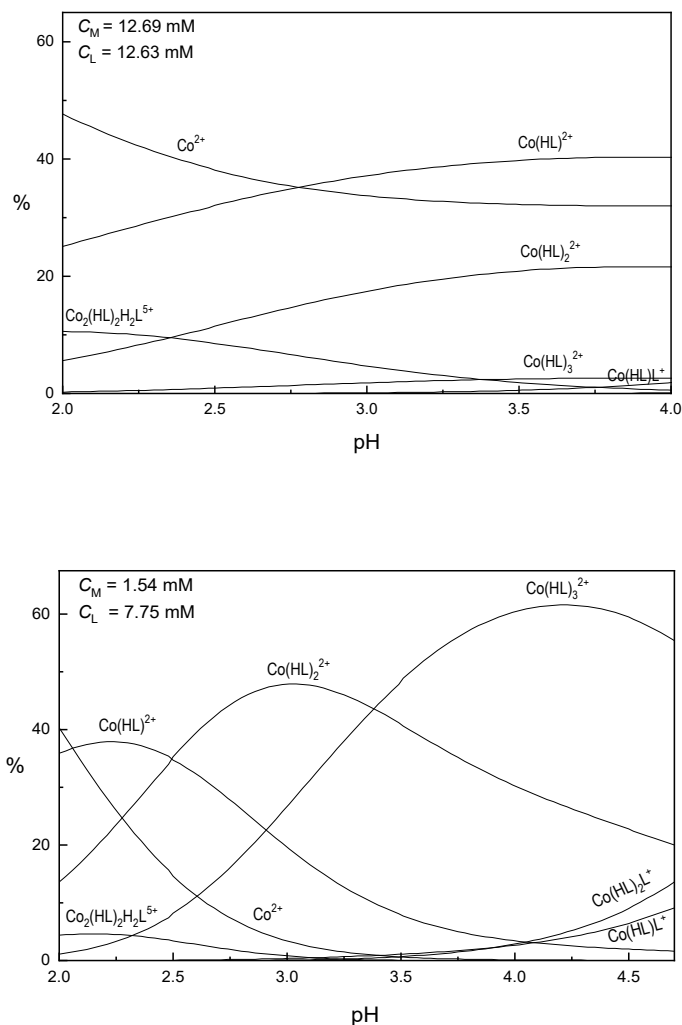


Figure 19. Examples of the concentration distribution of the cobalt(II) species vs. pH with pyridine-2-carboxamidoxime.

Co(HL)_2^{2+} ($\text{p}K_{a1} = 5.07$) and Co(HL)_3^{2+} (5.3) are about 2–3 log units stronger acid than Ni(HL)_2^{2+} (7.76), Zn(HL)_2^{2+} (7.80) and Ni(HL)_3^{2+} (8.23) proving that Co(HL)L^+ and $\text{Co(HL)}_2\text{L}^+$ are low spin. They are easily oxidized to cobalt(III) complexes, which causes the very slow attainment of equilibria in the pH range 3.7–4.8. Co(HL)^{2+} , Co(HL)_2^{2+} , and Co(HL)_3^{2+} are undoubtedly high spin and reach very high concentrations in the presence of fivefold ligand excess (Figure 19) without observable

oxidation. According to the Irving–Williams stability order,⁶⁰ they are less stable than the corresponding nickel(II) complexes. However, the low spin $\text{Co}(\text{HL})\text{L}^+$ ($\log \beta_{-112} = 2.44$) with $t_{2g}^6 e_g$ electron structure is even more stable than $\text{Ni}(\text{HL})\text{L}^+$ (1.76). This proves that $\text{Ni}(\text{HL})\text{L}^+$ is high spin and octahedral with $t_{2g}^6 e_g^2$ electron structure. The approximately equal acidity constants of $\text{Ni}(\text{HL})_2^{2+}$ ($\text{p}K_{a1} = 7.76$ and $\text{p}K_{a2} = 8.63$) and $\text{Zn}(\text{HL})_2^{2+}$ (7.80 and 8.63) prove that $\text{Ni}(\text{HL})_2^{2+}$ and NiL_2 are also octahedral and high spin.

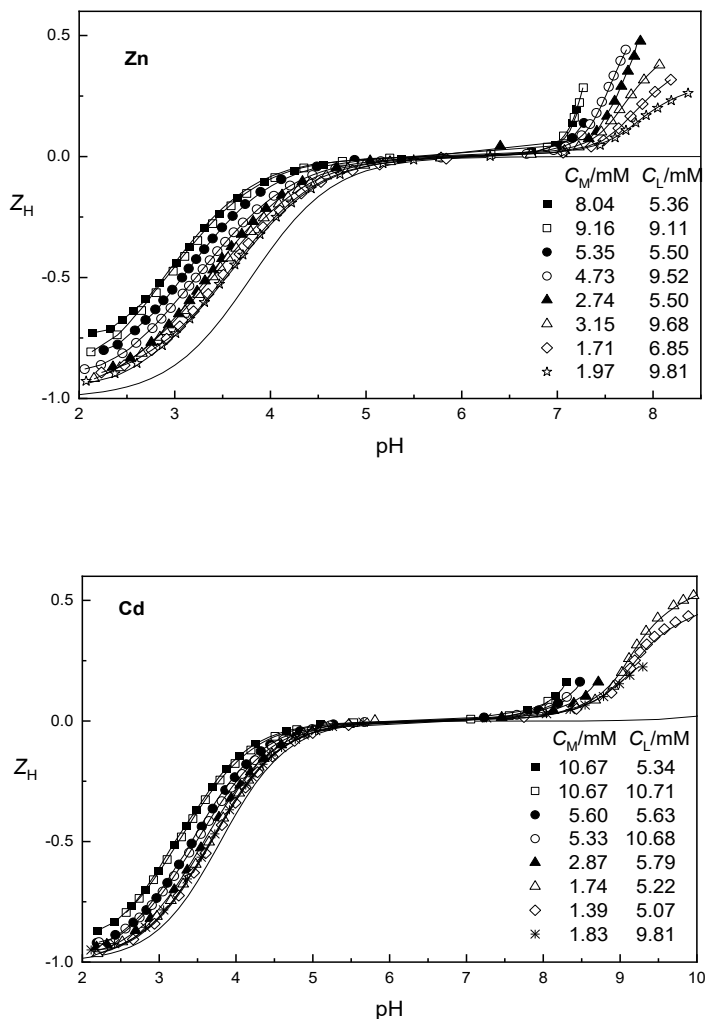


Figure 20. Part of the experimental data plotted as Z_H curves vs. pH for zinc(II) and cadmium(II) complex formation with pyridine-2-carboxamidoxime HL. The full lines have been calculated using sets of proposed stability constants in Table 5. The lowest line refers to the ligand alone

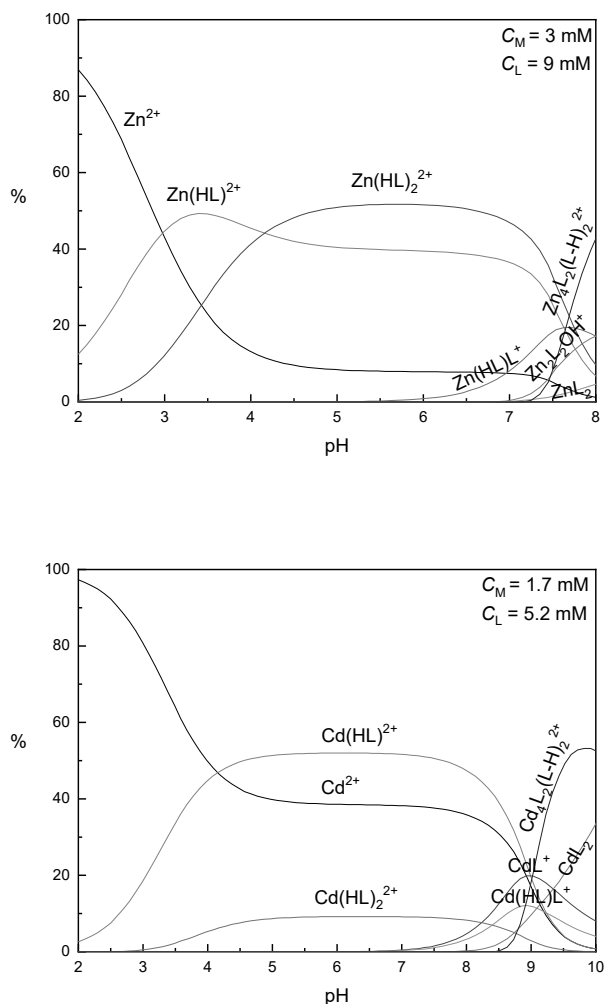


Figure 21. Examples of the concentration distribution of zinc(II) and cadmium(II) species vs. pH with pyridine-2-carboxamidoxime.

In aqueous 1.0 M NaClO_4 solution, 2-aminoacetamidoxime (Hao) and 2-(methylamino)-acetamidoxime (Hma) form orange-colored square-planar low spin complexes Ni(Hao)(ao)^+ and Ni(Hma)(ma)^+ ,¹ showing that Ni(Hao)_2^{2+} ($\text{p}K_a = 6.57$) and Ni(Hma)_2^{2+} (7.10) are considerably stronger acids than Zn(Hao)_2^{2+} (8.70), Zn(Hma)_2^{2+} (8.54),³ and the 2-(dimethylamino)acetamidoxime complex Ni(Hdma)_2^{2+} ($\text{p}K_a = 8.76$).¹ The crystalline $[\text{Ni(Hao)}_2(\text{H}_2\text{O})_2]\text{Cl}_2$ is octahedral, the oxime groups are *trans*-oriented in the equatorial plane and the aqua ligands in the axial position. The $\text{Ni}-\text{N}_{\text{ox}}$ distances are 2.049 Å and $\text{N}-\text{O}$ distances are 1.426 Å.¹¹¹ The formation of Ni(Hao)_3^{2+} requires that in its parent complex Ni(Hao)_2^{2+} the oxime ligands (Hao) are perpendicularly

coordinated. In the crystalline orange-red $[\text{Ni}(\text{Hao})(\text{ao})]\text{Cl}\cdot 1\frac{1}{2}\text{H}_2\text{O}$, the $\text{Ni}(\text{Hao})(\text{ao})^+$ molecules are square-planar and arranged so that every nickel(II) atom lies nearly perpendicularly above and below the amide $-\text{NH}_2$ nitrogen atoms of the adjacent molecules. The $\text{Ni}-\text{NH}_2$ distances are 3.189 and 3.325 Å. The oxime and oximate groups are *cis* oriented and intramolecular hydrogen bonded in $\text{O}\cdots\text{O}$ distance of 2.489 Å.¹¹¹ The $\text{Ni}-\text{N}_{\text{ox}}$ distances are 1.846–1.852 Å and the $\text{N}-\text{O}(\text{OH})$ distances are 1.391–1.397 Å.¹¹¹ The crystalline $[\text{Ni}(\text{Hdma})_2(\text{H}_2\text{O})_2]\text{Cl}_2$ is octahedral with bond angles $\text{N}_{\text{ox}}-\text{Ni}-\text{N}_{\text{ox}}$ 94.5°, $\text{Me}_2\text{N}-\text{Ni}-\text{NMe}_2$ 170.2°, and $\text{H}_2\text{O}-\text{Ni}-\text{OH}_2$ 82.8°, and with $\text{Ni}-\text{N}_{\text{ox}}$ distances of 2.064 and 2.086 Å.¹¹¹ Apparently, $\text{Ni}(\text{Hdma})(\text{dma})^+$ is also octahedral and high spin, because the dimethylamino ($\text{Me}_2\text{N}-$) groups cause steric interference with the planar *cis* orientation of the oxime and oximate groups.

Table 6. Stepwise stability and acidity constants of pyridine-2-carboxamidoxime complexes of type $\text{M}(\text{HL})_r^{z+}$ in aqueous 0.1 M Na(Cl) solution at 25 °C.^a

| M^{z+} | $\log K_1$ | $\text{p}K_{1a}$ | $\log K_2$ | $\text{p}K_{2a1}$ | $\text{p}K_{2a2}$ | $\log K_3$ | $\text{p}K_{3a1}$ | $\text{p}K_{3a2}$ | $\text{p}K_{3a3}$ | Ref. |
|------------------|---------------------|------------------|-----------------|-------------------|-------------------|-----------------|-------------------|-------------------|-------------------|------|
| H^+ | 3.798 ± 0.006^b | 11.7^c | | | | | | | | 9 |
| Co^{2+} | 3.94 ± 0.04 | | 3.57 | 5.07 | | 2.93 | 5.3 | | | II |
| Ni^{2+} | 4.93 ± 0.10 | | 4.59 ± 0.06 | 7.76 | 8.60 | 4.40 ± 0.03 | 8.23 | 9.68 | 10.85 | 9 |
| Cu^{2+} | $\geq 6^d$ | | 4.72 ± 0.03 | 4.61 ± 0.03 | | | | | | 9 |
| Zn^{2+} | 3.03 ± 0.02 | | 2.44 | 7.80 | 8.63 | | | | | IV |
| Cd^{2+} | 2.53 ± 0.01 | 9.06 | 1.64 | 8.45 | 9.16 | | | | | IV |

^a The stability constants (K_r) relate to the reaction $\text{M}(\text{HL})_{r-1}^{z+} + \text{HL} \rightleftharpoons \text{M}(\text{HL})_r^{z+}$. The acidity constants are for clarity symbolized as K_{ra} , K_{ra1} , K_{ra2} , and K_{ra3} . All the constants have been calculated disregarding the isomers using for example concentrations $[\text{M}(\text{HL})_r^{z+}] = \Sigma[\text{cis-M}(\text{HL})_r^{z+}] + \Sigma[\text{trans-M}(\text{HL})_r^{z+}]$. ^b $\log \beta_{101}(\text{M}(\text{HL})_r^{z+} = \text{H}_2\text{L}^+)$. ^c $= -\log \beta_{-101}$. ^d It could not be experimentally determined, because the formation $\text{Cu}(\text{HL})_2^{2+}$ was complete already at pH = 2. Its lower limit was estimated by using following data of a solution: $C_{\text{M}} = C_{\text{L}} = 4.997$ mM and $Z_{\text{H}} \approx 0$ (\approx constant) in pH range 2–3 (Figure 1 in Ref. 9).

$\text{Zn}(\text{Hao})_2^{2+}$ ($\text{p}K_{\text{a}} = 8.70$) and $\text{Zn}(\text{Hma})_2^{2+}$ (8.54) are weaker acids³ than $\text{Zn}(\text{HL})_2^{2+}$ (7.80), and also the free 2-aminoacetamidoxime ($\text{p}\beta_{-101} = 12.5 \pm 0.1$), 2-(methylamino)acetamidoxime (12.4 ± 0.1), and 2-(dimethylamino)acetamidoxime (12.3 ± 0.1) are weaker acids¹ than the free pyridine-2-carboxamidoxime (11.7).⁹ The electron-withdrawing pyridine ring increases the acidity of the oxime NOH group but lowers basicity of the pyridine and oxime nitrogens. Thus, copper(II), nickel(II), and zinc(II) ions form less stable complexes with pyridine-2-carboxamidoxime ($\log \beta_{101} = 3.798$) than with 2-aminoacetamidoxime (7.942) and 2-(methylamino)acetamidoxime (8.260).¹ In aqueous 1.0 M Na(ClO)₄ solution, the free 2-(dimethylamino)acetamidoxime ($\log \beta_{101} = 7.606$) is a stronger base and $\text{Cu}(\text{Hma})_2^{2+}$ ($\log \beta_{011} = 6.909 \pm 0.005$) and $\text{Cu}(\text{Hdma})_2^{2+}$ ($\log \beta_{012} = 11.894 \pm 0.009$, $\log K_2 = 4.985$)

more stable than in 0.1 M Na(ClO)₄ solution ($\log \beta_{101} = 7.214$, $\log \beta_{011} = 6.602 \pm 0.006$, $\log \beta_{012} = 11.284 \pm 0.021$), and $\log K_2 = 4.682$).² Due to the steric interference by the dimethylamino (Me₂N—) groups, Ni(Hdma)²⁺ ($\log \beta_{011} = 3.979$), Ni(Hdma)₂²⁺ ($\log \beta_{012} = 5.52$, $\log K_2 = 1.54$),¹ Zn(Hdma)²⁺ ($\log \beta_{011} = 2.500$), and Zn(Hdma)₂²⁺ ($\log \beta_{012} = 4.19$, $\log K_2 = 1.69$) are less stable than the corresponding pyridine-2-carboxamidoxime complexes. Zn(Hdma)(dma)⁺ and Zn(dma)₂ cannot be observed, because the uncomplexed aqua Zn²⁺ ion precipitates as Zn(OH)₂ in the pH range 7.0–7.5.³

Also, Ni(ao)₂, Ni(ma)₂, Ni(dma)₂,¹ Zn(ao)₂, and Zn(ma)₂,³ don't reach measurable concentrations in the pH range 8–9, where the precipitation or very slow attainment of equilibria in their solutions begins. Ni(Hao)(ao)⁺ displaces Ni(Hao)₃²⁺ as the main species in the pH range 8.0–8.5 and reaches about 80 % of C_M in the presence of fourfold ligand excess in the pH range 8.5–9.0. Ni(Hao)₃²⁺ does not deprotonate, although its proportion at pH = 9 is still about 20 % of C_M. Due to the steric requirements by the *N*-methyl groups the proportion of Ni(Hma)₃²⁺ remains only about 20 % of C_M even in the presence of 15-fold ligand excess, and Ni(Hma)(ma)⁺ reaches in the presence of fourfold ligand excess about 95 % of C_M.¹ This means that the pK_a value of *cis*-Ni(Hma)(ma)⁺ is at least 10–11. Apparently, the amide —NH₂ hydrogens form with their adjacent oxime and oximate oxygens some intramolecular hydrogen bonding N—H···O—H···[−]O···H—N strengthened also by the delocalization of the lone electron pair of the amide —NH₂ nitrogens.

ZnL₂ is probably formed in the pH range 7–8 (Figure 20) through deprotonation of *trans*-Zn(HL)₂²⁺ via *trans*-Zn(HL)L⁺. Ni(Hao)₂²⁺, Ni(Hma)₂²⁺, and Ni(Hdma)₂ disappear in the pH range 8–9 and the proportion of Ni(Hdma)(dma)⁺ remains only at about 5 % of C_M in the presence of fourfold ligand excess. Apparently also the proportions of the possible *trans*-Ni(Hao)(ao)⁺ and *trans*-Ni(Hma)(ma)⁺ remain so small that Ni(ao)₂ and Ni(ma)₂ cannot reach measurable concentration.

The octahedral high spin pyridine-2-carboxamidoxime complexes Ni(HL)L⁺ and NiL₂ cannot displace Ni(HL)₃²⁺ (pK_a = 8.23), Ni(HL)₂L⁺ (9.68), Ni(HL)L₂ (10.85), and NiL₃[−].⁹ In the crystalline [Ni(HL)₃](NO₃)₂·H₂O the oxime groups are *mer* oriented with N_{ox}—Ni—N_{ox} angles of 88.1, 96.8, and 171.1°. ¹¹² Apparently, the structure retains in the protonation of Ni(HL)₃²⁺ stepwise to NiL₃[−]. The formation of *mer*-Ni(HL)₃²⁺ requires the parent complex *trans*-Ni(HL)₂²⁺ with perpendicularly coordinated ligands HL (pyridine rings). However, other isomers of Ni(HL)₂²⁺ are also possible.

The crystalline [Ni(HL)₂(NO₃)₂] is distorted octahedral with *cis*-oriented nitrate NO₃[−] ions coordinated as monodentate ligands and *trans*-oriented oxime NOH groups. ¹¹² The Ni—N_{ox} bonds (2.048 Å) are shorter, and the N_{ox}—Ni—N_{ox} angle (168.7°) is slightly smaller than those in the corresponding 1-(2-pyridinyl)ethanone oxime complex (2.059 and 2.069 Å, and 169.88°, respectively). ⁹⁵ The structures of [M(HL)₂(OOCCH₃)₂], where M = Ni, ¹¹³ Zn, ¹¹⁴ or Cd, ¹¹⁵ are similar with bond lengths: Ni—N_{ox} 2.054, ¹¹³ Zn—N_{ox} 2.110, ¹¹⁴ and Cd—N_{ox} 2.315 Å, ¹¹⁵ and following angles

$N_{ox}-Ni-N_{ox}$ 166.2,¹¹³ $N_{ox}-Zn-N_{ox}$ 161.0,¹¹⁴ and $N_{ox}-Cd-N_{ox}$ 159.0°.¹¹⁵ Also, the structure of $[Zn(HL)_2(OOCPh)_2]$ is similar with bond lengths $Zn-N_{ox}$ 2.133 Å, $Zn-N_{py}$ 2.203 Å, and the $N_{ox}-Zn-N_{ox}$ angle of 156.7°.¹¹⁴ The pyridine nitrogens are generally 0.06–0.10 Å further from the central atom than the oxime nitrogens. The oxime groups are able to form intramolecular hydrogen bonds with the uncoordinated oxygen atoms of the adjacent monodentate acetate $-OOCCH_3$ or phenolate $-OOCPh$ ligand and also with the adjacent amide $-NH_2$ hydrogens ($N-H\cdots O-H\cdots OC$). In $[Ni(HL)_2(OOCCH_3)_2]$ the $NOH\cdots OC$ distances are 1.73 Å ($NO\cdots OC$ distances are 2.561 Å) and the $N-H\cdots OH$ distances are 2.23 Å ($N\cdots O$ distances are 2.589 Å).¹¹³ In the other complexes the $NOH\cdots OC$ distances are 1.77–1.86 Å ($O\cdots O$ distances are 2.544–2.600 Å).^{114,115} In aqueous acidic solution the monodentate ligands are readily replaced by aqua ligands, but the structure of the bis complexes with perpendicularly *trans* oriented oxime groups is preserved. The repulsive forces between the partially positively charged aqua and oxime hydrogens can lead to dissociation of the aqua ligand allowing isomerization of the *trans*- $M(HL)_2^{2+}$ to *cis*- $M(HL)_2^{2+}$, which is deprotonated at a sufficiently high pH to *cis*- $M(HL)L^+$ stabilized by the intramolecular hydrogen bonding between the oxime and oximate oxygens and their adjacent amide hydrogens $N-H\cdots O-H\cdots O\cdots H-N$.

It must be noted that the stepwise logarithmic stability differences between $Co(HL)^{2+}$ and $Co(HL)_2^{2+}$ $\log(K_1/K_2) = 0.37$ and between $Ni(HL)^{2+}$ and $Ni(HL)_2^{2+}$ (0.35) are smaller than the statistical difference between octahedral mono and bis complexes (0.68).⁷⁹ Also $\log(K_2/K_3)$ between $Ni(HL)_2^{2+}$ and $Ni(HL)_3^{2+}$ is small (0.19) but markedly greater between $Co(HL)_2^{2+}$ and $Co(HL)_3^{2+}$ (0.64). The statistically small stability differences show significant strengthening of the ligand fields from $Ni(HL)^{2+}$ to $Ni(HL)_3^{2+}$ and from $Co(HL)^{2+}$ to $Co(HL)_2^{2+}$. The aqueous $Co(HL)_2^{2+}$ may be partly tetrahedral and able to form also *fac*- $Co(HL)_3^{2+}$. Due to the repulsion forces between the positively charged oxime protons *fac*- $Co(HL)_3^{2+}$ is less stable than *mer*- $Co(HL)_3^{2+}$. It is also possible that $Co(HL)_3^{2+}$ is partly low spin (if the energy level difference between its t_{2g} and e_g orbitals is $\Delta_o \approx 15\,000\text{ cm}^{-1}$ or $\approx 180\text{ kJ/mole}$).⁵¹ Apparently, the $Co-N$ distances are about 1.8–1.9 Å in the *xy* plane of the low spin $Co(HL)_3^{2+}$ but due to the Jahn–Teller distortion about 2.6–2.7 Å on the *z* axis of the complex. For example, in the crystalline oxamide dioximato complex $[Co(Hoad)_2]\cdot H_2O$ the cobalt(II) ions are low spin chelated by two oxamide dioximato $Hoad^-$ anions in *s-cis* conformation through their oxime NOH and oximate NO^- nitrogens in $Co-N_{ox}$ distances of 1.885–1.889 Å.¹¹⁶ The adjacent oxime and oximate groups form two intramolecular hydrogen bridges in $O\cdots O$ distances of 2.561 Å in the chelate molecules. The individual chelate molecules $Co(Hoad)_2$ are stacked in the lattice parallel to each other so that the amide $-NH_2$ nitrogen occupies the fifth and sixth coordination of the cobalt(II) from the upper and lower chelate molecules. The $Co-NH_2$ distances of 2.639 Å are smaller than the sum of van der Waals radii (3.25 Å) of nitrogen (1.55 Å) and cobalt (1.70 Å).^{116,117}

So the cobalt(II) ions are rather in Jahn–Teller distorted octahedral than in square-planar coordination environments.¹¹⁶ The brick-red $[\text{Ni}(\text{Hoad})_2] \cdot \text{H}_2\text{oad}$ has very similar structure.¹¹⁸ The interplanar distances along the stacks are 3.22 and 3.23 Å, but Ni–NH₂ distances are only 3.04 Å proving some bonding interaction between Ni and the axial NH₂ groups.

Apparently, the low spin $\text{Co}(\text{HL})_3^{2+}$ decomposes completely by Jahn–Teller distortion, but in $\text{Co}(\text{HL})_2\text{L}^+$ the oxime and oximate group and also the amide groups are able to intramolecular hydrogen bonding $\text{N}-\text{H} \cdots \text{O}-\text{H} \cdots \text{O}^- \cdots \text{H}-\text{O} \cdots \text{H}-\text{N}$ stabilizing the Jahn–Teller distorted complex, especially if the oxime and oximate groups are *fac* oriented. The intramolecular hydrogen bonding can also cause significant deviation of the axial Co–N bonds from the *z* axis so that they are short enough to form chelate rings.

In $[\text{Zn}(\text{HL})_2\text{NO}_3]\text{NO}_3$ the Zn–N_{ox} distances are 2.088 and 2.122 Å, and the Zn–N_{py} distances are 2.084 and 2.086 Å. The nitrate NO₃[−] ligand is at the borderline of anisobidentate/monodentate: one of its O–Zn distances is 2.180 Å, but the other is 2.470 Å.¹¹⁴ The O–Zn–O angle of 53.0(1)° is abnormally small for an octahedral coordination environment. If the oxygen atom in the longer O...Zn distance is considered non-bonding, the geometry about Zn can be described as much distorted trigonal bipyramidal, with the *trans* oriented oxime nitrogens at the N_{ox}–Zn–N_{ox} angle of 173.3° occupying the axial positions. The angles of the shorter O–Zn with the pyridine nitrogens (O–Zn–N_{py}) are 98.1 and 145.9°, and the N_{py}–Zn–N_{py} angle is 114.9°.¹¹⁴ In 0.1 M Na(Cl) solution, the water activity is so high that the only nitrate NO₃[−] ligand of $\text{Zn}(\text{HL})_2\text{NO}_3^+$ is replaced by two rather than one aqua ligand. In the absence of ligand field stabilization, the aqua ligands are readily dissociated, allowing for the isomerization of $\text{Zn}(\text{HL})_2^{2+}$.

The crystalline $[\text{Cu}(\text{HL})_2(\text{H}_2\text{O})]\text{Cl}_2$ is square-pyramidal: the ligands HL lie on the bottom with *trans* oriented oxime NOH groups and the aqua ligand lies on the top of the pyramid.^{104,119} The Cu–N_{ox} distances are 1.969–1.971 Å, the Cu–OH₂ distance is 2.238–2.248 Å,^{104,119} and the N_{ox}–Cu–N_{ox} angle is 172.8°.¹¹⁹ All attempts to prepare *cis*- $\text{Cu}(\text{HL})_2(\text{H}_2\text{O})\text{Cl}_2$ by Pearse *et al.*¹⁰⁴ were unsuccessful. Apparently, the repulsive forces between the positively charged oxime protons caused in rotation of the oxime OH groups around the N–OH bonds expel the oxime groups from the *cis* positions.

In aqueous 0.1 M Na(Cl) solution $\text{Cu}(\text{HL})_2^{2+}$ is probably octahedral and the oxime ligands (HL) are *trans*-oriented on the *xy* plane of the complex and the aqua ligands on its *z* axis. Due to the Jahn–Teller distortion, the Cu–OH₂ bonds are weak. The dissociation of one aqua ligand allows the isomerization of *trans*- $\text{Cu}(\text{HL})_2^{2+}$ to *cis* and following deprotonation to $\text{Cu}(\text{HL})\text{L}^+$. The octahedral $\text{Co}(\text{HL})_2^{2+}$ can also isomerize via tetrahedral $\text{Co}(\text{HL})_2^{2+}$, but $\text{Co}(\text{HL})\text{L}^+$ can also be formed through coordination of free ligand HL to $\text{Co}(\text{HL})_2^{2+}$ with *cis* orientation of the oxime groups and following

deprotonation already in the pH range 2–3 (Figure 19). $\text{Zn}(\text{HL})\text{L}^+$ can be formed in a similar way in the pH range 6–8, where the proportion of $\text{Zn}(\text{HL})^{2+}$ is high (Figure 21). Thus, the *cis*- $\text{M}(\text{HL})_2^{2+}$ complexes can be much stronger acids but probably much less stable than their *trans* isomers.

$\text{Cd}(\text{HL})\text{L}^+$ is formed partly in a similar way than $\text{Zn}(\text{HL})\text{L}^+$ but mainly through coordination of free HL to CdL^+ with *cis* orientation of the oxime and oximate groups. According to the stepwise stability constants $\text{Cd}(\text{HL})\text{L}^+$ ($\log(\beta_{-112}/\beta_{-111}) = 2.25$) is more stable than $\text{Cd}(\text{HL})_2^{2+}$ ($\log(\beta_{012}/\beta_{011}) = 1.64$) but less stable than $\text{Cd}(\text{HL})_2^{2+}$ ($\log \beta_{011} = 2.53$) and even less stable than the corresponding 1-(2-pyridinyl)ethanone oxime complex $\text{Cd}(\text{HL})\text{L}^+$ ($\log(\beta_{-112}/\beta_{-111}) = 2.63$). The amidoximate oxygen is able to intramolecular hydrogen bonding in CdL^+ both with the adjacent aqua ligand and with the amide hydrogens ($\text{N}-\text{H}\cdots\text{O}^-\cdots\text{H}_2\text{O}-\text{Cd}$) but the ketoximate oxygen only with its adjacent aqua ligand ($\text{O}^-\cdots\text{H}_2\text{O}-\text{Cd}$). The methyl $-\text{CH}_3$ group is hydrophobic but the amide $-\text{NH}_2$ is hydrophilic and able also to intermolecular hydrogen bonding hydrogens with the water molecules ($\text{N}-\text{H}\cdots\text{OH}_2\cdots\text{O}-\text{N}$). Both the intramolecular and the intermolecular hydrogen bonding retard the forward coordination reaction of HL to CdL^+ and the hydrogen bonding between them ($\text{C}=\text{N}-\text{O}-\text{H}\cdots\text{O}-\text{N}-\text{Cd}$).

CdL_2 is formed partly through the deprotonation of *trans*- $\text{Cd}(\text{HL})_2^{2+}$ via *trans*- $\text{Cd}(\text{HL})\text{L}^+$ but mainly through the coordination of HL to CdL^+ with *trans* orientation of the oxime and oximate groups and following deprotonation. Due to the weak acidity of the oxime NOH group of the free HL ($\text{p}\beta_{-101} = 11.7$) the formation of CdL^+ and CdL_2 via reaction (32) is very small in the pH range 7–10. For the same reason, the stability constants and even also the conventional stability constants of CdL^+ ($\log \beta_1 = 5.17$) and CdL_2 ($\log \beta_2 = 9.96$, $\log K_2 = 4.72$) are smaller than those of the corresponding 1-(2-pyridinyl)ethanone oxime complexes ($\log \beta_1 = 5.31$, $\log \beta_2 = 10.02$, and $\log K_2 = 4.71$).

The weakly acidic pyridine-2-carboxamidoxime does not form binuclear complex $\text{Zn}_2\text{L}_2^{2+}$ with the six-membered $(\text{ZnNO})_2$ ring until in the pH range 7.0–7.5, where it is immediately deprotonated. The deprotonation of an aqua ligand leads to the formation of $\text{Zn}_2\text{L}_2\text{OH}^+$ with a hydroxo $-\text{OH}^-$ bridge besides the $(\text{ZnNO})_2$ ring, but also the amide groups of $\text{Zn}_2\text{L}_2^{2+}$ are deprotonable to form a tetramer. The structure of the tetramer is probably $\text{Zn}_4(\text{L}-\text{H})_2\text{L}_2^{2+}$ with a $(\text{ZnNO})_2$ central ring and two amido $-\text{NH}^-$ bridges (Figure 22). Ji *et al.*^{120,121} found that the reaction of $\text{NiX}_2 \cdot n\text{H}_2\text{O}$ ($\text{X}^- = \text{Cl}^-$, Br^- , NO_3^- , ClO_4^-) with pyridine-2-carboxamidoxime in aqueous acetonitrile solution (pH 9–10) produce red brown single-, double-, or triple-decker complexes, where two nickel(II) ions in square-planar NiN_3O environments and two nickel(II) ions in octahedral environments. Aqua ligands have been found only in double- or triple-decker compounds. In the double-decker compounds $[\text{Ni}_4(\text{L}-\text{H})_2\text{L}_2(\text{H}_2\text{O})_2]_2\text{X}_4 \cdot n\text{H}_2\text{O} \cdot (\text{CH}_3\text{CN})$ ($\text{X}^- = \text{ClO}_4^-$ and $n = 1$ or $\text{X}^- = \text{Br}^-$ and $n = 14$ without CH_3CN) each of the four octahedral coordination spheres is completed in its axial coordination

position by an aqua ligand and an oximate nitrogen or an oximate oxygen. Thus, the four octahedrally coordinated nickel(II) ions link the adjacent decks by four “pillars” (two Ni–N_{ox} and two Ni–O_{ox} bonds). In the triple-decker complexes, the adjacent decks are similarly linked by two Ni–N_{ox} and two Ni–O_{ox} bonds and the four octahedrally coordinated nickel(II) ions of two peripheral decks bind four terminal ligands.¹²⁰ Apparently, the formation of double and triple-decker compound instead of single-decker compounds with four aqua ligands is due to the formation of stronger ligand fields. The isolated single-decker compounds [Ni₄(L–H)₂L₂X₄](ClO₄)₂ have been isolated with X = imidazole,¹²⁰ 1-methylimidazole, pyridine, 3- or 4-methylpyridine¹²¹ coordinated axially to the octahedral nickel(II) ions through nitrogen atoms.

In the single-, double-, or triple-decker complexes the Ni–N/O distances are clearly shorter in the square-planar NiN₃O environments (generally 1.812–1.912 Å) than in the octahedral environments (2.009–2.269 Å). The N–O bonds of the doubly deprotonated (L–H)^{2–} ligands bridging two octahedral and one square-planar nickel(II) ions are longer (1.395–1.460 Å) than the N–O bonds of the singly deprotonated L[–] ligands bridging one square-planar and one octahedral nickel(II) ions (1.326–1.380 Å).^{120,121} This elongation is likely due to the coordination of the amido –NH[–] groups of the doubly deprotonated ligands.¹²¹ The Ni_{oct}–N–O–Ni_{oct} torsion angles of the central (NiNO)₂ rings are in the single-decker compounds generally 2.80–13.41° and in the double- and triple-decker compounds generally 11.06–18.70°.^{120,121} The inter-deck Ni–N_{ox} bond distances are 2.269–2.560 Å, the Ni_{oct}–N–Ni_{oct} angles are 91.55–93.7°, and the Ni_{oct}–O–Ni_{oct} angles are 97.37–104.7°.¹²¹

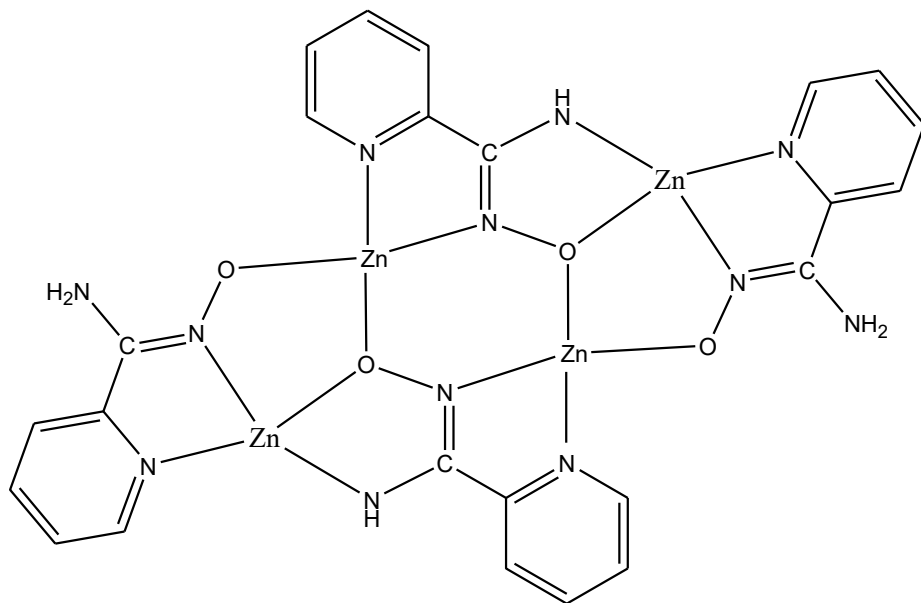


Figure 22. A proposed schematic representation for the tetranuclear complex ion [Zn₄(L–H)₂L₂]²⁺ projected in a plane. For clarity, the possible aqua ligands have been omitted.

Pyrazine-2-carboxamidoxime (Hpza) forms in aqueous 0.1 M NaCl solution $\text{Ni}_4(\text{pza-H})_2(\text{pza})_2^{2+}$ with $\log \beta_{-644} = -21.70$. It appears in the pH range 7.0–7.5 and its proportion in solution of $C_M = 1$ mM and $C_L = 3$ mM remains almost constant at about 10 % of C_M in the pH range 8–10. Brown $[\text{Ni}_4(\text{pza-H})_2(\text{pza})_2(\text{H}_2\text{O})_2](\text{NO}_3)_2 \cdot 2\text{H}_2\text{O}$ crystallized from aqueous methanol solution (pH = 9–10) has two square-planar and two octahedral nickel(II) ions, but each octahedrally coordinated nickel(II) ions binds an another tetramer in its pyrazine-4-nitrogen atom on the opposite site of the central $(\text{NiNO})_2$ ring.¹²² The aqua ligands complete the octahedral coordination. Each tetramer is surrounded by four other tetramers using two pyrazine-4-nitrogens as donor to coordinate with two nickel(II) ions and, in turn, two nickel(II) ions as acceptors for the coordination of two pyrazine-4-nitrogen atoms from another two adjacent tetramers. The Ni–N/O distances are 1.841–1.884 Å in the square-planar NiN_3O environments and 2.018–2.136 Å in the octahedral environments. The N–O bonds of the doubly deprotonated $(\text{pza-H})^{2-}$ ligands are 1.383 Å. In red-brown single-decker crystals of $[\text{Ni}_4(\text{pza-H})_2(\text{pza})_2\text{Py}_4]\text{X}_2 \cdot n\text{Py}$ ($\text{X}^- = \text{ClO}_4^-$ and $n = 2$ or $\text{X}^- = \text{NO}_3^-$ and $n = 4$) formed by slow diffusion of methanol to pyridine (Py) solution of $\text{NiX}_2 \cdot 6\text{H}_2\text{O}$ the octahedral nickel(II) ions are axially coordinated by two pyridine nitrogen atoms.¹²² Apparently, the complete formula of the aqueous tetramer is $\text{Ni}_4(\text{pza-H})_2(\text{pza})_2(\text{H}_2\text{O})_4^{2+}$, where both of the octahedral nickel(II) ions are axially coordinated by two water oxygen atoms.

Pyridine-2-carboxamidoxime does not form polynuclear nickel(II) complexes in aqueous solution.⁹ They are apparently displaced by $\text{Ni}(\text{HL})\text{L}_2$ ($\log \beta_{-213} = -3.99$) and NiL_3^- ($\log \beta_{-313} = -14.84$), which are much more stable than $\text{Ni}(\text{Hpza})(\text{pza})_2$ (–6.02) and $\text{Ni}(\text{pza})_3^-$ (–16.12). Also $\text{Ni}(\text{HL})^{2+}$ ($\log \beta_{011} = 4.93$), $\text{Ni}(\text{HL})_2^{2+}$ ($\log \beta_{012} = 9.52$), and $\text{Ni}(\text{HL})_3^{2+}$ ($\log \beta_{013} = 13.92$) are much more stable⁹ than $\text{Ni}(\text{Hpza})^{2+}$ (3.36), $\text{Ni}(\text{Hpza})_2^{2+}$ (5.97), and $\text{Ni}(\text{Hpza})_3^{2+}$ (8.37). Due to the second electron-withdrawing nitrogen atom, the pyrazine ring is a much weaker base than the pyridine ring. Thus, the free pyrazine ($\log \beta_{011} = 0.65$ at 1.0 M ionic strength¹²³) is a much weaker base than the free pyridine ($\log \beta_{101} = 5.25$ at 0 ionic strength⁴⁸ and 5.33 ± 0.01 in NaClO_4 solution at 0.1 M ionic strength⁴⁹). From this point of view, the protonation of the free pyrazine-2-carboxamidoxime ($\log \beta_{101} = 2.68$) is connected rather to the oxime nitrogen ($\text{H}^+ \text{—NOH}$) as in acetamidoxime ($\log \beta_{101} = 5.78$ at 0.0 M ionic strength) and benzamidoxime¹⁰² (4.85) than to the pyrazine-1-nitrogen.

2-(*N*-dimethylamino)- and 2-(*N*-diethylamino)acetamidoxime (Hdea) form similar tetranuclear complexes with copper(II) and nickel(II) ions in aqueous solution.^{1,2,4} The X-ray analysis proved that in the crystalline complexes $[\text{Cu}_4(\text{dma-H})_2(\text{dma})_2](\text{ClO}_4)_2 \cdot \text{H}_2\text{O}$ and $[\text{Cu}_4(\text{dea-H})_2(\text{dea})_2](\text{ClO}_4)_2$ all the four copper(II) atoms are in square-planar environments.^{2,4} In both of the tetramers, the Cu–N/O distances are 1.873–2.054 Å in the square-planar CuN_3O environments and 1.89–2.090 Å in the square-planar CuN_2O_2 environments.⁴ The N–O bonds of the doubly deprotonated ligands $(\text{dma-H})^{2-}$ (1.42 Å) and $(\text{dea-H})^{2-}$ (1.431 Å) bridging two copper(II) atoms of the central $(\text{CuNO})_2$ rings and one

copper(II) atom of a CuN_3O environment are also in these tetramers longer than the N—O bonds of the singly deprotonated ligands dma^- (1.34 Å) and dea^- (1.347 Å) bridging two copper(II) atoms of one CuN_3O and one CuN_2O_2 environments.⁴

The larger size of cadmium(II) ion especially weakens the Cd—O bonds and the polymerization of CdL^+ in this way. For this reason, the $(\text{CdNO})_2$ ring is much weaker than the $(\text{ZnNO})_2$ ring. $\text{Cd}_4(\text{L-H})_2\text{L}_2^{2+}$ is probably formed similar to $\text{Zn}_4(\text{L-H})_2\text{L}_2^{2+}$, but in the higher pH range 8.5–9.0 where the amido bridges outnumber the hydroxo bridges. Although $\text{Cd}_4(\text{L-H})_2\text{L}_2^{2+}$ is the major species in the pH range 9–10, CdL^+ and CdL_2 are remarkable competing species (Figure 21). In the further increase of pH, $\text{Cd}_4(\text{L-H})_2\text{L}_2^{2+}$ is seemingly displaced by CdL_2 . In $\text{Zn}_4(\text{L-H})_2\text{L}_2^{2+}$ and $\text{Cd}_4(\text{L-H})_2\text{L}_2^{2+}$ probably all the zinc(II) and cadmium(II) ions are in octahedral environments. The square-planar coordination is very improbable for the d^{10} structured metal ions.

The connection often found between the composition of the ternary hydrolytic complexes and the binary hydroxo species $\text{Cu}_2(\text{OH})_2^{2+}$, $\text{Ni}_4(\text{OH})_4^{2+}$, and $\text{Cd}_4(\text{OH})_4^{2+}$ of the metal ions^{124–129} would suggest competing amidoximato complexes with structures $\text{Cu}_4(\text{OH})_2\text{L}_4^{2+}$, $\text{Ni}_4(\text{OH})_4(\text{HL})_2\text{L}_2^{2+}$, and $\text{Cd}_2(\text{OH})_4(\text{HL})_2\text{L}_2^{2+}$ in aqueous solution. But for zinc(II) complexes, such structures are improbable. The binary hydrolysis of zinc(II) produces only ZnOH^{2+} and $\text{Zn}_2\text{OH}^{3+}$ before precipitation commences in the neutral region.^{58,28} Both zinc(II) and cadmium(II) ions form mainly binary complexes ZnIm_n^{2+} and CdIm_n^{2+} ($n = 1-4$) with imidazole (Im) and only at low $C_L:C_M$ ratios in small amounts also ternary complexes $\text{Zn}(\text{OH})\text{Im}^+$, $\text{Zn}(\text{OH})\text{Im}_3^+$, $\text{Zn}_2(\text{OH})\text{Im}_2^{3+}$, $\text{Zn}_2(\text{OH})\text{Im}_3^{3+}$,¹²⁷ and $\text{Cd}(\text{OH})\text{Im}^+$.¹²⁹ The d^{10} electron structures of zinc(II) and cadmium(II) favor coordination of nitrogen over oxygen. Thus, the dimer $\text{Zn}_2\text{L}_2^{2+}$ is mainly polymerized via two amido —NH— bridges to $\text{Zn}_4(\text{L-H})_2\text{L}_2^{2+}$, which becomes the major species in the pH range 7.5–8.0 (Figure 21). The proportions of the competing species $\text{Zn}_2\text{L}_2\text{OH}^+$ and ZnL_2 in the same pH range remain smaller. This is reflected as relatively large inaccuracies in the values of $\log \beta_{-322}$ and $\log \beta_{-212}$.

The alternative binuclear structure $\text{Zn}_2(\text{L-H})\text{L}^+$ or $\text{Zn}(\text{L-H})\text{ZnL}^+$ with an uncoordinated oximate oxygen (NO^-) atom in L^- can be excluded in the pH range 7.0–7.5. The ternary hydroxo complex $\text{Zn}_2\text{L}_2\text{OH}^+$ is much more probable, although in its parent complex $\text{Zn}_2\text{L}_2^{2+}$ ($\text{p}K_a < 7.0$) the $(\text{ZnNO})_2$ ring is probably in chair conformation as in $\text{Zn}_2\text{L}_2(\text{acac})_2$ crystallized from methanol with the Zn—N—O—Zn torsion angle of 59.5° (and the zinc(II) ions in distorted trigonal bipyramidal ZnN_2O_3 environments).¹¹⁴ In aqueous $\text{Zn}_2\text{L}_2^{2+}$ the $(\text{ZnNO})_2$ ring is flexible and bends easily to boat conformation, which allows the formation of a hydroxo bridge beside the oximato bridges. In the tetramers $\text{Zn}_4(\text{L-H})_2\text{L}_2^{2+}$ and $\text{Cd}_4(\text{L-H})_2\text{L}_2^{2+}$ the central $(\text{MNO})_2$ rings are apparently so rigid and that no hydroxo bridge can be formed beside their oximato bridges.

The structure of the binuclear complex $\text{Co}_2(\text{HL})_2\text{H}_2\text{L}^{5+}$ is very difficult to predict. It probably involves a combination of $\text{Co}(\text{HL})^{2+}$, $\text{Co}(\text{HL})_2^{2+}$, and a proton H^+ that connects the complex nuclei

with a hydrogen bridge. The bridge is broken by the deprotonation of H_2L^+ to HL. $\text{Co}_2(\text{HL})_2\text{H}_2\text{L}^{5+}$ reaches its maximum concentration in the pH range 1.7–2.1 and disappears in the same pH range (3.2–3.7), where $\text{Co}(\text{HL})\text{L}^+$ appears (Figure 19).

3.5. Pyridine-2-acetamidoxime complexes

Orama and Saarinen⁹ have determined for pyridine-2-acetamidoxime the protonation and acidity constants and the stability constants for its copper(II) and nickel(II) complexes in aqueous 0.1 M NaCl solution at 25 °C. In this work, the stability constants have been determined for cobalt(II), zinc(II), and cadmium(II) complexes.

In the free pyridine-2-acetamidoxime HL ($\log \beta_{101} = 5.017 + 0.003$),⁹ the protonation is about 0.2–0.3 log units weaker than in the free pyridine ($\log \beta_{101} = 5.25$ at 0 ionic strength,⁴⁸ 5.33 ± 0.01 at 0.1 M ionic strength in NaClO_4 solution⁴⁹) and about 0.7–0.8 log units weaker than in the free acetamidoxime ($\log \beta_{101} = 5.78$ at 0.0 M ionic strength).¹⁰² The $-\text{CH}_2-$ group effectively isolates the amidoxime group and the pyridine nitrogen and allows also the amide $-\text{NH}_2$ group to protonate with a stepwise protonation constant $\log (\beta_{201}/\beta_{101}) = 2.29 \pm 0.01$.⁹ This protonation is of same order or higher than in 2-aminoacetamidoxime ($\log (\beta_{201}/\beta_{101}) = 2.467$) and in its *N*-alkyl derivatives (1.351–2.112),^{1,2,4} but 1–2 log units smaller than in 3-aminopropanamidoxime (4.005) and in its *N*-alkyl derivatives (3.660–3.823).^{5,7} At low pH the free rotations around the C–C bonds allow intramolecular hydrogen bonding between the pyridine (or amino) and oxime nitrogens ($\text{N}-\text{H}^+\cdots\text{N}$) and in the higher pH range between the amide hydrogens and pyridine (or amino) nitrogens ($\text{N}-\text{H}\cdots\text{N}$). The oxime dissociation is in the free pyridine-2-acetamidoxime HL ($\text{p}K_{\text{a}} = 12.3$) weaker or about equally weak than in the free pyridine-2-carboxamidoxime (11.7),⁹ 2-aminoacetamidoxime (12.5),¹ 3-aminopropanamidoxime (11.5),⁵ and in their *N*-alkyl derivatives (12.0–12.4),^{1,5,7} but clearly stronger than in the free acetamidoxime ($\text{p}K_{\text{a}} = 13.21$ in NaCl solution at 0.3 M ionic strength).¹⁰² The increased acidity of 3-aminopropanamidoxime ($\text{p}K_{\text{a}} = 11.5$) is probably due to the intramolecular hydrogen bonding between the amino, oximate, and amide groups ($\text{N}-\text{H}\cdots\text{N}-\text{O}^-\cdots\text{H}-\text{N}$).

The formation of the cobalt(II) complexes could be followed up to pH range 6.0–6.2. Also, these cobalt(II) ion solutions changed during titrating from pink to yellow and finally to brown. Formation and oxidation of some low spin cobalt(II) complexes was observed in the SUPERQUAD calculation. All of the solutions with a more than twofold excess of ligand led to large χ^2 and *s* values and had to be removed from the SUPERQUAD calculation, which was run with only three solutions. The Z_{H} curves of the solutions are shown in Figure 23. The stability constants are given in Table 7 with the

earlier determined stability constants of the copper and nickel(II) complexes and the protonation constants of the ligand (HL) used in the SUPERQUAD calculation.

Table 7. Stability constants ($\log \beta_{pqr} \pm 3\sigma$) of pyridine-2-acetamidoxime complexes relating to reaction $p\text{H}^+ + q\text{M}^{2+} + r\text{HL} \rightleftharpoons (\text{H}^+)_p(\text{M}^{2+})_q(\text{HL})_r$ in aqueous 0.1 M NaCl) solution at 25 °C.

| M^{2+} | $\log \beta_{111}$ | $\log \beta_{011}$ | $\log \beta_{012}$ | $\log \beta_{-111}$ | $\log \beta_{-112}$ | $\log \beta_{-222}$ | $\log \beta_{-322}$ | Ref. |
|------------------|---------------------|---------------------|--------------------|---------------------|---------------------|---------------------|---------------------|------|
| H^+ | 7.307 ± 0.013^a | 5.017 ± 0.003^b | | -12.3^c | | | | 9 |
| Co^{2+} | 6.0 ± 0.5 | 2.56 ± 0.05 | 4.73 ± 0.07 | | -1.87 ± 0.14 | | | II |
| Ni^{2+} | | 3.59 ± 0.01 | 6.86 ± 0.02 | | -1.56 ± 0.05 | | -13.82 ± 0.02 | 9 |
| Cu^{2+} | | 5.31 ± 0.01 | 9.55 ± 0.03 | | | 4.7 ± 0.1 | | 9 |
| Zn^{2+} | | 1.79 ± 0.02 | | | | | -16.29 ± 0.05 | IV |
| Cd^{2+} | | 1.72 ± 0.02 | | -8.05 ± 0.11 | | | | IV |

^a = $\log \beta_{201}$. ^b = $\log \beta_{101}$. ^c = $\log \beta_{-101}$.

The proposed formulas of the cobalt(II) complexes in Table 7 are from left to right: $\text{Co}(\text{H}_2\text{L})^{3+}$, $\text{Co}(\text{HL})^{2+}$, $\text{Co}(\text{HL})_2^{2+}$ and $\text{Co}(\text{HL})\text{L}^+$. This model gives $\chi^2 = 7.87$ and $s = 1.28$ with $\sigma_E = \pm 0.1$ mV and $\sigma_V = \pm 0.02$ ml. The SUPERQUAD program rejects all other stability constants. The addition of a solution with $C_M: C_L \approx 1:3$ to the used series of the three solutions gives greater stability constants to all complexes in Table 3 with $\chi^2 = 82.6$ and $s = 3.86$. This indicates the formation of low spin cobalt(II) complexes in the increase of pH and their increasing oxidation to cobalt(III) complexes in the presence of a great ligand excess. The SUPERQUAD program interprets the formed cobalt(III) complexes probably as $\text{Co}(\text{HL})_2^{2+}$ and $\text{Co}(\text{HL})\text{L}^+$ and a part of complexes $\text{Co}(\text{HL})_2^{2+}$ as $\text{Co}(\text{HL})^{2+}$. This leads to unreliably great stability constants for the three complexes.

$\text{Co}(\text{HL})\text{L}^+$ ($\log \beta_{-112} = -1.87$) is only 0.3 log units less stable than $\text{Ni}(\text{HL})\text{L}^+$ (-1.56), although $\text{Co}(\text{HL})_2^{2+}$ ($\log \beta_{012} = 4.73$) is over two log units less stable than $\text{Ni}(\text{HL})_2^{2+}$ (6.86). This proves that $\text{Co}(\text{HL})\text{L}^+$ is low spin, but $\text{Co}(\text{HL})_2^{2+}$, $\text{Co}(\text{HL})^{2+}$, and $\text{Co}(\text{H}_2\text{L})^{3+}$ are high spin. $\text{Co}(\text{H}_2\text{L})^{3+}$ ($\log \beta_{111} = 6.0 \pm 0.5$) exists at low pH and deprotonates to $\text{Co}(\text{HL})^{2+}$ with $\text{p}K_a \approx 3.4$. Analogous complexes are also formed by 3-aminopropanamidoxime and its *N*-methylated derivatives with cobalt(II)⁸ and copper(II) ions.⁵ The positively charged pyridinium or ammonium group must be sufficiently far from the central metal ion (there are five atoms between the positive charges), and the chelate ring is possibly not closed. No polynuclear cobalt(II) complexes could be found. An example on the concentration distribution of the cobalt(II) species in solutions is given in Figure 24.

The zinc(II) solutions could be titrated only to pH range 7.0–7.5 and cadmium(II) solutions to pH range 8–9. The slight dispersion of the Z_H curves (Figure 25) demonstrates only weak complex formation for both metal ions. The Z_H curves exceed the zero level in the end of the titrations proving

some formation of deprotonated complexes. SUPERQUAD calculations gave the best χ^2 and s statistics for models $\text{Zn}(\text{HL})^{2+}$ and $\text{Zn}_2\text{L}_2\text{OH}^+$ ($\chi^2 = 11.7$, $s = 1.47$, 255 points from eight titrations) and $\text{Cd}(\text{HL})^{2+}$ and CdL^+ ($\chi^2 = 39.7$, $s = 1.11$, 230 points from eight titrations). The stability constants are given in Table 7. Examples of the concentration distributions of the zinc(II) and cadmium(II) species are given in Figure 26.

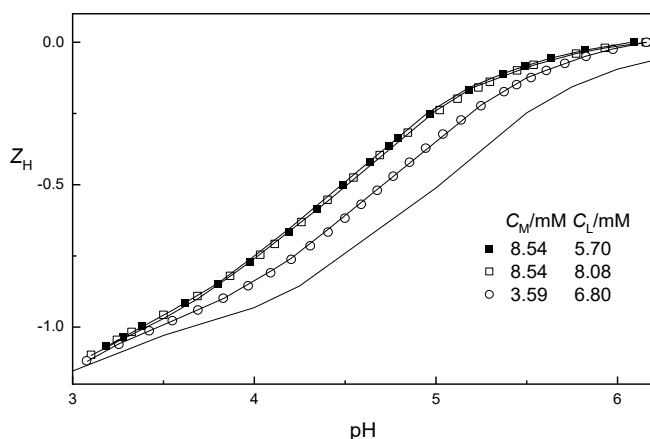


Figure 23. Part of the experimental data plotted as Z_H curves vs. pH for cobalt(II) complex formation with pyridine-2-acetamidoxime HL. The full lines have been calculated using sets of proposed stability constants in Table 7. The lowest line refers to the ligand alone.

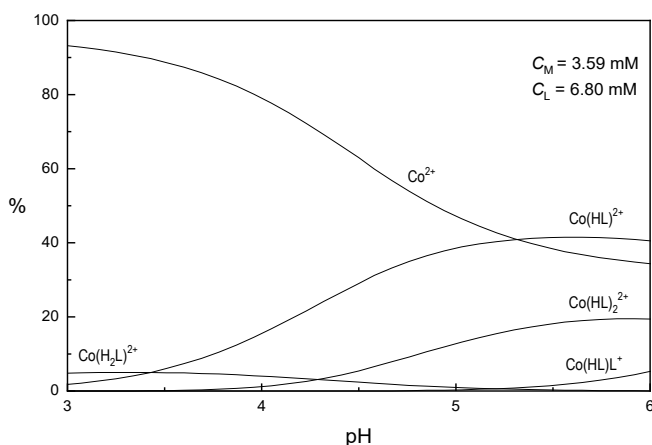


Figure 24. An example of the concentration distribution of the cobalt(II) species vs. pH with pyridine-2-acetamidoxime.

$\text{Zn}_2\text{L}_2\text{OH}^+$ is probably formed through dimerization of two deprotonated $\text{Zn}(\text{HL})^{2+}$ complexes (ZnL^+) via two oximato $-\text{NO}^-$ bridges to $\text{Zn}_2\text{L}_2^{2+}$, which in the pH range 7.0–7.5 immediately

deprotonates to $\text{Zn}_2\text{L}_2\text{OH}^+$ through forming a hydroxo $-\text{OH}^-$ bridge besides the six-membered $(\text{ZnNO})_2$ ring. Nickel(II) ion forms an analogous complex $\text{Ni}_2\text{L}_2\text{OH}^+$.⁹ $\text{Cd}(\text{HL})^{2+}$ does not deprotonate until in the pH range 8–9. Although the proportion of CdL^+ was small in all the solution (Figure 26), it was accepted because it would be very difficult to find reasons to exclude the deprotonation of the parent complex $\text{Cd}(\text{HL})^{2+}$ in the pH range 8.0–8.8. $\text{Cd}(\text{HL})^{2+}$ ($\text{pK}_a = 9.77$) is, as expected, about 0.7 pK_a units weaker acid than the corresponding pyridine-2-carboxamidoxime complex (9.06). Similar to this is the calculated acidity difference between the $\text{Ni}(\text{HL})_2^{2+}$ complexes with pyridine-2-acetamidoxime ($\text{pK}_a = 8.42$) and with pyridine-2-carboxamidoxime (7.76).⁹ The small amounts of

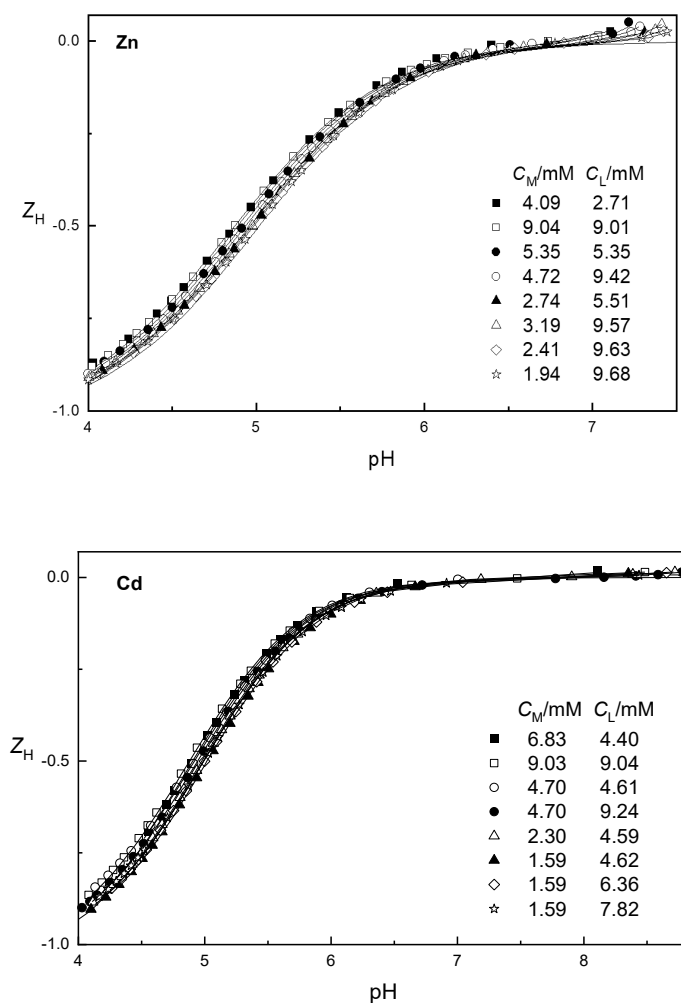


Figure 25. Part of the experimental data plotted as Z_H curves vs. pH for zinc(II) and cadmium(II) complex formation with pyridine-2-acetamidoxime HL. The full lines have been calculated using sets of proposed stability constants in Table 7. The lowest line refers to the ligand alone.

CdL^+ explain the slight exceeding of the Z_{H} curves above the zero level before the precipitation of $\text{Cd}(\text{OH})_2$.

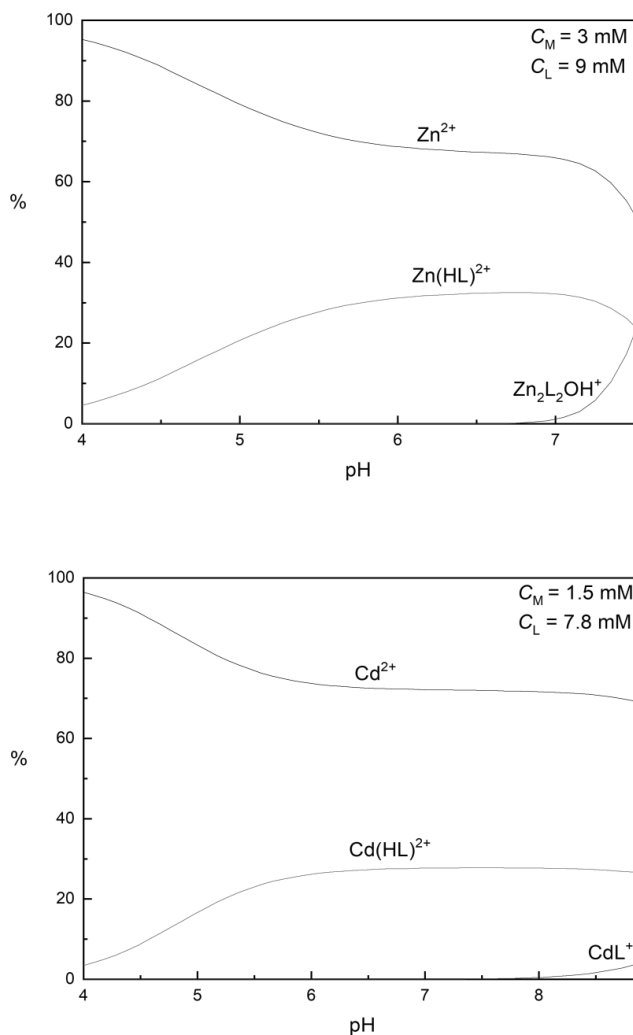


Figure 26. Examples of the concentration distributions of the zinc(II) and cadmium(II) species vs. pH with pyridine-2-acetamidoxime.

Due to the six-membered chelate rings, the complex formation of the pyridine-2-acetamidoxime with zinc(II) and cadmium(II) ions is very small. The cobalt(II), nickel(II), and copper(II) complexes are stabilized by ligand fields. The stepwise logarithmic stability differences $\log(K_1/K_2)$ between $\text{Co}(\text{HL})^{2+}$ ($\log K_1 = 2.56$) and $\text{Co}(\text{HL})_2^{2+}$ ($\log K_2 = 2.17$) and between $\text{Ni}(\text{HL})^{2+}$ ($\log K_1 = 3.59$) and $\text{Ni}(\text{HL})_2^{2+}$ ($\log K_2 = 3.27$) are (0.32–0.39) smaller than the statistic difference between octahedral

mono and bis complexes (0.68).⁷⁹ $\text{Cu}(\text{HL})^{2+}$ ($\log \beta_{011} = 5.31$) and $\text{Cu}(\text{HL})_2^{2+}$ ($\log \beta_{012} = 9.55$) are even more stable⁹ than the corresponding pyridine-2-aldoxime complexes ($\log \beta_{011} = 3.93$ and $\log \beta_{012} = 7.48$).¹¹ Also, the 3-aminopropanamidoxime complexes $\text{Ni}(\text{ap})^{2+}$ ($\log \beta_{011} = 4.89$) and $\text{Ni}(\text{ap})_2^{2+}$ ($\log \beta_{012} = 8.35$) are in 0.1 M NaCl solution⁷ more stable than the corresponding pyridine-2-aldoxime complexes ($\log \beta_{011} = 4.190$ and $\log \beta_{012} = 7.620$) in 1.0 M NaCl solution,¹⁰ but the corresponding pyridine-2-acetamidoxime complexes $\text{Ni}(\text{HL})^{2+}$ ($\log \beta_{011} = 3.59$) and $\text{Ni}(\text{HL})_2^{2+}$ ($\log \beta_{012} = 6.86$) are less stable. The electron-withdrawing pyridine rings weaken also the stabilities of these complexes as the basicity of the free ligand HL. Thus, the pyridine nitrogen of the free pyridine-2-acetamidoxime ($\log \beta_{101} = 5.017$) is a much weaker base than the amine nitrogens of 3-aminopropanamidoxime (9.061) and its *N*-alkyl derivatives (8.577–9.375).^{5–7} All these oximes form with copper(II) and nickel(II) ions pentanuclear complexes, and the crystal structure has been determined by X-ray diffraction for the solid 3-(*N*-methylamino)propanamidoxime complex $[\text{Cu}_5(\text{mp-H})_4]\text{Br}_2 \cdot 2\text{H}_2\text{O}$.⁵ The pentamer consists of four $\text{Cu}(\text{mp-H})$ units linked together via amido $-\text{NH}^-$ and oximato $-\text{NO}^-$ bridges, from which the oximato bridges are branched to form a square-planar CuO_4 central core. In the aqueous pentanuclear nickel(II) complexes, the central core is probably octahedral (NiO_6) with two aqua ligands. This structure allows the deprotonation of $\text{Ni}_5(\text{ap-H})_4^{2+}$ to $\text{Ni}_5(\text{ap-H})_4\text{OH}^+$. $\text{Ni}_5(\text{ap-H})_4^{2+}$ ($\text{p}K_a = 9.6$), $\text{Ni}_5(\text{mp-H})_4^{2+}$ (9.4), and the 3-(*N*-dimethylamino)propanamidoxime complex $\text{Ni}_5(\text{dmp-H})_4^{2+}$ (9.5) are weak acids⁷ as the aqua Ni^{2+} ion ($\text{p}K_a = 9.85$).²⁸

$\text{Ni}_2\text{L}_2\text{OH}^+$ is probably formed via two oximato $-\text{NO}^-$ bridges and a hydroxo $-\text{OH}^-$ bridge between the nickel(II) ions. At high $C_L:C_M$ ratios a precipitate or slow attainment of equilibria appears in the pH range 8–9 and at low $C_L:C_M$ ratios in the pH range 7–8. $\text{Cu}_2\text{L}_2^{2+}$ is formed at lower pH ranges (pH < 5.9) only via two oximato $-\text{NO}^-$ bridges. The available pH ranges remain too narrow to observe possible tetra- or pentanuclear pyridine-2-acetamidoxime complexes.⁹

3.6. Pyridine-2,6-dicarboxamidoxime complexes

Pyridine-2,6-dicarboxamidoxime is a tridentate ligand with two amidoxime groups. Because both of the oxime groups are deprotonable, it is best to symbolize the uncharged form of the ligand as H_2L instead of HL. In evaluating the equilibrium constants, the binary two-component equilibria (35–41) are considered:





In evaluation the stability constants of the three-component (H^+ , M^{2+} , and H_2L) equilibria equation (11) is replaced with



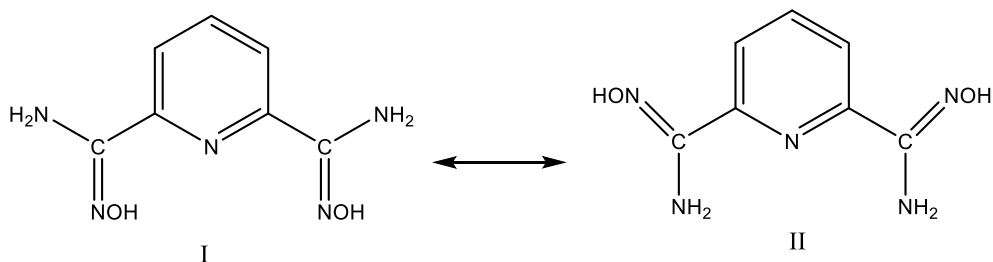
Bovenzi and Pearse¹³⁰ have reported the crystal structures of the solid ligand H_2L , $[\text{Cu}(\text{H}_2\text{L})\text{SO}_4] \cdot 2\text{H}_2\text{O}$, and $[\text{Ni}(\text{H}_2\text{L})_2]\text{SO}_4 \cdot 5\text{H}_2\text{O}$. In this work the protonation and acidity constants of the free ligand H_2L and the stability constants for its copper(II) and nickel(II) complexes in aqueous 0.1 M NaCl solution at 25 °C have been determined. To find out the role of the deprotonation of the oxime function on these complexes, the crystal structure of $[\text{Ni}(\text{HL})_2] \cdot 4\text{H}_2\text{O}$ has also been determined.

To determine the values of protonation and acidity constants only ligand added to the solution of 50.00 ml 0.100 M NaCl + 7.00 ml 0.1 M HCl after the determination of E_0 . The solutions were then titrated with the accurately known 0.1 M NaOH solution. Only dilute solutions could be used without precipitation. In solution with an initial $C_L \geq 3$ mM, a white precipitate was formed already at pH 3–4 and dissolved again in the pH range 10–11. Titration points after the dissolution had to be used in data treatment to determine of the acidity constants K_{a1} and K_{a2} . The protonation and acidity constants calculated from 246 titration points of five titration with $\chi^2 = 8.37$ and $s = 1.75$ are shown in Table 8. The values of constants $\log \beta_{101} = 3.817$ and $\text{p}K_{a1} = 11.2$ prove that the precipitate was formed by the uncharged ligand H_2L .

Bovenzi and Pearse¹³⁰ used infrared stretching assignments of NH_2 and OH groups to show that there are considerable intermolecular hydrogen bonds between the adjacent ligand molecules (H_2L) in the solid state involving amide and oxime hydrogens with oxime oxygens ($\text{N}-\text{H} \cdots \text{O}$ and $\text{O}-\text{H} \cdots \text{O}$) and with amide nitrogens ($\text{N}-\text{H} \cdots \text{N}$ and $\text{O}-\text{H} \cdots \text{N}$).¹³⁰ Every uncharged ligand molecule (H_2L) has four groups capable of intermolecular hydrogen bonding, which probably promotes the precipitation in aqueous solution.

The interactions of the amidoxime groups in pyridine-2,6-dicarboxamidoxime H_2L can be understood by comparing its acidity constants ($\text{p}K_{a1} = 11.2$, $\text{p}K_a = 12.2$) with those of pyridine-2-carboxiamidoxime⁹ ($\text{p}K_a = 11.7$) and benzamidoxime (12.36 in aqueous NaCl solution at $I = 0.3$ M).¹⁰² Comparable acidity differences are found between pyridine-2,6-dialdoxime ($\text{p}K_{a1} = 9.7$ and $\text{p}K_{a2} =$

10.7 in NaClO₄ solution at $I = 0.01$ M),¹³¹ pyridine-2-aldoxime ($pK_a = 10.17$ at $I < 0.001$ M),⁴⁷ and benzaldoxime (10.7 at low ionic strength).⁵⁰ The pyridine nitrogen increases the acidity of the 2-amidoxime and 2-aldoxime groups by 0.5–0.7 log units and the additional 6-amidoxime or 6-aldoxime group by about 0.5 log units. Pyridine-2,6-dialdoxime ($\log \beta_{101} = 2.34$) is in NaClO₄ solution at 0.005 M ionic strength¹³¹ a much weaker base than pyridine-2-aldoxime ($\log \beta_{101} = 3.56$) at low (< 0.001 M) ionic strength.⁴⁷ The additional electron-withdrawing 6-aldoxime groups lowers the basicity of the pyridine nitrogen about 1.2 log units, but there are no essential difference between the protonation constants of pyridine-2,6-dicarboxamidoxime H₂L ($\log \beta_{101} = 3.817 \pm 0.015$) and pyridine-2-carboxamidoxime HL (3.798 ± 0.006).⁹ The increased electron densities by the delocalization of lone electron pairs of the amide nitrogens allow the amidoxime nitrogens to form a much stronger intramolecular hydrogen bonding with pyridine nitrogen ($H-O-N \cdots H^+ \cdots N-O-H$) than the aldoxime groups. In the decrease of pH, pyridinium-2,6-dicarboxamidoxime H₃L⁺ protonates further to H₄L²⁺ with a stepwise protonation constant $\log (\beta_{201}/\beta_{101}) = 2.336 \pm 0.015$. It is of same order with those of pyridine-2-acetamidoxime ($\log (\beta_{201}/\beta_{101}) = 2.29 \pm 0.01$),⁹ 2-aminoacetamidoxime (2.467),¹ and its *N*-alkyl derivatives (1.351–2.112).^{1,2,4} It was previously estimated that the amide group would be protonated.^{5,9,13} However, observations of the structures of the protonated acetamidoxime and benzamidoxime¹⁰² suggest that the proton would be attached also in other amidoximes to the oxime nitrogen rather than to the amide nitrogen. The protonation of the amidoxime group lowers the basicity of the pyridine nitrogen in *ortho* position and probably transfers the proton to the other amidoxime nitrogen. Both of the protonated amidoxime groups of H₄L²⁺ rotate around the C_{py}–C_{ox} bonds and the pyridine nitrogen forms intramolecular hydrogen bonding with the amide hydrogens ($N-H \cdots N \cdots H-N$). Bovenzi and Pearse¹³⁰ have shown with X-ray analysis that in the crystalline state both of the amide –NH₂ groups and the pyridine nitrogen of the free H₂L are on the same side of the C_{py}–C_{ox} bonds as the only amide group in the crystalline pyridine-2-carboxamidoxime.^{103,104} This conformation (II below) is probable also in aqueous H₂L and H₄L²⁺ because of the intramolecular hydrogen bonding ($N-H \cdots N \cdots H-N$) and the repulsion forces between the protons in H₄L²⁺ or between the lone electron pairs of the oxime ($H_2N-C=N-OH \leftrightarrow H_2N^+=C-N^--OH$) and pyridine nitrogens in H₂L.



The formation of the copper(II) complexes occurs in very acidic conditions. At beginning of the measurements, the solutions were blue or blueish-green and the green color strengthened during titration. The Z_H curves (Figure 27) of the solutions show very strong complex formation already at $\text{pH} = 2$. The same is true in the system Cu^{2+} –pyridine-2-carboxamidoxime.⁹ Here, the stability constant of the mono complex $\text{Cu}(\text{H}_2\text{L})^{2+}$ could be determined only by using very dilute solutions with $C_M = 0.347\text{--}0.681$ mM and $C_L = 0.347\text{--}0.689$ mM in 1:1 titrations. The best fit to the data from eight titrations and 208 points ($\chi^2 = 36.7$ and $s = 1.02$) was obtained with a simple model consisting of mononuclear species $\text{Cu}(\text{H}_2\text{L})^{2+}$, $\text{Cu}(\text{H}_2\text{L})_2^{2+}$, $\text{Cu}(\text{H}_2\text{L})\text{HL}^+$, and $\text{Cu}(\text{HL})_2^{2+}$ (or $\text{Cu}(\text{H}_2\text{L})\text{L}$). Their stability constants are given in Table 8. The useful experimental data were restricted to $\text{pH} < 6.8$, preventing further analysis.

Because of the high stability of $\text{Cu}(\text{H}_2\text{L})^{2+}$ no accurate value of β_{011} could be obtained. The values of the other β -constants calculated seemed to be affected by the given β_{011} value and sensitive to its systematic errors, but the stepwise stability and acidity constants of $\text{Cu}(\text{H}_2\text{L})_2^{2+}$ reported in Table 8 were practically independent of the β_{011} value (in the wide prefixed $\log \beta_{011}$ range 6.4–7.0) and more precise. An example of the concentration distribution of the copper(II) species is shown in Figure 28.

Although pyridine-2,6-dicarboxamidoxime (H_2L) is a tridentate ligand, $\text{Cu}(\text{H}_2\text{L})^{2+}$ ($\log \beta_{011} = 6.66 \pm 0.13$) is less stable than the 2-aminoacetamidoxime complex $\text{Cu}(\text{Hao})^{2+}$ (8.787), and also $\text{Cu}(\text{Hma})^{2+}$ (8.108) and $\text{Cu}(\text{dma})^{2+}$ (6.909 in 1.0 M NaClO_4) despite of the steric requirements by the *N*-methyl groups.² Even $\text{Cu}(\text{Hap})^{2+}$ (7.53 ± 0.01) and $\text{Cu}(\text{Hmp})^{2+}$ (6.82 ± 0.01) are more stable despite their six-membered chelate rings.⁵ The electron-withdrawing pyridine ring weakens significantly the basicity of the free pyridine-2,6-dicarboxamidoxime ($\log \beta_{101} = 3.817$) and also stability of $\text{Cu}(\text{H}_2\text{L})^{2+}$. The free 2-aminoacetamidoxime¹ ($\log \beta_{101} = 7.942$) and the free 3-aminopropanamidoxime⁵ (9.061) are much stronger bases and able to form more stable metal complexes than the tridentate pyridine-2,6-dicarboxamidoxime.

The stepwise stability constant of $\text{Cu}(\text{H}_2\text{L})_2^{2+}$ ($\log K_2 = 3.53$) is due to the Jahn–Teller distortion much smaller than $\log K_1 = 6.66$. Attempts to synthesize any crystalline complex with copper(II) chloride were unsuccessful. Bovenzi and Pearse¹³⁰ reported that the ligand does not form the expected monomeric product with copper(II) sulfate but rather a two-dimensional Jahn–Teller distorted polymer $\{[\text{Cu}(\text{H}_2\text{L})\text{SO}_4] \cdot 2\text{H}_2\text{O}\}_n$. Each of the copper–ligand units are bonded to two sulfate groups by Cu–O bonds resulting in five-coordinate copper(II) ions.

The Z_H curves (Figure 27) show measurable formation of nickel(II) complexes at the beginning of the measurements, where the solutions were almost colorless. In the course of the titration, the solutions had weak violet tone but after the neutralization of the added acid, they became yellow, later light brown and in the pH range 9–10 turned dark brown. The best fit to the experimental data from nine titrations and 265 points ($\chi^2 = 28.2$, $s = 1.07$) was obtained by assuming the mononuclear species

$\text{Ni}(\text{H}_2\text{L})^{2+}$, $\text{Ni}(\text{H}_2\text{L})_2^{2+}$, $\text{Ni}(\text{H}_2\text{L})\text{HL}^+$, $\text{Ni}(\text{HL})_2$, $\text{Ni}(\text{HL})\text{L}^-$, and NiL_2^{2-} . The stability constants and the acidity constants of $\text{Ni}(\text{H}_2\text{L})_2^{2+}$ are given in Table 8.

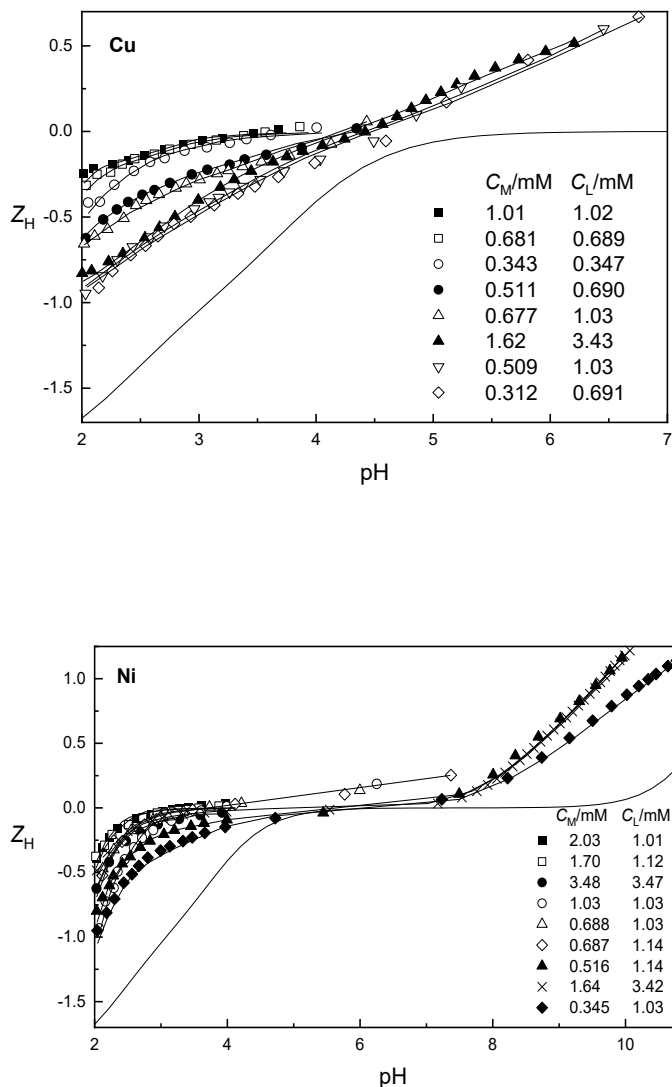


Figure 27. Part of the experimental data plotted as Z_H curves vs. pH for copper(II) and nickel(II) complex formation with pyridine-2,6-dicarboxamidoxime H_2L . The full lines have been calculated using sets of proposed stability constants in Table 5. The lowest line refers to the ligand alone.

The stability constant of $\text{Ni}(\text{H}_2\text{L})^{2+}$ ($\log \beta_{011} = 5.67 \pm 0.15$) is fairly inaccurate, and it is therefore not clear whether it is more stable than $\text{Ni}(\text{Hao})^{2+}$ (5.720 ± 0.005). However, unlike $\text{Cu}(\text{H}_2\text{L})^{2+}$, it is clearly more stable than $\text{Ni}(\text{Hma})^{2+}$ (5.253) and $\text{Ni}(\text{Hap})^{2+}$ (4.89).

Unlike the copper(II) complexes, the inaccuracy of the stability constant of $\text{Ni}(\text{H}_2\text{L})^{2+}$ is not markedly cumulated to the other β -constants calculated. The overall stability constants of $\text{Ni}(\text{H}_2\text{L})_2^{2+}$, $\text{Ni}(\text{H}_2\text{L})\text{HL}^+$, $\text{Ni}(\text{HL})_2$, and $\text{Ni}(\text{HL})\text{L}^-$ could be exactly determined in the pH range 8–10. Such accuracy for the stability constant of NiL_2^{2-} ($\log \beta_{-412} = -27.25 \pm 0.23$) could not be obtained, because the complex was observed in the solutions in the pH range > 9.7 and in the calculations it was necessary to use data points up to pH 11.0. An example of the concentration distribution of the nickel(II) species is shown in Figure 28.

Table 8. Proposed formulas and stability constants ($\log \beta_{pqr}$) of pyridine-2,6-dicarboxamidoxime complexes relating to the reaction $p\text{H}^+ + q\text{M}^{2+} + r\text{H}_2\text{L} \rightleftharpoons (\text{H}^+)_p(\text{M}^{2+})_q(\text{H}_2\text{L})_r$ and their first acidity constants ($\text{p}K_a$) in aqueous 0.1 M Na(Cl) solution at 25 °C.

| $p\ q\ r$ | Proposed formula | $\log \beta_{pqr} \pm 3\ \sigma$ | $\text{p}K_a \pm 3\ \sigma$ |
|-----------|------------------------------------------------------------------------|----------------------------------|-----------------------------|
| 1 0 1 | H_3L^+ | 3.817 ± 0.015 | 3.817 ± 0.015 |
| 2 0 1 | H_4L^{2+} | 6.153 ± 0.013 | 2.336 ± 0.013 |
| -1 0 1 | HL^- | -11.2 ± 0.2^a | 12.2 ± 0.2^a |
| -2 0 1 | L^{2-} | -23.4 ± 0.2^a | |
| 0 1 1 | $\text{Cu}(\text{H}_2\text{L})^{2+}$ | 6.66 ± 0.13 | |
| 0 1 2 | $\text{Cu}(\text{H}_2\text{L})_2^{2+}$ | $3.53^b \pm 0.04$ | 4.92 ± 0.05 |
| -1 1 2 | $\text{Cu}(\text{H}_2\text{L})\text{HL}^+$ | 5.23 ± 0.15 | 6.71 ± 0.12 |
| -2 1 2 | $\text{Cu}(\text{HL})_2$ (or $\text{Cu}(\text{H}_2\text{L})\text{L}$) | -1.48 ± 0.20 | |
| 0 1 1 | $\text{Ni}(\text{H}_2\text{L})^{2+}$ | 5.67 ± 0.15 | |
| 0 1 2 | $\text{Ni}(\text{H}_2\text{L})_2^{2+}$ | 11.31 ± 0.08 | 8.17 ± 0.04 |
| -1 1 2 | $\text{Ni}(\text{H}_2\text{L})\text{HL}^+$ | 3.14 ± 0.09 | 9.18 ± 0.04 |
| -2 1 2 | $\text{Ni}(\text{HL})_2$ | -6.04 ± 0.09 | 9.96 ± 0.05 |
| -3 1 2 | $\text{Ni}(\text{HL})\text{L}^-$ | -16.00 ± 0.10 | 11.25 ± 0.22 |
| -4 1 2 | NiL_2^{2-} | -27.25 ± 0.25 | |

^a $\pm 10\ \sigma$. ^b $= \log K_2$ relating to the reaction $\text{Cu}(\text{H}_2\text{L})^{2+} + \text{H}_2\text{L} \rightleftharpoons \text{Cu}(\text{H}_2\text{L})_2^{2+}$.

The structure of the crystallized complex with the formula $[\text{Ni}(\text{HL})_2] \cdot 4\text{H}_2\text{O}$ could be determined by X-ray diffraction. A crystal was selected for the X-ray measurement and mounted to the glass fiber using the oil drop method,¹³² data were collected at 173 K on Nonius Kappa CCD diffractometer (Mo-K α radiation, graphite monochromator, $\lambda = 0.71073$). The intensity data were corrected for Lorentz and polarization effects and for absorption. The programs COLLECT,¹³³ SHELXS-97,¹³⁴ and SHELXS-97-2¹³⁴ were used for data reduction, structure solution, and structure refinement, respectively. The non-hydrogen atoms were refined anisotropically. The H atoms were introduced in calculated positions and refined with fixed geometry with respect to their carrier atoms. The H atoms of the water molecules were determined from the difference map. One of the water molecules was

disordered. The crystal structure is orthorhombic, space group *phen* with $a = 12.601(3)$, $b = 9.3990(19)$, $c = 17.195(3)$ Å, $\alpha = \beta = \gamma = 90^\circ$ and $Z = 4$. The structure is shown in Figure 29.

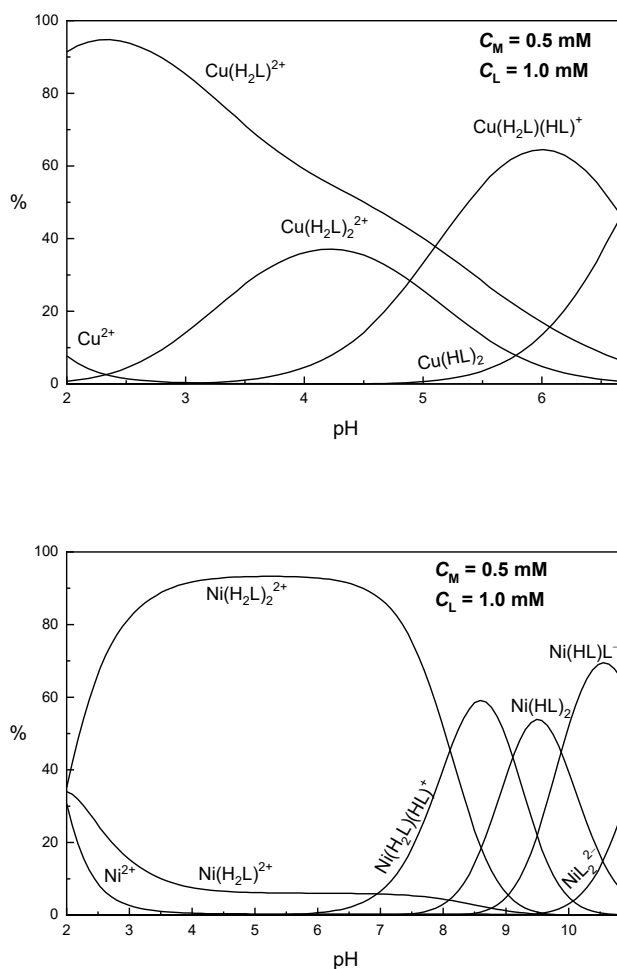


Figure 28. Examples of the concentration distributions of copper(II) and nickel(II) species vs. pH with pyridine-2,6-carboxamidoxime.

The crystal structure of the solid $\text{Ni}(\text{HL})_2$ confirms that two tridentate ligands are approximately perpendicularly coordinated to each other. The nickel(II) ion is six-coordinated through the oxime, oximato and pyridine nitrogens of the two ligands. The resulting configuration is a slightly distorted octahedron, the distortion rising from the rigid structures of the ligands. The $\text{N}(1)\text{—Ni—N}(9)$ angle (153.05°) is approximately equal to the sum of the angles $\text{N}(10)\text{—Ni—N}(1)$ and $\text{N}(10)\text{—Ni—N}(9)$ (153.12°), proving a planar coordination by both ligands. The Ni—N_{py} bonds (2.0042 Å) are shorter

than in the crystalline octahedral high spin pyridine-2-carboxamidoxime complexes $\text{Ni}(\text{HL})_2(\text{NO}_3)_2$ (2.084–2.090 Å),¹¹² $\text{Ni}(\text{HL})_2(\text{OOCCH}_3)_2$ (2.116 Å),¹¹³ and $\text{Ni}(\text{HL})_3^{2+}$ (2.079–2.109 Å),¹¹² but only slightly shorter than in $[\text{Ni}(\text{H}_2\text{L})_2]\text{SO}_4 \cdot 5\text{H}_2\text{O}$ (2.007 Å).¹³⁰ The $\text{Ni}-\text{NO}^-$ (2.1361 Å) bonds are longer than the $\text{Ni}-\text{NOH}$ bonds (2.1326 Å) and the $\text{N}(9)-\text{Ni}-\text{N}(9\text{A})$ angle (100.56°) is larger than the $\text{N}(1)-\text{Ni}-\text{N}(1\text{A})$ (96.44°), $\text{N}(1)-\text{Ni}-\text{N}(9\text{A})$, and $\text{N}(1\text{A})-\text{Ni}-\text{N}(9)$ angles (87.70°) apparently because of the repulsion forces between the oximate NO^- groups. Due to the rigid structures of the tridentate ligands, the $\text{Ni}-\text{NOH}$ bonds are also in $\text{Ni}(\text{H}_2\text{L})_2^{2+}$ (2.117–2.136 Å) longer than in the octahedral high spin nickel(II) complexes of bidentate amidoximes (2.048–2.086 Å).^{111–113} In $\text{Ni}(\text{HL})_2$ the $\text{N}-\text{O}(\text{H})$ bond lengths (1.4239 Å) are typical for the octahedral high spin amidoxime complexes^{112–115} but the $\text{N}-\text{O}^-$ bonds are shorter (1.3752 Å). The deprotonation of the oxime group shortens the $\text{N}-\text{O}$ bond and opens the $\text{C}=\text{N}-\text{O}$ bond angle, which closes both the adjacent $\text{Ni}-\text{N}-\text{O}$ and $\text{Ni}-\text{N}=\text{C}$ angles and seems to affect the whole ligand geometry. For example, in $\text{Ni}(\text{HL})_2$ the $\text{C}=\text{N}-\text{O}(\text{H})$ angles are 110.93° but the $\text{C}=\text{N}-\text{O}^-$ angles are 115.26° . The $\text{C}(2)-\text{N}(1)-\text{Ni}$ and $\text{C}(8)-\text{N}(9)-\text{Ni}$ angles are 117.15° and 114.45° , respectively, but in $\text{Ni}(\text{H}_2\text{L})_2$ the corresponding angles are 116.3° .¹³⁰ The $\text{C}=\text{N}-\text{O}(\text{H})$ angles in the free pyridine-2,6-carboxdiamidoxime H_2L are

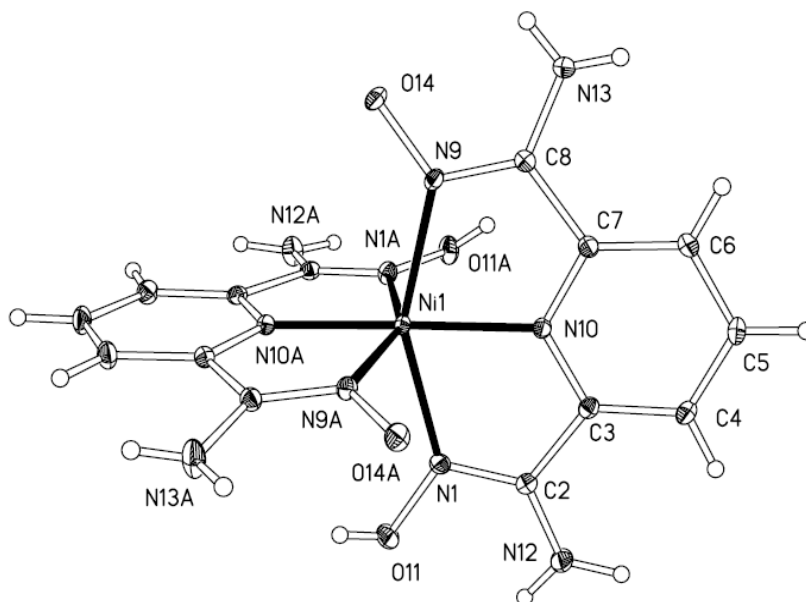


Figure 29. Crystal structure of $[\text{Ni}(\text{HL})_2] \cdot 4\text{H}_2\text{O}$ showing the atomic numbering scheme. The water molecules have been omitted for clarity.

108.7°, ¹³⁰ in the free pyridine-2-carboxamidoxime HL 108.89°, ¹⁰³ or 109.1°, ¹⁰⁴ and in other free amidoximes generally 109.0–110.7°. ^{106–109} In high spin pyridine-2-carboxamidoxime complexes the C=N–O(H) angles are generally 111.3–112.6°, ^{112–115} and in other amidoxime complexes 110.6–111.8°. ^{111,136,137} The deprotonation of the oxime group opens the C=N–O angles and the intramolecular hydrogen bonding C=N–O–H···[−]O–N=C opens also the C=N–OH angles. For example, in the following 1-(2-pyridinyl)ethanone oxime complexes Ni(HL)₂Br₂ the C=N–O(H) angles are 114.7° and 115.3°, in [Ni(HL)L(H₂O)₂]₂NO₃ the C=N–OH angle is 116.5° and the C=N–O[−] angle is 119.1°, ⁹⁴ in Cu(HL)Cl the C=N–OH angle is 118.3° and the C=N–O[−] is 117.7°, ⁹³ and in [PtL₂] C=N–O angles are 119.5°. ⁹⁶ In the pyridine-2-aldoxime complex [PtL₂]₂·2H₂O the C=N–O angles are 119.1°, ⁷⁴ and in the dimeric complex Ni(HL)L₂·6½H₂O the C=N–OH angles are 120.7°, the hydrogen bridged C=N–O[−] angles are 117.2°, and the non-bridged C=N–O[−] angles are 118.8°. ¹⁰ In the octahedral 2-aminoacetamidoxime complex [Ni(Hao)₂(H₂O)₂]Cl₂ the C=N–O angles are 111.6° but in the square-planar [Ni(Hao)(ao)]Cl·½H₂O 114.8° and 116.3°. ¹¹¹ In mononuclear metal chelates (M = Cu²⁺, Ni²⁺, Zn²⁺, Co³⁺), where all the oxime groups are deprotonated, the C=N–O angles are in general within 119–123°. ^{138,139}

The titration and crystallographic analyses (Figure 29) show that the *bis* complex Ni(H₂L)₂²⁺ dissolves with increasing pH stepwise to Ni(HL)₂, which further dissolves to NiL₂^{2−}. According to its conventional stability constant $\log \beta_2 = (\log \beta_{-212} + 2p\beta_{-101}) = 16.4$, Ni(HL)₂ is more stable but according to its acidity constants $pK_{a1} = 9.96$ and $pK_{a2} = 11.25$ (pK_{a3} and pK_{a4} of Ni(H₂L)₂²⁺, respectively) 2–3 log units weaker acid than the corresponding pyridine-2,6-dialdoxime complex ($\log \beta_2 = 15.7$, $pK_{a1} = 7.3$, $pK_{a2} = 8.9$ in NaClO₄ solution at $I = 0.01$ M). ¹³¹ The delocalization of the lone electron pairs of the amide NH₂ nitrogens increases electron density in the oxime nitrogens strengthening the Ni–N_{py} and oxime NO–H bonds and weakens the acidity of Ni(HL)₂. The pyridine-2-carboxamidoxime complexes Ni(HL)₂L⁺ ($pK_a = 9.68$) and Ni(HL)L₂ ($pK_a = 10.85$) are clearly weaker acids⁹ than Ni(H₂L)(HL)⁺ (9.18) and Ni(HL)₂ (9.68) and also the pyridine-2-aldoxime complex Ni(HL)L₂ ($pK_a = 7.71$ in 1.0 M NaCl) solution¹⁰) is a weaker acid than the pyridine-2,6-dialdoxime complex Ni(HL)₂ (7.3 in NaClO₄ solution at $I = 0.01$ M). ¹³¹ The bidentate ligands apparently stabilize Ni(HL)₂L⁺ and Ni(HL)L₂ with some intramolecular hydrogen bonding (O–H···O[−]···H–O and O[−]···H···O, respectively). The tridentate ligands are so rigid that no intramolecular hydrogen bonding can be observed in the solid Ni(HL)₂ between the perpendicularly coordinated oxime and oximate groups.

The Jahn–Teller distortion weakens the acidity of the ligand coordinated on the *z* axis of Cu(H₂L)₂²⁺, explaining the rather large difference between the values of $pK_{a1} = 4.92$ and $pK_{a2} = 6.71$. Figure 29 shows that in NiH₂L₂ both ligands are present in the form HL[−] giving the structure Ni(HL)₂.

In the case of the copper(II) complex $\text{Cu}(\text{H}_2\text{L})\text{HL}^+$, deprotonation to $\text{Cu}(\text{HL})_2$ is questionable; it is also possible that both of the protons dissociate from the same ligand in the *xy* plane giving a complex $\text{Cu}(\text{H}_2\text{L})\text{L}$. Pinart *et al.*¹⁴⁰ proposed that the structure of the corresponding pyridine-2,6-dialdoxime complex is $\text{Cu}(\text{HL})_2$ with intramolecular hydrogen bonding ($=\text{N}-\text{O}-\text{H}\cdots\text{O}=\text{N}=\text{O}$) between the adjacent oxime and oximato groups. In the copper(II) complexes $\text{Cu}(\text{H}_2\text{L})\text{HL}^+$ and $\text{Cu}(\text{HL})_2$, Jahn–Teller distortion can cause such a marked deviation on the *z* axis to the ligand that some intramolecular hydrogen bonding is possible. The absence of $\text{Cu}(\text{HL})^+$ even in the pH range 6.0–6.7 can be due to forming of deprotonated bis complexes $\text{Cu}(\text{H}_2\text{L})\text{HL}^+$ and $\text{Cu}(\text{HL})_2$ with some stabilizing intramolecular hydrogen bonding. The detection of $\text{Ni}(\text{HL})^+$ is difficult, because the proportion of its parent complex $\text{Ni}(\text{H}_2\text{L})^{2+}$ is small (< 5 %) in the pH range 8–9 (Figure 28). Due to the stronger ligand field the stepwise stability constant of $\text{Ni}(\text{H}_2\text{L})_2^{2+}$ ($\log K_2 = 5.64$) is nearly equal to that of $\text{Ni}(\text{H}_2\text{L})^{2+}$ ($\log K_1 = 5.67 \pm 0.15$). In a weaker ligand field, $\text{Ni}(\text{H}_2\text{L})^{2+}$ is a weaker acid than $\text{Ni}(\text{H}_2\text{L})_2^{2+}$ ($\text{p}K_a = 8.17$).

4. SUMMARY AND CONCLUSIONS

Pyridine-2-aldoxime and its methyl or amide derivatives coordinate as uncharged ligands HL to metal ions through their pyridine and oxime nitrogens. As Figure 30 shows the stability of the mono complexes $\text{M}(\text{HL})^{2+}$ increases with few exceptions in the order $\text{Cd} < \text{Zn} < \text{Co} < \text{Ni} < \text{Cu}$.

Pyridine-2-carboxiamidoxime ($\log \beta_{101} = 3.798$) and 1-(2-pyridinyl)ethanone oxime (3.968) are stronger bases and form clearly more stable mono complexes than pyridine-2-aldoxime ($\log \beta_{101} = 3.590$) does. The methyl $-\text{CH}_3$ and amide $-\text{NH}_2$ groups increase the electron density of the oxime and the pyridine nitrogens. The increased electron density strengthens the basicity of the pyridine ring and the oxime $\text{NO}-\text{H}$ nitrogen weakening the acidity of the oxime NOH group. The three ligands form also bis complexes and with nickel(II) and partly with cobalt(II) ion also tris complexes. Pyridine-2-acetamidoxime and 6-methylpyridine-2-aldoxime don't form tris complexes because of the six-membered chelate rings and the steric interferences by the 6-methyl groups. Pyrazine-2-carboxamidoxime is taken in Figure 30, because its electron-withdrawing 4-nitrogen significantly weakens the basicity ($\log \beta_{101} = 2.68$) and complexing ability of the ligand. Therefore, the pyrazine-2-carboxamidoxime complexes are less stable than the corresponding pyridine-2-aldoxime complexes. An exception is $\text{Cu}(\text{Hpza})^{2+}$ ($\log K_1 = 4.16$), which is more stable than $\text{Cu}(\text{Hpyal})^{2+}$ (3.93). $\text{Cu}(\text{Hpyac})^{2+}$ ($\log K_1 = 5.31$) is despite its six-membered chelate ring almost as stable as $\text{Cu}(\text{Hpyet})^{2+}$ (5.63). Pyrazine-2-carboxamidoxime forms tris complexes only with nickel(II) ion. The stepwise stability orders of the complexes $\text{M}(\text{HL})_r^{2+}$ are with all the ligands: $K_1 > K_2 > K_3$.

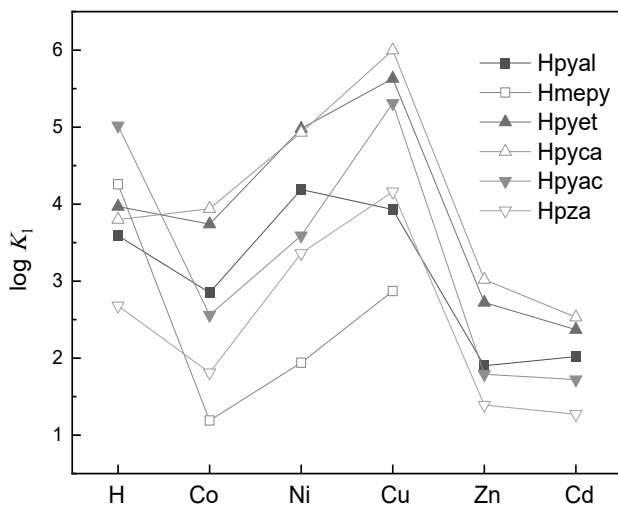


Figure 30. The stepwise stability constants of the mono complexes $M(HL)^{2+}$ vs. divalent metal ion (M^{2+}) and hydrogen ion (H^+). Abbreviations: Hpyal = pyridine-2-aldoxime, Hmepy = 6-methylpyridine-2-aldoxime, Hpyet = 1-(2-pyridinyl)ethanone oxime, Hpyca = pyridine-2-carboxamidoxime, Hpyac = pyridine-2-acetamidoxime, Hpza = pyrazine-2-(carbox)amidoxime. For the metal ions $\log K_1 = \log \beta_{011}$ and for H^+ $\log K_1 = \log \beta_{101}$. The stability constant of $Ni(Hpyal)^{2+}$ was determined in 1.0 M Na(Cl), the other constants in 0.1 M Na(Cl) solution, all at 25 °C.

It seems that copper(II) ion favors amidoximes over aldoximes. $Ni(Hpyal)^{2+}$ ($\log \beta_{011} = 4.19$) is in 1.0 M Na(Cl) solution more stable than $Cu(Hpyal)^{2+}$ (3.93) in 0.1 M Na(Cl). This is probably because the free pyridine-2-aldoxime (Hpyal) is in 1.0 M Na(Cl) a stronger base (3.865) than even pyridine-2-carboxamidoxime (Hpyca) in 0.1 M Na(Cl) solution (3.798). However, $Ni(Hpyal)^{2+}$ is in 1.0 M Na(Cl) solution clearly less stable than $Ni(Hpyca)^{2+}$ ($\log \beta_{011} = 4.93$) and $Ni(Hpyet)^{2+}$ (4.98) in 0.1 M Na(Cl) solution. This is probably due the weaker ligand field in the pyridine-2-aldoxime complexes.

In the increase of pH the complexes deprotonate. The deprotonated bis complexes $M(HL)L^+$ are stabilized by an intramolecular hydrogen bridge between the *cis* oriented oxime and oximate groups ML_2 , the oxime and oximate groups are probably *trans* oriented due to the repulsion forces between the negatively charged oximate groups and between the positively charged oxime protons. The complexes are apparently octahedral, and the dissociation of their aqua ligands allows the isomerization of the *trans* oriented oxime groups to *cis*. It is also possible that the $trans-M(HL)_2^{2+}$ complexes deprotonate via $trans-M(HL)L^+$ to $trans-ML_2$. The intermediates $trans-M(HL)L^+$ are much less stable but stronger acids than their *cis* isomers. In the tris complexes, the oxime groups are apparently *mer* oriented, and the structure is prevented in the deprotonated nickel(II) complexes $Ni(HL)_2L^+$, $Ni(HL)L_2$, and NiL_3^- .

The cobalt(II) complexes $\text{Co}(\text{HL})^{2+}$ and $\text{Co}(\text{HL})_2^{2+}$ are mainly octahedral high spin complexes with $t_{2g}^5 e_g^2$ electron structure, but some tetrahedral complexes also exist with two fully occupied lower e and three half-occupied higher energy t_2 orbitals ($e^4 t_2^3$) in equilibrium. The bis complexes $\text{Co}(\text{HL})_2^{2+}$ are except the pyridine-2-aldoxime complex about 2–3 log units stronger bases than the corresponding $\text{Ni}(\text{HL})_2^{2+}$ and $\text{Zn}(\text{HL})_2^{2+}$ complexes, because the $\text{Co}(\text{HL})\text{L}^+$ complexes are low spin with $t_{2g}^6 e_g$ electron structure. Pyridine-2-carboxamidoxime forms also tris complex $\text{Co}(\text{HL})_3^{2+}$, which deprotonates with $\text{p}K_a = 5.3$ to $\text{Co}(\text{HL})_2\text{L}^+$. $\text{Co}(\text{HL})_3^{2+}$ is probably mainly high spin with *mer* oriented oxime groups, but $\text{Co}(\text{HL})_2\text{L}^+$ is low spin. In $\text{Co}(\text{HL})_2\text{L}^+$ the *mer* oriented oxime and oximate groups are not obvious. The octahedral low spin cobalt(II) complexes are Jahn–Teller distorted because of the uneven electron occupation in their e_g orbitals. The *fac* oriented oxime and oximate are more capable of intramolecular hydrogen bonding $\text{O}=\text{H}\cdots\text{O}^-\cdots\text{H}-\text{O}$ in the Jahn–Teller distorted complexes than the *mer* oriented ones. Also, pyridine-2-aldoxime forms $\text{Co}(\text{HL})_2\text{L}^+$, which is low spin, but its parent complex $\text{Co}(\text{HL})_3^{2+}$ never reaches measurable concentrations. The low spin cobalt(II) complexes oxidize easily to cobalt(III) complexes, because their only e_g electron detaches very easily. The t_{2g}^6 electron structured cobalt(III) complexes are very inert and their substitution reactions are very slow. The oxidation of the low spin cobalt(II) complexes is very strong in acid solution but no longer in the pH range 8–10. With the increase in the concentration of low spin cobalt(II) complexes, the attainment of equilibria becomes slow often already in the pH range 4–5. Using very small cobalt(II) ion concentration ($C_M \leq 0.36$ mM) a pyridine-2-aldoxime solution could be titrated to pH range 8–9, but very small NaOH additions had to be used in the pH range 5–8. In the increase of pH $\text{Co}(\text{HL})_2\text{L}^+$ is completely displaced by CoL_2 and the deprotonated complexes $\text{Co}(\text{HL})\text{L}_2$ and CoL_3^- never reach measurable concentrations.

It is possible that 1-(2-pyridinyl)ethanone oxime also forms tris complexes with cobalt(II) ion. They cannot be detected, because $\text{Co}(\text{HL})_2^{2+}$ ($\text{p}K_{a1} \approx 2.8$) is about 2–3 log units stronger acid than $\text{Ni}(\text{HL})_2^{2+}$ (4.82) and $\text{Zn}(\text{HL})_2^{2+}$ (5.16), $\text{Co}(\text{HL})\text{L}^+$ is low spin and oxidizes to cobalt(III) complex already in the pH range 2.5–2.9. The high spin structure of the pyridine-2-aldoxime complex $\text{Co}(\text{HL})\text{L}^+$ and the weaker acidity of the pyridine-2-carboxamidoxime complex $\text{Co}(\text{HL})_2^{2+}$ ($\text{p}K_a = 5.07$) allow the detections of the tris complexes with these ligand.

6-methylpyridine-2-aldoxime forms $\text{Co}(\text{HL})^{2+}$, CoL^+ , CoL_2 , $\text{Co}_2\text{L}_2\text{OH}^+$, Co_2L_3^+ , and $\text{Co}_2\text{L}_3\text{OH}$ with cobalt(II) ion. The 6-methyl groups cause steric interference with the *cis* orientation of the oxime groups in a plane. Apparently, CoL_2 is octahedral low spin and due to the Jahn–Teller distortion, at least one of the oximate $-\text{NO}^-$ groups lies on the z axis of the complex. Co_2L_3^+ is probably formed through combination of CoL_2 and CoL^+ via three oximate $-\text{NO}^-$ bridges. One of the cobalt(II) ions in CoN_4O_2 environment is probably low spin, but the other in CoN_2O_4 environment is high spin. The octahedral low spin part and one of the oximate bridges is Jahn–Teller distorted. The deprotonation

of Co_2L_3^+ to $\text{Co}_2\text{L}_3\text{OH}$ in the pH range 6–9 requires formation of a hydroxo $-\text{OH}^-$ bridge and breaking of an oximate bridge, if the coordination spheres of $\text{Co}_2\text{L}_3\text{OH}$ are still octahedral. The Jahn–Teller distorted oximate bridge of Co_2L_3^+ is easily broken and after bending of the remaining $(\text{CoNO})_2$ ring, the hydroxo bridge is formed on the opposite side of the of the opened oximate $-\text{NO}^-$ group. $\text{Co}_2\text{L}_2\text{OH}^+$ is probably formed through dimerization of two deprotonate mono complexes (CoL^+) via two oximate bridges and a hydroxo bridge between the cobalt(II) ions. Both of the cobalt(II) ions are in CoN_2O_4 probably high spin.

Pyrazine-2-carboxamidoxime forms similar cobalt(II) complexes, but instead of CoL^+ and CoL_2 , it forms $\text{Co}(\text{HL})\text{L}^+$ and $\text{Co}_2\text{L}_2(\text{OH})_2$. As in $\text{Co}_2\text{L}_3\text{OH}$, only three bridges are possible in $\text{Co}_2\text{L}_2(\text{OH})_2$ between the cobalt(II) ions, if their coordination spheres are still octahedral. The bending of the $(\text{MNO})_2$ rings easily breaks the hydroxo bridge and causes a collision of two adjacent aqua ligands on the opposite site of the broken hydroxo bridge. One of the two aqua ligands is then released as oxonium H_3O^+ ion and the other deprotonated to OH^- ligand, which forms a new hydroxo bridge. Soon, the formed hydroxo bridge is broken and the former hydroxo ligand is again bridged. The two hydroxo ligands of $\text{M}_2\text{L}_2(\text{OH})_2$ form alternatively short-lived hydroxo bridges between metal ions.

The pyrazine-2-carboxamidoxime complexes $\text{Co}(\text{HL})\text{L}^+$ and $\text{Ni}(\text{HL})\text{L}^+$ disappear in the pH range 9–10 without deprotonation to CoL_2 and NiL_2 . In amidoxime complexes, the delocalization of the lone electron pairs of the amide nitrogens stabilize the intramolecular hydrogen bonding between the oxime and oximate oxygen and the adjacent amide hydrogens are also able to intramolecular hydrogen bonding: $\text{N}-\text{H}\cdots\text{O}-\text{H}\cdots\text{O}\cdots\text{H}-\text{N}$.

Both 6-methylpyridine-2-aldoxime and pyrazine-2-carboxamidoxime form also $\text{Ni}(\text{HL})_2^{2+}$ and Ni_2L_3^+ but neither form $\text{Ni}_2\text{L}_3\text{OH}$. The three oximate bridges of Ni_2L_3^+ must be *fac* oriented and none of them is Jahn–Teller distorted. If one of the oximate ligands is located in the *xy* plane of the NiL_2 unit (NiN_4O_2 environment) and the other pyridine nitrogen on the *z* axis of the unit, none of the three oximate bridges can be replaced by a hydroxo bridge without significant isomerization of the complex. 6-methylpyridine-2-aldoxime forms also NiL_2 , where the oximate groups are *trans* oriented and the $\text{Ni}-\text{N}_{\text{py}}$ bonds are perpendicular to each other. This structure allows NiL_2 to form insoluble polymers with deprotonated mono complexes via oximate and hydroxo bridges starting with $\text{Ni}_3\text{L}_4(\text{OH})_2$. In all solutions with $C_L \geq 1.5 C_M$, a precipitate or very slow attainment of equilibrium appears already in the pH range 6.5–7.5. 6-methyl groups cause steric interference with the *cis* orientation of the oxime or oximate groups and with the formation of tris complexes. Pyrazine-2-carboxamidoxime forms soluble tris complexes and a tetramer $\text{Ni}_4\text{L}_2(\text{L}-\text{H})_2^{2+}$ with a $(\text{NiNO})_2$ central ring and two amido $-\text{NH}^-$ bridges binding the central $\text{Ni}_2(\text{L}-\text{H})_2$ unit and two NiL^+ units.

6-methylpyridine-2-aldoxime forms with zinc(II) and cadmium(II) ions only deprotonated complexes: $\text{Zn}_2\text{L}_2^{2+}$ ($\text{p}K_a = 6.31$), $\text{Zn}_2\text{L}_2\text{OH}^+$ (8.29), and $\text{Zn}_2\text{L}_2(\text{OH})_2$, CdL^+ , CdL_2 , and $\text{Cd}_2\text{L}_2\text{OH}^+$. In

$\text{Zn}_2\text{L}_2^{2+}$, only two oximato bridges combine the zinc(II) ions. Its proportion remains small, because the hydroxo bridge is already formed in the pH range 6–7 beside the $(\text{ZnNO})_2$ ring. The polymerization of CdL^+ is rather weak, and the proportion of $\text{Cd}_2\text{L}_2\text{OH}^+$ remains small.

Also, pyridine-2-aldoxime and 1-(2-pyridinyl)ethanone oxime form $\text{Zn}_2\text{L}_2^{2+}$ ($\text{p}K_a = 6.54\text{--}6.83$) $\text{Zn}_2\text{L}_2\text{OH}^+$ (7.99–9.36), $\text{Zn}_2\text{L}_2(\text{OH})_2$, and $\text{Cd}_2\text{L}_2\text{OH}^+$ in addition to mono and bis complexes. Pyridine-2-aldoxime forms also $\text{Cd}_2\text{L}_2^{2+}$ ($\text{p}K_a = 8.64$) and the 1-(2-pyridinyl)ethanone oxime complex $\text{Cd}_2\text{L}_2\text{OH}^+$ deprotonates with $\text{p}K_a = 9.83$ to $\text{Cd}_2\text{L}_2(\text{OH})_2$. Due to the larger size of cadmium(II) ion, the cadmium(II) complexes are weaker acids and also the polymerization of CdL^+ is rather weak. The pyridine-2-aldoxime complex $\text{Zn}(\text{HL})_2^{2+}$ doesn't reach measurable concentrations. The proportion of $\text{Zn}(\text{HL})_2^{2+}$ ($\text{p}K_a = 6.71$) is in the pH range 6–7 still so large that ZnL^+ reaches measurable concentrations. Similarly, the cadmium(II) complexes CdL^+ reach measurable concentrations with all the six oximes. Except the pyridine-2-carboxamidoxime complex, none of the complex of type $\text{Cd}(\text{HL})_2^{2+}$ reaches measurable concentrations. The other oxime complexes $\text{M}(\text{HL})_2^{2+}$ are so stable and the mono complexes $\text{M}(\text{HL})^{2+}$ so weak acids that they do not deprotonate to ML^+ before they disappear in the increase of pH.

Pyridine-2-carboxamidoxime forms $\text{Zn}_2\text{L}_2\text{OH}^+$ and $\text{Zn}_4(\text{L-H})_2\text{L}_2^{2+}$ in the pH range 7–8. Apparently, their parent complex is $\text{Zn}_2\text{L}_2^{2+}$, which immediately forms a hydroxo bridge or polymerizes to the tetramer via amido —NH— and oximato —NO— bridges. Cadmium(II) ion forms similarly $\text{Cd}_4(\text{L-H})_2\text{L}_2^{2+}$ in the pH range 8–10, but not $\text{Cd}_2\text{L}_2\text{OH}^+$. The larger size of cadmium(II) ion weakens especially the Cd—O bonds. The d^{10} electron structures of zinc(II) and cadmium(II) favor coordination to nitrogen over the oxygen.

Pyridine-2-carboxamidoxime forms in the low pH range a binuclear complex $\text{Co}_2(\text{HL})_2\text{H}_2\text{L}^{5+}$, where one of the ligands is positively charged. The structure of the dimer is very difficult to predict. The deprotonation of the ligand H_2L^+ to HL in the pH range 2–3 causes decomposing of $\text{Co}_2(\text{HL})_2\text{H}_2\text{L}^{5+}$ to $\text{Co}(\text{HL})_2^{2+}$ and $\text{Co}(\text{HL})_2^{2+}$. Cobalt(II) ion forms also a complex $\text{Co}(\text{H}_2\text{L})_3^{3+}$ with a positively charged pyridine-2-acetamidoxime H_2L^+ . It deprotonates to $\text{Co}(\text{HL})_2^{2+}$ in the pH range 4–5, where the proportion of $\text{Co}(\text{HL})_2^{2+}$ is rather small. Apparently, the positively charged ligands H_2L^+ are coordinated to the cobalt(II) ion as monodentate ligand. Nickel(II) and zinc(II) ions do not form complexes with positively charged ligands. Apparently, nickel(II) ion displaces the protons in the pH range 2–3 and zinc(II) cannot form stable complexes with positively charged ligands.

Both pyridine-2-acetamidoxime and pyrazine-2-carboxamidoxime form only $\text{Zn}(\text{HL})_2^{2+}$ and $\text{Zn}_2\text{L}_2\text{OH}^+$ with zinc(II) and only $\text{Cd}(\text{HL})_2^{2+}$ and CdL^+ with cadmium(II). The aqua Zn^{2+} ion precipitates as $\text{Zn}(\text{OH})_2$ in the pH range 7.0–7.5, where the proportions of the $\text{Zn}_2\text{L}_2\text{OH}^+$ complexes are very small. $\text{Cd}(\text{OH})_2$ starts to precipitate at (pH =) 8–9, where also the proportion of CdL^+ complexes are also very small.

It is obvious that the formation of polynuclear species originates from the weak stabilities of the mononuclear bis and tris complexes. Due to the Jahn–Teller distortion, copper(II) ion does not form tris complexes with bidentate oximes. For the same reason also the structure of $\text{Cu}_2\text{L}_2\text{OH}^+$ would be highly unstable. Pyridine-2-acetamidoxime forms $\text{Cu}_2\text{L}_2^{2+}$, but pyridine-2-aldoxime and its methylated derivatives form trinuclear species $\text{Cu}_3\text{L}_3\text{OH}^{2+}$ and $\text{Cu}_3\text{L}_3\text{O}^+$ (or $\text{Cu}_3\text{L}_3(\text{OH})_2^+$).

Pyridine-2,6-dicarboxamidoxime H_2L is a tridentate ligand and forms more stable complexes $\text{Cu}(\text{H}_2\text{L})^{2+}$ ($\log \beta_{011} = 6.66$), $\text{Ni}(\text{H}_2\text{L})^{2+}$ (5.67), and $\text{Ni}(\text{H}_2\text{L})_2^{2+}$ ($\log \beta_{012} = 11.31$, $\log K_2 = 5.64$) than the bidentate oxime ligands HL. However, due to the Jahn–Teller distortion the stepwise stability constant $\log K_2$ of $\text{Cu}(\text{H}_2\text{L})_2^{2+}$ is only 3.53. The crystal structure of $[\text{Ni}(\text{HL})_2] \cdot 4\text{H}_2\text{O}$ determined with X-ray diffraction shows that in NiH_2L_2 both ligand are in the form HL^- , but the structure of $\text{Cu}(\text{HL})_2$ is not clear in CuH_2L_2 . The structure of $\text{Cu}(\text{HL})_2\text{L}$ is also possible; because the Jahn–Teller distortion weakens also the acidity of the ligand coordinated on the z axis of $\text{Cu}(\text{H}_2\text{L})_2^{2+}$.

REFERENCES

1. H. Saarinen, M. Orama, T. Raikas, and J. Korvenranta, *Acta Chem. Scand.* **A 37** (1983) 631.
2. H. Saarinen, M. Orama, T. Raikas, and J. Korvenranta, *Acta Chem. Scand.* **A 40** (1986) 396.
3. M. Orama, H. Saarinen, T. Raikas, and J. Korvenranta, *Finnish Chem. Lett.* **13** (1986) 59.
4. M. Orama, H. Saarinen, and J. Korvenranta, *Acta Chem. Scand.* **A 43** (1989) 834.
5. M. Orama, H. Saarinen, and J. Korvenranta, *Acta Chem. Scand.* **A 48** (1994) 127.
6. M. Orama, H. Saarinen, J. Korvenranta, and T. Raikas, *Acta Chem. Scand.* **A 46** (1992) 1083.
7. M. Orama and H. Saarinen, *Acta Chem. Scand.* **A 50** (1996) 1168.
8. M. Salonen, M. Orama, and H. Saarinen, *The 9th Symposium on Inorganic and Analytical Chemistry*, Helsinki, 1996, Programme and Abstracts, s. 67; The University of Helsinki, Institute of Chemistry, Laboratory of Inorganic Chemistry.
9. M. Orama and H. Saarinen, *Acta Chem. Scand.* **A 50** (1996) 1087.
10. M. Orama and H. Saarinen, *Acta Chem. Scand.* **A 43** (1989) 407.
11. M. Orama, H. Saarinen, and J. Korvenranta, *J. Coord. Chem.* **22** (1990) 183.
12. H. Saarinen and M. Orama, *Acta Chem. Scand.* **A 52** (1998) 1209.
13. M. Salonen, *Ph. Lic. Thesis*, University of Helsinki (2002).
14. H. Hartkamp, *Naturwissenschaften* **45** (1958) 211.
15. H. Hartkamp, *Z. Analyt. Chem.* **170** (1959) 399.
16. H. Hartkamp, *Z. Analyt. Chem.* **176** (1960) 185.
17. I. Wojciechowska, K. Wieszczycka, and A. Wojciechowska, *Sep. Purif. Technol.* **173** (2017) 372.

18. M. Krupa, K. Wieszczycka, A. Wojciechowska, and A. Olszanowski, *Sep. Sci. Technol.* **50** (2015) 654.
19. A. Demeke, F. Chekol, S. Admassie, and S. Mehretie, *Anal. Bioanal. Electrochem.* **9** (2017) 704.
20. G. A. Petroianu, *Pharmazie* **68** (2013) 916.
21. M. C. Moffett, J. H. McDonough, J. D. McMonagle, and T. M. Myers, *Int. J. Toxicol.* **35** (2018) 352.
22. B. Kumar, K. K. Prasad, and S. K. Srivastava, *Asian J. Chem.* **23** (2011) 1680.
23. R. Banks and R. F. Brookes, *Chem. Ind.* (1974) 617.
24. R. Näsänen and K. Paakkola, *Suom. Kemistil.* **B 34** (1961) 19.
25. R. Näsänen and P. Meriläinen, *Suom. Kemistil.* **B 33** (1960) 149.
26. H. S. Harned and R. A. Robinson, *Trans. Faraday Soc.* **36** (1940) 973.
27. S. Sjöberg, Y. Häggglund, A. Nordin, and N. Ingri, *Marine Chem.* **13** (1985) 35.
28. C. F. Baes, Jr. and R. E. Mesmer, *The Hydrolysis of Cations*, John Wiley & Sons, New York, 1976.
29. Y. Kanekiyo, S. Aizawa, N. Koshino, and S. Funahashi, *Inorg. Chim. Acta* **298** (2000) 154.
30. M. H. Huntington, W. C. E. Higginson, *J. Chem. Soc., Dalton Trans.* (1973) 1247.
31. K. J. Powell, P. L. Brown, R. H. Byrne, T. Gajda, G. Hefter, A.-K. Leuz, S. Sjöberg, and H. Wanner, *Pure Appl. Chem.* **83** (2011) 1163.
32. S. Chaberek, Jr., R. C. Courtney, and A. E. Martell, *J. Am. Chem. Soc.* **74** (1952) 5057.
33. R. Arnek and W. Kakolowicz, *Acta Chem. Scand.* **21** (1967) 2180.
34. K. J. Powell, P. L. Brown, R. H. Byrne, T. Gajda, G. Hefter, S. Sjöberg, and H. Wanner, *Pure Appl. Chem.* **79** (2007) 895.
35. K. J. Powell, P. L. Brown, R. H. Byrne, T. Gajda, G. Hefter, A.-K. Leuz, S. Sjöberg, and H. Wanner, *Chem. International* **37** (2015) 15.
36. Stability Constants Database and Mini-SC Database, IUPAC and Academic Software, Version 5.3, Sourby Old Farm, Timble Otley, Yorks, UK, 2011 schbase@acadsoft.co.uk.
37. P. Gans, A. Sabatini, and A. Vacca, *J. Chem. Soc., Dalton Trans.* (1985) 1195.
38. N. Bjerrum, *Z. Anorg. Allg. Chem.* **119** (1921) 179.
39. J. Bjerrum, *Metal Ammine Formation in Aqueous Solution*, P. Haase and Sons, Copenhagen, 1957, p. 20.
40. C. H. Liu and C. F. Liu *J. Am. Chem. Soc.* **83** (1961) 4167, 4169.
41. B. Kirson, *Bull. Soc. Chim. France* (1962) 1030.
42. G. I. H. Hanania and D. H. Irvine, *J. Chem. Soc.* (1962) 2745.
43. Y. Israeli and E. Jungreis, *Bull. Res. Council of Israel* **11 A** (1962) 121.
44. S. Bolton and R. I. Ellin, *J. Pharm. Sci.* **51** (1962) 533.
45. K. Burger, I. Egyed, and I. Ruff, *J. Inorg. Nucl. Chem.* **28** (1966) 139.
46. C. Petitfaux, *Ann. Chim.* **8** (1973) 33.
47. R. W. Green and I. R. Freer, *J. Phys. Chem.* **65** (1961) 2211.
48. J. Bjerrum, *Acta Chem. Scand.* **18** (1964) 843.
49. K. Kahlmann, H. Siegler, and H. Erlenmeyer, *Helv. Chim. Acta* **47** (1964) 1754.

50. O. L. Brady and R. F. Goldstein, *J. Chem. Soc.* (1926) 1918.
51. F. A. Cotton, G. Wilkinson, C. A. Murillo, and M. Bochmann, *Advanced Inorganic Chemistry*, John Wiley & Sons, New York, 6. Edition, 1999.
52. H. Taube, *Chem. Rev.* **50** (1952) 69.
53. A. E. Martell and R. J. Motekaitis, *Determination and Use of Stability Constants*, VCH Publishers, 1988.
54. K. Burger and I. Ruff, *Talanta* **10** (1963) 329.
55. R. A. Krause and D. H. Busch, *J. Am. Chem. Soc.* **82** (1960) 4830.
56. K. Burger and B. Pintér, *J. Inorg. Nucl. Chem.* **29** (1967) 1717.
57. K. Burger, B. Pintér, E. Papp-Molnár, and S. Nemes-Kósa, *Acta Chim. Acad. Sci. Hung. Tomus* **57** (1968) 363.
58. R. G. Pearson, *J. Chem. Educ.* **45** (1968) 581, 643.
59. R. D. Shannon, *Acta Cryst.* **A 32** (1976) 751.
60. H. Irving and J. P. Williams, *J. Chem. Soc.* (1953) 3192.
61. L. Bologni, A. Sabatini, and A. Vacca, *Inorg. Chim. Acta* **69** (1983) 71.
62. P. Schindler, H. Althaus, and W. Feitnecht, *Helv. Chim. Acta* **47** (1964) 982.
63. P. Schindler *Helv. Chim. Acta* **42** (1959) 2736.
64. A. Chakravorty, *Coord. Chem. Rev.* **13** (1974) 1.
65. C. F. Liu and C. H. Liu, *J. Am. Chem. Soc.* **83** (1961) 2615.
66. C. F. Liu and C. H. Liu, *Inorg. Chem.* **2** (1963) 706.
67. K. W. Nordquest, D. W. Phelps, W. F. Little, and D. J. Hodgson, *J. Am. Chem. Soc.* **98** (1976) 1104.
68. L. Helm, L. I. Elding, and A. E. Merbach, *Inorg. Chem.* **24** (1985) 1719.
69. L. Helm, L. I. Elding, and A. E. Merbach, *Helv. Chim. Acta* **67** (1984) 1453.
70. L. Helm and A. E. Merbach, *Chem. Rev.* **105** (2005) 1923.
71. Y. Si, *Acta Cryst.* **E 68** (2012) m554.
72. E. B. Coropceanu, L. Croitor, A. A. Ciloci, Zh. P. Tyurina, E. G. Dvornina, C. Z. Codreanu, and M. S. Fonari, *Russ. J. Coord. Chem.* **43** (2017) 278.
73. S. A. Shirvan and S. Haydari Dezfuli, *Acta Cryst.* **E 68** (2012) m1080.
74. S. Mukherjee, B. A. Patel, and S. Bhaduri, *Organometallics* **28** (2009) 3074.
75. B. J. Coe and S. J. Glenwright, *Coord. Chem. Rev.* **203** (2000) 5.
76. V. Amani, D. Sharafie, N. Faal Hamedani, and M. Naseh, *J. Iran. Chem. Soc.* **17** (2020) 441.
77. T. Weyhermüller, R. Wagner, S. Khanra, and P. Chaudhuri, *J. Chem. Soc., Dalton Trans.* (2005) 2539.
78. M. Dey, A. Goswami, and N. Gogoi, *Transit. Met. Chem.* **41** (2016) 509.
79. F. R. Hartley, C. Burgess, and R. M. Alcock, *Solution Equilibria*, John Wiley & Sons, New York, 1980.
80. R. Beckett and B. F. Hoskins, *J. Chem. Soc., Dalton Trans.* (1972) 291.
81. P. F. Ross, R. K. Murmann, and E. O. Schlemper, *Acta Cryst.* **B 30** (1974) 1120.
82. S. Ross, T. Weyhermüller, E. Bill, K. Wieghardt, and P. Chaudhuri, *Inorg. Chem.* **40** (2001) 6656.

83. S. Ross, T. Weyhermüller, E. Bill, E. Bothe, U. Flörke, K. Wieghardt, and P. Chaudhuri, *Eur. J. Inorg. Chem.* (2004) 984.
84. Y. Couturier and C. Petitfaux, *Bull. Soc. Chim. France* (1973) 439, 445.
85. F. Pantani, *Ricerca Sci.* **34** (1964) 417.
86. G. Anderegg, *Helv. Chim. Acta* **43** (1960) 414.
87. N. Kumar, G. S. Manku, A. N. Bhat, and B. D. Jain, *Talanta* **17** (1970) 873.
88. A. Pajunen, I. Mutikainen, H. Saarinen, and M. Orama, *Z. Kristallogr. NCS* **214** (1999) 217.
89. V. L. Pecoraro, A. J. Stemmler, B. R. Gibrey, J. J. Bodwin, H. Wang, J. W. Kampf, and A. Barwinski, *Prog. Inorg. Chem.* **45** (1997) 83.
90. SciFinder *Chemical Abstracts Service* (2017). Predicted pK_a calculated using Advanced Chemistry Development (ACD/Labs) Software V11.02 (© 1994-2017 ACD/Labs).
91. X. Han, V. K. Balakrishnan, G. W. van Loon, and E. Buncel, *Langmuir* **22** (2006) 9009.
92. C. V. King and A. P. Marion, *J. Am. Chem. Soc.* **66** (1944) 977.
93. X. Qui, L. Li, and D. Li, *Acta Cryst. E* **67** (2011) m1810.
94. K. Riggle, T. Lynde-Kernell, and E. O. Schlemper *J. Coord. Chem.* **25** (1992) 117.
95. L. Martínez, J. S. Gancheff, F. E. Hahn, R. A. Burrow, R. González, C. Kremer, and R. Chiozzone, *Spectrochim. Acta A Mol. Biomol. Spectrosc.* **105** (2013) 439.
96. D. W. Phelps, W. F. Little, and D. J. Hodgson, *Inorg. Chem.* **15** (1976) 2263.
97. E. Grunwald, P. J. Karabatsos, R. A. Kromhout, and E. L. Purlee, *J. Chem. Phys.* **33** (1960) 556.
98. M. Eigen and K. Kustin *J. Am. Chem. Soc.* **82** (1960) 5952.
99. D. L. Cole, E. M. Eyring, D. T. Rampton, A. Silzars, and R. P. Jensen, *J. Phys. Chem.* **71** (1967) 2771.
100. L. P. Holmes, D. L. Cole, and E. M. Eyring, *J. Phys. Chem.* **72** (1968) 301.
101. M. Eigen and W. Krause, *Z. Naturforsch.* **18 b** (1963) 857.
102. N. Mehio, M. A. Lashely, J. W. Nugent, L. Tucker, B. Correlia, C.-L. Do-Thanh, S. Dai, R. D. Hancock, and V. S. Bryantsev, *J. Phys. Chem.* **B 119** (2015) 3567.
103. P. A. Suchetan, S. Sreenivasa, B. S. Palakshamurthy, T. Madhu Chakrapani Rao, and Vijithkumar, *Acta Cryst. E* **69** (2013) o1180.
104. G. A. Pearse, P. R. Raithby, and J. Lewis, *Polyhedron* **8** (1989) 301.
105. G. A. Pearse, Jr., *Acta Chem. Scand.* **B 33** (1979) 742.
106. D. Hall, *Acta Cryst.* **18** (1965) 955.
107. H. Gozlan and C. Riche, *Acta Cryst.* **B 32** (1976) 1662.
108. A. Gieren and B. Dederer, *Acta Cryst.* **B 33** (1977) 3296.
109. X. Solans, C. Mirravittles, J. P. Declercq, G. Germain, *Acta Cryst.* **B 36** (1980) 3121.
110. H. Gozlan, R. Michelot, C. Riche and R. Rips, *Tetrahedron* **33** (1977) 2535.
111. H. Saarinen, J. Korvenranta M. Orama, and T. Raikas *Acta Chem. Scand.* **A 38** (1984) 265.
112. G. A. Pearse, P. R. Raithby, C. M. Hay, and J. Lewis, *Polyhedron* **8** (1989) 305.

113. M. Werner, J. Berner, and P. G. Jones, *Acta Cryst. C* **52** (1996) 72.
114. K. F. Konidaris, V. Bekiari, E. Katsoulakou, C. P. Raptopoulou, V. Psycharis, S. P. Perlepes, T. C. Stamatatos, and E. Manessi-Zoupa, *Inorg. Chim. Acta* **376** (2011) 470.
115. J. Liu, *Acta Cryst. E* **70** (2014) 142.
116. Ö. Bekaroglu, S. Sarisaban, A. R. Koray, and M. L. Ziegler, *Z. Naturforsch.* **32 b** (1977) 387.
117. D. W. J. Cruickshank, *Acta Cryst.* **9** (1956) 747.
118. H. Enders, T. Jannack, and B. Prickner, *Acta Cryst.* **B 36** (1980) 2230.
119. M. Näsäkkälä, H. Saarinen, J. Korvenranta, and M. Orama *Acta Cryst.* **C 45** (1989) 1514.
120. C.-M. Ji, H.-J. Yang, C.-C. Zhao, V. Tangoulis, A.-L. Cui, and H.-Z. Kou, *Cryst. Growth Des.* **9** (2009) 4607.
121. H.-Z. Kou, G.-Y An, C.-M. Ji, B.-W. Wang, and A.-L. Cui, *Dalton Trans.* **39** (2010) 9604.
122. G.-Y An, C.-M. Ji, A.-L. Cui, and H.-Z. Kou, *Inorg. Chem.* **50** (2011) 1079.
123. J. M. Malin and R. E. Shepherd, *J. Inorg. Nucl. Chem.* **34** (1972) 3203.
124. W. Forsling, *Acta Chem. Scand.* **A 32** (1978) 857.
125. S. Sjöberg, *Acta Chem. Scand.* **27** (1973) 3721.
126. S. Sjöberg, *Acta Chem. Scand.* **A 31** (1977) 729.
127. W. Forsling, *Acta Chem. Scand.* **A 31** (1977) 759.
128. L.-O. Öhman and S. Sjöberg, *Acta Chem. Scand.* **A 36** (1982) 47.
129. I. Granberg, and S. Sjöberg, *Acta Chem. Scand.* **A 35** (1981) 193.
130. B. A. Bovenzi and G. A. Pearse, Jr., *J. Chem. Soc., Dalton Trans.* (17) 2793.
131. S. P. Bag, Q. Fernando, and H. Freiser, *Anal. Chem.* **35** (1963) 719.
132. T. Kottle and D. Stalke, *J. Appl. Crystallogr.* **26** (1993) 615.
133. Nonius *COLLECT*, Nonius BV: Delft, The Netherlands (2002).
134. G. M. Sheldrick, *SHELXS-97 Program for Crystal Structure Determination*, University of Göttingen, Germany (1997).
135. G. M. Sheldrick, *SHELXS-97-2 Program for Crystal Structure Determination*, University of Göttingen, Germany (1997).
136. D. L. Cullen and E. C. Lingafelter, *Inorg. Chem.* **9** (1970) 1865.
137. H. Endress and T. Jannack, *Acta Cryst.* **B 36** (1980) 2136.
138. H. Saarinen, J. Korvenranta, and E. Näsäkkälä, *Acta Chem. Scand.* **A 32** (1978) 303.
139. H. Saarinen, J. Korvenranta, and E. Näsäkkälä, *Finnish Chem. Lett.* (1979) 81.
140. J. Pinart, C. Petitfaux, and J. Faucherre, *Bull. Soc. Chim. France* (1974) 1786.

